Order Number 9510743

Electrochemical study of artemisinin and analogs and computer simulation programming of cyclic voltammetric experiments

Zhang, Feng, Ph.D.

City University of New York, 1994

U·M·I
300 N. Zeeb Rd.
Ann Arbor, MI 48106

Electrochemical Study of Artemisinin and Analogs and Computer Simulation Programming of Cyclic Voltammetric Experiments

by

Feng Zhang

A dissertation submitted to the Graduate Faculty in Chemistry in partial fulfillment of the requirement for the degree of Doctor of Philosophy
The City University of New York

1994

This manuscript has been read and accepted for the Graduate Faculty in Chemistry in satisfaction of the dissertation requirement for the degree of Doctor of Philosophy.

6/26/94

Date

Chairman of Examining Committee

6/28/94

Date

Executive Officer

Supervisory Committee

The City University of New York

Abstract

Electrochemical Study of Artemisinin and Analogs and Computer Simulation Programming of Cyclic Voltammetric Experiments

by

Feng Zhang

Thesis Advisor: Professor David K. Gosser

This thesis includes two parts of works in electroanalytical chemistry. Part 1 describes the computer simulation programming of Cyclic Voltammetric experiments. The simplex routine was added into the original CV program which developed by Prof. Gosser (called CVFIT) and an error estimation program was also developed for the new version of CV program (named EET). These programs have been tested by me and Dr. Qingdong Huang, a graduate from City College. This work has been written in Prof. David K. Gosser's new book-"Cyclic Voltammetry-Simulation and Analysis of Reaction Mechanisms". Part 2 describes the study of artemisinin and its analogs by electrochemical techniques. The reactions of artemisinin and its analogs with hemin can be monitored by CV experiments and the electrochemical parameters can be determined from various electrochemical methods. This work is very useful to the biologists to understand the artemisinin's antimalarial mechanism in vivo.

To My Parents

Acknowledgment

I wish to thank my thesis advisor Professor David K. Gosser for his excellent direction and friendship during the years when I was at City College. I would also like to thank my thesis committee members, Professors Ronald L. Birke and David C. Locke, for their precious advice and finding time in their busy schedule. Also I want to thank my best friend Dr. Qingdong Huang. We worked together for years at City and I learned a lot from you. Finally, I would like to thank my wife Yihong Zhuang, my brother John Q. Zhang and all the members in my family, without their love, support and understanding this work could have never been done.

Table of Contents

Lists of Figures & Tables

Chapter 1

Chapter 2

Chapter 3

Chapter 4

Part 1
The Development of Programming for the Simulation and Analysis of Cyclic Voltammetric Experiments

Chapter 1: The Principles
1-1: Introduction

The theoretical description of an electrochemical experiment usually requires the solution of a set of coupled partial differential equations based on the diffusion equation. When a diffusing species is involved in a chemical reaction, reaction rate terms must be added to the equation describing its concentration. The set of equations often has time-dependent boundary conditions and can be devilishly difficult to solve. The analytical solution is always to be preferred since it leads to an exact equation relating experimental measurables to kinetic parameters. However, range of applicability is limited to relatively simple experiments, so computer simulation techniques must be employed.

Computer simulation by the explicit finite difference method has been used to treat a variety of electrochemical diffusion-kinetic problems[1-5]. The shape of a cyclic voltammetric curve reflects both electron transfer at the electrode and the chemical reactions in the solution which are coupled to the electron transfer. Simulations are often helpful in the preliminary stages of a cyclic voltammetric study, assisting in predicting mechanism(s) that can give rise to the cyclic voltammograms observed. Once a particular mechanism is decided upon, experimental results can be compared with successive simulations in order to extract rate and equilibrium parameters of the chosen mechanism.

Although adsorption processes can be included in the simulation, it is

not considered in our program (also the double-layer effects on the concentration of species in the outer Helmholtz plane are ignored). A planar electrode and linear diffusion are assumed throughout.

1-2: Basics of electrochemical digital simulation

1-2-1: Electron transfer process without following chemical reactions

Most commonly, the basic equation we need to solve is the diffusion equation, relating concentration C to time t and distance x from the electrode surface, as described in Fick's second diffusion equation:

$$\frac{\partial C}{\partial t} = D\frac{\partial^2 C}{\partial x^2} \qquad (1)$$

Fick's second law modified with a homogeneous chemical kinetics term describes the process involving following chemical reactions in the solution.

$$\frac{\partial C_q}{\partial t} = D_q \frac{\partial^2 C_q}{\partial x^2} \pm \sum k_g C_{g1} C_{g2} \qquad (2)$$

Where C_q = concentration of species q; k_g = chemical rate constant for the n^{th} solution chemical reaction; C_{gn} = concentrations for the first and second species in the n^{th} chemical reaction.

Near the electrode the concentrations will be determined in part by the potential of the electrode (through the Butler-Volmer equation). At a distance beyond the diffusion layer the concentrations will be the bulk values. These are the boundary conditions for Fick's second law.

Concentrations are functions of both time and distance from the electrode, C(x,t). The simplest approach is to divide the time and distance axes into discrete elements of size δt and δx and rewrite equation (1) as a finite difference equation through the application of a Taylor series approximations

of a function around a point. The "forward" and "backward" series are

$$y(z+\Delta z) = y(z) + \Delta z\frac{\partial y}{\partial z} + \frac{1}{2}\Delta z^2\frac{\partial^2 y}{\partial z^2} \quad (3)$$

$$y(z-\Delta z) = y(z) - \Delta z\frac{\partial y}{\partial z} + \frac{1}{2}\Delta z^2\frac{\partial^2 y}{\partial z^2} \quad (4)$$

Adding the two series, and regarding the variables y and z as concentration and distance respectively, we arrive at:

$$\frac{\partial^2 C}{\partial x^2} = \frac{D\left[C_{i-1} - 2C_i + C_{i+1}\right]}{\Delta x^2} \quad (5)$$

This is the discrete version of the right side of Fick's second law, where i is an index that keeps track of spatial points.

Considering only the first two terms of the forward series, and regarding the variables y and z as concentration and time (and introducing the time index j), we have the left side of Fick's second law:

$$\frac{\partial C}{\partial t} = \frac{\left[C_{j+1} - C_j\right]}{\Delta t} \quad (6)$$

Rearranging the above two equations and we can get the discrete version of Fick's second law:

$$C_{i,j+1} = C_{i,j} + D\frac{\delta t}{\delta x^2}\left(C_{i-1,j} - 2C_{i,j} + C_{i+1,j}\right) \quad (7)$$

Where i is the distance increment and j is the time increment. The three points thus give us a new point at the next time.

$$D^* = D\frac{\delta t}{\delta x^2} \quad (8)$$

D^* is a dimensionless diffusion coefficient. Equation (7) is equivalent to the creation of a space and time grid (**see Fig. 1-1-Space-time grid**). In any one time increment δt, diffusion can only propagate to neighboring concentration cells, this brings the value of $D^* \leq 0.5$. δt and δx are related which can be seen from equation (8).

If the concentration of each species is calculated at every space and time grid point, then the experiment is described. But the most difficult aspect of

the simulation is the calculation of the surface boundary conditions.

Let's review a simple one electron transfer example.

$A + e^- \Leftrightarrow B \quad k_f$ and k_b

k_f and k_b are the forward and backward electron transfer rate constants.

In electrochemical cells, the net current flowing will often be partly determined by the kinetics of electron transfer between electrode and the electroactive species in solution. The current in such cases is obtained from the Butler-Volmer equation relating current to electrode potential.

$$J_A = k_f C_{A0} - k_b C_{B0} \tag{9}$$

J is the current flux and defined as

$$J = \frac{i}{nFA}$$

The k_f and k_b have the following relationships with the standard rate constant k^0

$$k_f = k^0 e^{-\left(\frac{\alpha nF}{RT}\right)(E-E^{\circ})} \tag{10}$$

$$k_b = k^0 e^{(1-\alpha)\left(\frac{nF}{RT}\right)(E-E^{\circ})} \tag{11}$$

E^0 is the formal potential and α is the transfer coefficient.

Both forward (reduction) current i_f and reverse (oxidation) current i_b may be flowing simultaneously. The net current is then the sum: $i = (i_f + i_b)$.

If a reaction is very fast, it may be simpler to make the assumption of complete reversibility or electrochemical equilibrium at a given potential E. The Nernst equation then applies:

$$E = E^0 - \frac{RT}{nF} \ln\left(\frac{C_{B0}}{C_{A0}}\right) \tag{12}$$

or

$$\frac{C_{A0}}{C_{B0}} = \exp\left[\frac{nF}{RT}\left(E - E^0\right)\right] \tag{13}$$

If the electron transfer is not sufficiently fast, i.e., the standard heterogeneous rate constant k^0 is relatively small, the system is not in

equilibrium and the Nernst equation is not valid. The Butler-Volmer equation for electrochemical kinetics must be used.

A generalized approach to solve the Fick's diffusion equation is to develop the appropriate surface boundary conditions. A set of equations may be written describing it:

$$J_A = 2D_A(C_{A1} - C_{A0}) \tag{14}$$

$$J_A = k_f C_{A0} - k_b C_{B0} \tag{15}$$

$$J_B = 2D_B(C_{B1} - C_{B0}) \tag{16}$$

$$J_B = -J_A \tag{17}$$

$$J_{FAR} = J_A \tag{18}$$

Equations (14) and (16) are representations of the Fick's first law (19).

$$(J)_{x=0} = -D\left(\frac{dC}{dx}\right)_{x=0} \tag{19}$$

Considering the spatial cells near the electrode (**see Fig. 1-2-Space-time grid near the electrode surface**). The distance between the center of the first spatial element and the surface of the electrode is 1/2 δx. The discrete form of Fick's first law becomes

$$J = \frac{-D(C_1 - C_0)}{\frac{1}{2}\delta x} \tag{20}$$

The concentrations expressed in the finite difference equations are

For $i \geq 2$,

$$\Delta C_{i,j} = D^*\left(C_{i-1,j} - 2C_{i,j} + C_{i+1,j}\right) \tag{21}$$

For $i = 1$,

$$\Delta C_{1,j} = D^*\left(C_{2,j} - C_{1,j}\right) - J \tag{22}$$

For $i = 0$, from equation (20),

$$C_{0,j} = C_{1,j} - \frac{J_k \delta x}{2D_k} \tag{23}$$

Evaluation of the flux terms can be done by relatively simple algebraic

manipulations of equations (14) to (18). First, eliminate the surface concentration terms, i.e., from the equation (14) obtain equation (23) and substitute in equation (15). Similarly rearrange equation (16) and substitute in equation (15); Second, rearrange the resulting equations so that the flux terms and their coefficients form the left-hand side of an equation and constants and knowns form the right-hand side;

$$J_A\delta x\left(1+\frac{k_f}{2D_A}\right)-J_B\delta x\left(\frac{k_b}{2D_B}\right)=k_fC_{A1}-k_bC_{B1} \qquad (24)$$

Finally, solve for each flux term using the determinants method.

$$J_A\delta x=\frac{k_fC_{A1}-k_bC_{B1}}{1+\frac{k_f}{2D_A}+\frac{k_b}{2D_B}} \qquad (25)$$

C_{A1} and C_{B1} are the concentrations when i = 1 (i is distance increment). The remaining equations for J_B and J_{FAR} have in fact already been established in equations (17) and (18). They are all that are needed to calculate the flux terms for one-electron transfer.

The flux expression can be incorporated into an expression similar to equation (7). The flux (mol cm^{-2} s^{-1}) is converted to a concentration change by multiplying the appropriate dimensional factors.

$$C_{i,j+1}=C_{i,j}+D\frac{\delta t}{\delta x^2}\left(C_{i-1,j}-C_{i,j}\right)+J\frac{\delta t}{\delta x} \qquad (26)$$

This approach can be extended to two or more consecutive electron transfers. For multi-electron transfer, all heterogeneous reactions must be considered in the surface boundary calculations. It follows the same approach but the results will be more complicated.

For another example of a two-electron transfer process

$A+e^- \Leftrightarrow B$ $\quad k_{f1}$ and k_{b1}

$B+e^- \Leftrightarrow C$ $\quad k_{f2}$ and k_{b2}

The pertinent surface boundary equations are:

$$J_A = 2D_A(C_{A1} - C_{A0}) \tag{27}$$

$$J_A = k_{f1}C_{A0} - k_{b1}C_{B0} \tag{28}$$

$$J_C = 2D_C(C_{C1} - C_{C0}) \tag{29}$$

$$J_C = k_{f2}C_{C0} - k_{b2}C_{B0} \tag{30}$$

$$J_B = 2D_B(C_{B1} - C_{B0}) \tag{31}$$

$$J_B = -J_A - J_C \tag{32}$$

$$J_{FAR} = k_{f1}C_{A0} - k_{b1}C_{B0} + k_{f2}C_{B0} - k_{b2}C_{C0} = J_A - J_C \tag{33}$$

Following the procedure provided in one-electron transfer example, a set of three equations is obtained:

$$J_A\left(1 + \frac{k_{f1}}{2D_A}\right) - J_B\frac{k_{b1}}{2D_B} = k_{f1}C_{A1} - k_{b1}C_{B1} \tag{34}$$

$$J_A = J_B + J_C = 0 \tag{35}$$

$$-J_B\frac{k_{f2}}{2D_B} + J_C\left(1 + \frac{k_{b2}}{2D_C}\right) = k_{b2}C_{C1} - k_{f2}C_{B1} \tag{36}$$

Solving for J_A gives

$$J_A = \frac{k_{f1}C_{A1} - k_{b1}C_{B1} - \frac{k_{b1}}{2D_B}\left(\frac{k_{b2}C_{C1} - k_{f2}C_{B1}}{1 + \frac{k_{b2}}{2D_C} + \frac{k_{f2}}{2D_B}}\right)}{1 + \frac{k_{f1}}{2D_A} + \frac{k_{b1}}{2D_B}\left(\frac{1 + \frac{k_{b2}}{2D_C}}{1 + \frac{k_{b2}}{2D_C} + \frac{k_{f2}}{2D_B}}\right)} \tag{37}$$

Where $\delta x = 1$ here. When $k_{f2} = k_{b2} = 0$, equation (37) reduces to (25). The terms J_B, J_C and J_{FAR} can then be solved.

1-2-2: Electron transfer followed by chemical reactions

Although diffusion and chemical reaction are concurrent processes, in the explicit finite difference method they are calculated separately. This procedure, which is valid if the time increments are small enough, leads to

the possibility of a very general treatment of the chemical kinetic term in equation (2).

There are three approaches to homogeneous chemical kinetics when estimating the extent of reaction in a spatial box during a time increment 1) an analytical solution to the rate equations; 2) a differential approximation; and 3) the modified Euler method.

For example, $A \rightarrow B$, k_{chem}

With differential rate law,

$$\frac{dC_A}{dt} = -k_{chem} C_A \tag{38}$$

The concentration changes during δt,

$$\delta C_A = -\delta C_B = C_A\left[1 - e^{(-k_{chem}\delta t)}\right] \tag{39}$$

Most approaches to digital simulation have used the differential approximation,

$$\delta C_A \approx -k_{chem}\delta t C_A \tag{40}$$

Which is reasonably accurate for small values of $k_{chem} x \delta t$, (≤ 0.1). This means that for large k_{chem}, we have to use a small δt and thus many time increments.

In general, the number of time increments NT required for an accurate simulation is determined by the rate constants of homogeneous reactions. Since the δx is related to δt, δx must also be decreased for simulations involving fast homogeneous chemical reactions.

The modified Euler method makes use of the easily calculable time derivatives to estimate concentration changes and then corrects the derivatives using the new concentrations. Thus, the n^{th} approximation is given by,

$$C_{A,n} = C_{A,0} + \frac{\delta t}{2}\left[\left(\frac{dC_A}{dt}\right)_0 + \left(\frac{dC_A}{dt}\right)_{n-1}\right] \tag{41}$$

This method is equivalent to averaging the rate based on the initial concentrations with rates based on the successive approximations to the concentration after time δt.

Let's go back to the $A \rightarrow B$ example, the n^{th} approximation to the concentration of A is,

$$C_{A,n} = C_{A,0} - \left(\frac{1}{2}\right) k_{chem} \delta t \left(C_{A,0} + C_{A,n-1}\right) \qquad (42)$$

The first iteration is identical with the solution by the differential approximation, but subsequent iterations improve the result to approximate the equation (39).

If the kinetic scheme is the following

$A \rightarrow B$ $\quad k_1$

$B \rightarrow C$ $\quad k_2$

The nth concentrations $C_{a,n}$ and $C_{b,n}$ for A and B respectively are calculated as:

$$C_{A,n} = C_{A,0} - \frac{k_1 \delta t}{2}\left(C_{A,0} + C_{A,n-1}\right) \qquad (43)$$

and

$$C_{B,n} = C_{B,0} + \frac{k_1 \delta t}{2}\left(C_{A,0} + C_{A,n-1}\right) - \frac{k_2 \delta t}{2}\left(C_{B,0} + C_{B,n-1}\right) \qquad (44)$$

More details of analytical solutions for different types for chemical reactions are listed in table (1) and (2) in Gosser and Reiger's paper[3].

Table 1-1 lists the calculation results of the three methods of a simple A $\rightarrow$ B reaction with $C_{A,0}$ = 1.0 mM, δt = 0.5, and k_{chem} = 1.0. The results show that the time increment used for modified Euler solutions to rate equations can be as large as $k_{chem} \times \delta t$ = 0.5 without introducing serious errors. While this method is less efficient than the analytical solution when the latter is available, it can be applied to complex reaction schemes for which analytical solutions are unavailable, and it is used in our program.

1-2-3: Inclusion of non-ideal effects

Charging current and resistance of the solution can affect the electrochemical parameters in the simulation, especially in cases dealing with fast scan rates, non-aqueous solvents, low-temperatures, and microelectrodes[6-7].

The potential E in the Butler-Volmer equation can be corrected for IR drop in a number of ways. In this work, following the method of Boyer et al.[8], the IR term is included by reading an experimental current file and using a measured (or estimated) resistance to calculate IR.

$$E = E_{applied} + IR \tag{45}$$

The capacitance current can be corrected by analytical or numerical solutions.

For CV, $E = E_i + \upsilon t$

$$E = E_R + E_C = IR + \frac{Q}{C} = R\frac{dQ}{dt} + \frac{Q}{C} \tag{46}$$

Q is the charge. Thus, for t = 0, Q = 0, the analytical solution is

$$I_C = \upsilon C + \left[\left(\frac{E_i}{R} - \upsilon C\right)e^{\left(\frac{-t}{RC}\right)}\right] \tag{47}$$

The capacitance and resistance of the solution are easily determined by double potential step experiments in the potential region where there is no Faraday current. The forward step charging current is expressed as,

$$I_C = \frac{\Delta E}{R}e^{\left(\frac{-t}{RC}\right)} \tag{48}$$

and the backward charging current is,

$$I_C = \frac{-\Delta E}{R}\left[1 - e^{\left(\frac{-\tau}{RC}\right)}\right]e^{\left[\frac{-(t-\tau)}{RC}\right]} \tag{49}$$

The capacitive current is calculated by equation (47) as in Boyer's paper[8], by using the potential corrected for IR drop at each time step in the

simulation.

Advanced methods of digital simulations are beyond the scope of my thesis. For further details see listed references[9-10].

1-3: Introduction of simplex optimization

In order to fully exploit the power of digital simulation for the analysis of cyclic voltammograms, it is necessary to have a quantitative method for comparison of experimental and simulated results. A method that lends itself to a general treatment is nonlinear least-squares fitting, in which the parameters of interest (e.g., reduction potentials, heterogeneous or homogeneous rate constants) are varied in a systematic way until a simulation is found that minimizes the least-squares difference between the experimental result and the simulation. Here, we have utilized the simplex method, a robust algorithm for function minimization.

The simplex method was first introduced for experimental optimization. It has been used extensively for mathematical optimization such as the nonlinear regression of data. For example, for an instrument to perform at its best, a procedure that involves adjusting several instrumental parameters until optimum response is obtained; also, when fitting experimental data to a known mathematical model, variables in the theoretical equation(s) are adjusted until calculated values are in close agreement with the experimental values[11-14].

If the variables do not interact with each other, each variable can be optimized independently of the others. In general, however, variables do interact with each other and the one-factor-at-a-time approach will not always result in an optimum set of conditions.

A simplex is a geometric figure defined by the number of points equal

to one more than the number of dimensions of the space. For example, for 2 variables (n = 2), the simplex is a triangle (n + 1 = 3); for 3 variables (n = 3), the simplex is a tetrahedron (n + 1 = 4); etc. The series can be extended to higher dimensions but then simplexes are not easily visualized. The simplex method allows as many variables as you want , but when the variables are more than 5, simplex will become less efficient than other optimization methods, and also the computing time is proportional to the number of variables. Our PC 20 MHz 386 AT computer takes about 1, 3, 6, 8-10 hours to calculate 2, 3, 4, 5 variables in our simulation program.

The modified simplex method by Nelder and Mead has the ability to accelerate the progress of the simplexes and reduces the chance of failure on the ridge. There are 3 operations in the method: reflection, expansion, and contraction. A simple example will be given here to introduce this method instead of listing the rules **(see Fig. 1-3 & 1-4-Simplex procedure)**.

A diffusion coefficient D and a standard rate constant k are the variables in a CV experiment. The simplex has 2 + 1 = 3 points and is composed of P_1 (D_1, k_1), P_2 (D_2, k_2), P_3 (D_3, k_3).

The selection of initial points is important to the result. If the points are too far away from the optimum, the simplex may reach the local optimum of the error surface instead of the global optimum, and the parameter values would be erroneous. There are 3 ways to avoid or judge the local optimum: 1) comparing the simulated graph with the experimental one; 2) running several simulations with different starting values; 3) comparing the sum of square errors with different simulations.

The 3 initial points are input in the simulation program to calculate the theoretical current-potential relationship and the sum of square errors.

$$\chi^2 = \sum_{i=1}^{n} W_i [y_i(\text{meas.}) - y_i(\text{simu.})]^2 \qquad (50)$$

w_i is the weighing factors. In case of constant variance, $w_i = 1$.

The calculated currents and χ^2 of the initial points are shown in **Table 1-2-Potential-current chart with calculation of χ^2**. Comparing the χ^2 values, P_1 is the best, P_3 is the second best, and the P_2 is the worst. So the P_2 is discarded and replaced with its mirror image across the hyperface of the remaining points to the new P_4. This is called reflection.

There are 3 possibilities for P_4:

1) If χ^2 (P_4) < χ^2 (P_1), it means that simplex moves in the right direction. P_4 expands to P_5 which is generally double the distance from the hyperface (the expansion coefficient equals 2).

a) If P_5 is better than P_1 then P_5 is retained;

b) If P_5 is not better than P_1 then P_4 is retained.

This is called expansion.

2) If χ^2 (P_1) < χ^2 (P_4) < χ^2 (P_3) then P_4 is retained.

3) If χ^2 (P_4) > χ^2 (P_3), this means that the simplex moves in a wrong direction and P_4 should move away from this region.

a) If χ^2 (P_4) < χ^2 (P_2) then P_4 is contracted to P_6 which is closer to P_4 than P_2.

b) If χ^2 (P_4) > χ^2 (P_2), that means the direction is totally unsatisfactory, the P_4 is contracted to P_7 which is closer to P_2 than P_4. This is called contraction. (the contraction coefficient usually is 0.5).

Following these rules, the simplex can grow and contract as it moves to search for the optimum. The procedure can be stopped when the χ^2 and/or the fitting variables are smaller than the preset termination criteria.

1-4: Error estimation of the simplex results

In curve fitting by least squares, it is desirable to obtain an estimate of

the errors in the fitted parameters. However, once the simplex algorithm is complete, the estimates of the errors in the parameters have not been determined because the simplex method suffers from the absence of error estimation. This is not a significant problem for experimental optimization. However, when data are fit to theoretical models, the lack of error estimates is a fundamental problem. Analytical results are incomplete without a measure of uncertainty in addition to an estimate for the unknown quantity.

In all electrochemical simulations, the numerical method solves the diffusion equation (with perhaps some extra terms) for unknown concentrations. The current will then be calculated from these concentrations. If the concentrations used are not exact, the calculated current will be in error. Actually when we rewrite the diffusion equation from the differential form to the difference form, errors are introduced by the discrete approximations. (I assume there are no programming errors here, even though it is very possible. Please see next chapter for how to check for program bugs). Obviously, the validity of the simulation will depend on the dimensions of Δx and Δt; as these approach zero, the problem approaches differential form. Making these smaller, however, increases the computational time; therefore, some optimization is required. Roundoff error used to be a serious problem, however, using the extended variable type in Turbo Pascal, which gives a precision of 20 decimal places can reduce the roundoff error to a minimum. The goodness of the simulation result, e.g., the errors in the simulated electrochemical parameters, can be evaluated by error estimation methods.

Most error estimates are derived from the curvature matrix evaluated at the minimum in the error surface[15-17]. Qualitatively, if the curvature with respect to a parameter, θ_i, is small, then χ^2 is relatively insensitive to the variation in that parameter. Therefore, θ_i is not well-defined and will have a

large uncertainty. Conversely, if the curvature is large, that parameter will be well-defined and have a small uncertainty (see Fig. 1-5-χ^2 vs. θ_i curvature graph).

The curvature matrix A, contains the second partial derivatives of χ^2,

$$A_{ij} = \frac{\partial^2 \chi^2}{\partial \theta_i \partial \theta_j} \tag{51}$$

The variance-covariance matrix contains estimates of the errors in the parameters and is given by,

$$\varepsilon = s^2 A^{-1} \tag{52}$$

The quantity s^2 is the mean square error and equals,

$$s^2 = \frac{\chi^2}{(n-k)} \tag{53}$$

n is the number of data points, k is the number of parameters.

The estimated standard deviation in the i^{th} parameter is given by,

$$\sigma_{\theta_i} = \sqrt{\varepsilon_{ii}} \tag{54}$$

Where ε_{ii} is the i^{th} diagonal element of ε.

This suggests that the simplex estimates can be used to calculate partial derivatives and form the curvature matrix. This matrix is then inverted and used to compute the variance-covariance matrix ε. Finally, the errors of the parameters can be calculated from equation (54).

The problem is that the simplex method does not yield any estimate of curvature matrix of second derivatives at the minimum. The following method due to Phillips and Eyring[16] can be used to construct the curvature matrix without the evaluation of derivatives and can solve the simplex problem.

As we mentioned in the last section, the final simplex consists of n + 1 vertices in n dimensional parameter space.

$P_0\,(\theta_{0,1}, \theta_{0,2}, \ldots)$, $P_1\,(\theta_{1,1}, \theta_{1,2}, \ldots)$, $P_2\,(\theta_{2,1}, \theta_{2,2}, \ldots)$, ...

$\chi^2_0 , \chi^2_1 , \chi^2_2 , \cdots$

Where χ^2_0 is the minimum sum of squares error.

A quadratic equation is used to fit the error surface in the vicinity of the final simplex.

$$\chi^2 = \chi_0^2 + \vec{a}^{\,t} Q^{-1} \vec{\Delta} + \vec{\Delta}^{\,t} \left(Q^{-1}\right)^t B Q^{-1} \vec{\Delta} \tag{55}$$

the **a** vector is:

$$a_i = 2\chi^2_{oi} - \frac{\left(\chi_i^2 + 3\chi_0^2\right)}{2} \tag{56}$$

the **B** matrix is:

$$b_{ii} = 2\left(\chi_i^2 + \chi_0^2 - 2\chi^2_{0i}\right) \tag{57}$$

$$b_{ij} = 2\left(\chi_{ij}^2 + \chi_0^2 - \chi^2_{0i} - \chi^2_{0j}\right) \tag{58}$$

the **Q** matrix is:

$$q_{ij} = \vec{\theta}_{j,i} - \vec{\theta}_{j,0} \tag{59}$$

$i = 1,.., k; j = 1,.., k; i \neq j$; θ_{ij} and χ^2_{ij} are half-way points parameters and χ^2. The vector $\vec{\Delta}$, which is related to corrections in q_0, is never actually used. t is the transpose.

The parameter vector corresponding to the minimum of the quadratic equation is

$$\vec{\theta}_{min} = \vec{\theta}_0 - QB^{-1}\vec{a} \tag{60}$$

In order to satisfy the quadratic approximation, the inequality should be less than 1, otherwise the final simplex is so large that the quadratic approximation is not valid. Therefore the curvature matrix will not exist.

$$\vec{a}^{\,t} B^{-1} B^{-1} \vec{a} < 1 \tag{61}$$

If this inequality is not valid, θ_0 is replaced by the θ_{min}, the **a, B, Q** are recalculated, and a new θ_{min} is calculated until the inequality is satisfied.

The curvature matrix is equal to

$$(Q^{-1})^{t} B Q^{-1} \tag{62}$$

The error matrix or variance-covariance matrix is calculated from

$$\varepsilon = s^2 Q B^{-1} Q^{t} \tag{63}$$

and

$$\sigma_{\phi_i} = \sqrt{\varepsilon_{ii}} \tag{64}$$

Phillips and Eyring[16] point out that the convergence criterion can significantly affect the estimated errors unless some precautions are considered: 1) the final simplex can not be too small, otherwise the **B** matrix is largely the result of rounding errors in the calculation of χ^2; 2) the simplex can not be too large, otherwise the quadratic equation is not valid. Using double or higher precision in the calculation can overcome the first problem and using smaller convergence criterion can solve the second problem.

Part 1

Chapter 2: The applications of the simulation program

2-1: Programming and sample programs

Turbo-Pascal from Borland International versions 5 to 7 were used for our programming. Turbo-Pascal is a powerful, integrated applications development package that includes a compiler, an editor, a debugger, and a library manager. We can create highly readable, modular programs that generate fast, efficient executable code. Comparing Turbo-Pascal with FORTRAN, Turbo-Pascal is much easier to use, is almost as efficient, and the price is affordable.

There are two separate programs for doing simplex calculation and error analysis. The simplex calculations of the electrochemical mechanisms are very time consuming for complicated mechanisms. This program is called CVFIT. The CVFIT program quantitatively compares experimental and simulated data by the Nelder-Mead simplex algorithm to minimize the least squares difference between the simulated and experimental voltammograms **(Fig. 2-2 Flow-chart of CVFIT)**. The CV simulation program, named CVSIM **(Fig. 2-1 Flow-chart of CVSIM)**, does the theoretical calculations. The CVFIT program calls the interactive CVSIM once at the beginning, so the user can provide a first guess of the simulation parameters (like E^0, k^0, α, k_{chem}, diffusion coefficient, electrode area, concentrations, etc.). The initial simplex is based on a uniform random distribution centered on the input guesses (see the random program in Appendix 3). CVFIT subsequently repeatedly calls an automated version of CVSIM with new guesses that are provided from the simplex until a best fit is reached within a preset tolerance. If the simulation involves fast chemical reaction(s), the computing time will be much longer because $k_{chem} \times \delta t \leq 0.1$ to 0.5 for stable calculations.

After CVFIT finishes its calculations, another program can be carried out to estimate the errors in the simulated parameters. This program is called EET. Phillips and Eyring's procedure[1], is used in EET in which the error estimate is obtained from a quadratic approximation of the error surface from a simplex minimization (**Fig. 2-3 Flow-chart of EET**). It calls the last set of simplexes (k + 1) and does the calculations. This program also calls CVSIM to calculate the intermediate parameters. EET finishes in minutes, which depends on the CVSIM running time.

Some selected programs presented in Appendices show how the theories we have discussed are converted into computer languages. For details on writing and using the programs, please refer to the book of Gosser[2].

Appendix 1-Program of simplex segment in CVFIT

Appendix 2-Program of EET

Appendix 3-Program of random noise generator

Appendix 4-Program of background subtraction with a straight line

Appendix 5-Program of data addition to 1 mV per point at fast scan rate of BAS-100A

2-2: Test of CVFIT with simulated data

In order to test the correctness of CVFIT program, the easiest way is to fit the simulated data which is generated by CVSIM. The CVSIM program can be tested by comparing the simulated data (peak currents, peak potentials, number of electrons, transfer coefficient, etc.) with the theoretical values.

For reversible electron transfer systems, the E_p and i_p can be calculated from equation (1) and (2):

$$\left|E_p - E_{p/2}\right| = 2.2\frac{RT}{nF} = \frac{56.5mV}{n} \qquad \text{at } 25\,^{o}C \qquad (1)$$

$$I_p = 2.69\times10^{5} n^{\frac{3}{2}} A D_0^{\frac{1}{2}} \upsilon^{\frac{1}{2}} C_0^{*} \qquad (2)$$

For total irreversible electron transfer systems, E_p and i_p can be obtained from equation (3) and (4):

$$\left|E_p - E_{p/2}\right| = 1.857\frac{RT}{\alpha n_a F} = \frac{47.7mV}{\alpha n_a} \qquad (3)$$

$$I_p = 2.99\times10^5 n(\alpha n_a)^{\frac{1}{2}} A D_0^{\frac{1}{2}} \upsilon^{\frac{1}{2}} C_0^* \qquad (4)$$

For E_rC_i (reversible electron transfer with an irreversible following chemical reaction) mechanisms, E_p can be calculated from equation (5):

$$E_p = E_{1/2} - 0.78\frac{RT}{nF} + \frac{RT}{2nF}\ln\lambda \qquad (5)$$

Where

$$\lambda = \frac{k_{chem}\left(\frac{RT}{nF}\right)}{\upsilon} \qquad (6)$$

For mechanisms involving second order chemical reactions, an example of E_rC_i' (catalytic reaction) can be considered for a pseudo-first-order reaction when the concentration of catalyst (Z) is in larger excess than the reactant (O), that is, $C_Z^* >> C_O^*$.

$O + ne^- \Leftrightarrow R$

$R + Z \rightarrow O + Y \qquad k$

All of the curves tend to a limiting value of current i_∞ at sufficiently negative potentials, independent of scan rate υ, given by:

$$I_\infty = nFAC_0^*\left(DkC_z^*\right)^{\frac{1}{2}} \qquad (7)$$

Several different sets of parameters in each category were tested for CVSIM and all the simulated values fall within 99% accuracy of the theoretical values.

CVFIT was tested by using the correct version of CVSIM to generate the data files for different mechanisms plus some random noise. If CVFIT runs correctly, it will return the exact parameters as were input in the CVSIM.

Case 1: E mechanism

$1 + e^- \Leftrightarrow 2$

Table 2-1 Simulation results

Fig. 2-4 Simulation curve of CV

Case 2: EC mechanism

$1 + e^- \Leftrightarrow 2$

$2 \rightarrow 3$

Table 2-2 Simulation results

Fig. 2-5 Simulation curve of CV

2-3: Analysis of cyclic voltammetric data with CVFIT

In order to run the CVFIT successfully, some practical concerning the experiments are critical. First of all, only diffusion processes can be simulated in our program and any mechanism involved adsorption will fail to work. Second, the background current from impurities or charging current should be subtracted from the experimental data. In some cases where the experimental background data are not available, the theoretical approximation can generate similar background data by reading the slope and intercept of the experimental data in the region where there is no Faraday process occurring and then creating a straight line with same number of data points as the experimental data. (See the program in Appendix) Third, the capacitance and resistance of the solution should be measured from double potential step experiments at a potential where no Faraday current This is very important in fast scan experiments (capacitive current is very large) and high solution resistances (low temperatures, in aprotic solvents, microelectrode systems).

Example 1:

The simplest mechanism is the one electron reduction or oxidation of a chemical species at the working electrode surface. Ferricyanide/ferrocyanide is such a standard redox couple in electrochemistry. It bears a single reversible electron transfer between Fe^{3+} and Fe^{2+}. The electron transfer is totally reversible at slow scan rates and only the reduction potential is measurable from the Nernst equation. There is no kinetic information available because the kinetics are so facile and the electrochemical reaction is always under equilibrium. As we know that the reversibility depends on the scan rate ($k^0 > 0.3\upsilon^{1/2}$ cm/sec is reversible or Nernstian system), increasing the scan rate is equivalent to increasing the rate of diffusion. Any system can be reversible, quasi-reversible, or irreversible which will depend on the scan rates. We selected relatively fast scan rates (5 to 15 V/sec) in the simulation tests in order to extract the kinetic parameters.

Experiments were performed with a BAS-100A electrochemical analyzer. The data sets were transferred to a PC-compatible computer. The electrochemical cell utilized a 3-mm diameter glassy carbon working electrode (Area = 0.07 cm^2) and a silver/silver chloride reference electrode. The sample solution was 2.0 mM ferricyanide in 0.30 M potassium chloride, adjusted to pH = 2.0. The uncompensated resistance and capacitance were less than 100 Ω and 17 $\mu F/cm^2$ with the BAS-100A. (The capacitance for most electrodes falls in the range 10 to 20 $\mu F/cm^2$). The BAS-100A does this by assuming an RC circuit and the zero-time current for a potential step is extrapolated for the current decay[3].

The formal reduction potential $E^{0'}$, the heterogeneous rate constant k^0, the transfer coefficient α, and the electrode area A were fitted in the CVFIT program to give the best fit to the cyclic voltammograms of $Fe(CN)_6^{3-}$ at scan rates of 5, 10 and 15 V/sec. (fitting the electrode area will correct the small

error in the concentration and diffusion coefficients). Literature values[4] for the diffusion coefficients of ferricyanide 7.6×10^{-6} cm^2/sec and ferrocyanide 6.3×10^{-6} cm^2/sec, were used in the simulation. Background current was subtracted before the fitting procedure. No IR and capacitive current corrections were used in the simulations because IR was very small and most capacitive current was subtracted from background.

The best-fit simulations are compared with experimental data in **Fig. 2-6** and the best fits are summarized in **Table 2-3**. The results are in line with previous estimates of k^0 and α[5]. Comparing the relative average deviations among the fitted parameters, the $E^{0'}$ is the most precisely calculated parameter with an RAD less than 0.1% and the k^0 is the worst one with an RAD 3.7%.

Example 2:

Methylcobalamin is a member of vitamin B_{12} family. The electrochemical reaction of methylcobalamin in non-aqueous solvent follows an EC mechanism[6]. The experiment was carried out with 2 mM methylcobalamin (Sigma) in 60% methanol (Fisher Scientific) - 40% DMF (Burdick & Jackson), 0.3 M of TBAF (Fisher) as supporting electrolyte, at -30 ^oC. The DMF was dried over type 3A molecular sieves (Alfa). A Ag amalgam working electrode shows the best response to methylcobalamin among the commonly used working electrodes (Au, Pt, C, Hg, Ag and their amalgams) with no adsorption on the electrode surface in the experimental period. The Ag/AgCl reference electrode in ethanol saturated with LiCl (ultrapure grade, Alfa) is useful to -85 ^oC. Pt was the auxiliary electrode. The following chemical rate constant (k_{chem} = 590 sec^{-1}) was determined by double potential step experiment with a 0.25 mm diameter Ag amalgam electrode and a pulse width of 1-2 msec. Background current obtained from a CV

collected in the absence of electroactive species was subtracted from the current collected in the presence of the electroactive species in all simulations. This procedure eliminates the capacitive current and the residual Faraday current from electrolyte and solvent impurities.

It is difficult to determine the formal reduction potential $E^{0'}$ by cyclic voltammetry (CV) for this system because there is no reverse wave at slow scan rates. IR and capacitive current at fast scans cause problems in simulation accuracy. Slow electron transfer also obviates the use of fast scan rates. Using the CVFIT with the predetermined k_{chem} value from double potential experiment gives $E^{0'}$ within a few millivolts.

CVFIT includes the correction of IR and capacitive current. Only IR is corrected in this case because the capacitive current is not significant at slow scan rates in the range 50 to 300 mV/sec, and the majority of it has been subtracted from the background current. The resistance and capacitance are measured in the double potential step experiment. The initial potential was set the same as the one in CV experiment and then a potential step of -50 mV was applied for 1 or 2 msec. There is no Faraday current in this potential range and only the charging current exists. From the equation (48) in Chapter 1, a plot of ln (i_C) vs. time has a slope of $-(RC)^{-1}$ and an intercept ln ($\Delta E/R$). In this way the capacitance and resistance can be measured. R = 1650 Ω was determined and used as a constant in all simulations in this example.

The formal reduction potential $E^{0'}$, the heterogeneous rate constant k^0 and the transfer coefficient α are the fitting variables. The constancy of the fitted parameters for the experiments at three different scan rates provides strong evidence that the values obtained are not spurious or the result from a local minimum (**see Table2-4 and Fig. 2-7**). The fitted parameters have physical meaning[6].

Part 2

The study of artemisinin (Qinghaosu) and other anti-malarial drugs

Chapter 3: Introduction

3-1: History of malaria

Malaria is one of the most widespread parasitic diseases caused by invasion of human body by the protozoan parasites of the class of Plasmodium. It is estimated that about 300 million people are infected and 1-2 million die worldwide every year[1-4].

Malaria is transmitted by the female anopheles mosquito which infects humans with one of four species of parasite, Plasmodium malariae, P. ovale, P. vivax and P. falciparum. Three of them produce the mild forms of malaria by destroying red blood cells in peripheral capillaries and thus causing anemia. The bouts of fever correspond to the reproductive cycle of the parasite. However, the most dangerous is the fourth species, P. falciparum. In this case the infected red blood cells become sticky and form clumps in the capillaries of the deep organs of the body and cause microcirculatory arrest. If this happens in the brain delirium, coma, convulsions, and death may ensue.

Once the role of the mosquito had been established its eradication became the key factor in the control of malaria. The draining of marshes to remove the mosquitoes' habitat is highly effective but too expensive to implement in poor countries. The use of DDT to kill mosquitoes was, at one time, widely practiced but the toxic properties of DDT, its increased cost following the oil crisis of 1974, and the appearance of DDT-resistant mosquitoes have led to the re-emergence of malaria as a major world health problem. To make matters worse, strains of P. falciparum resistant to the principal antimalarial drug chloroquine **(Fig.3-1-a)** and to some of the

prophylactics, have been detected in mosquitoes. Thus drugs can no longer treat all forms of malaria and it now seems unlikely that it will be possible, on a worldwide scale, to eliminate all the habitats of the mosquito by ecologically acceptable means. In the absence of an effective vaccine the only answer seems to be improved drugs for the destruction of the malarial parasite, particularly P. falciparum, while in the human host. In the early 1980s the need for a new antimalarial drug became a matter of great urgency as malaria is, once again, the most important of all tropical diseases.

3-2: History of antimalarial drugs

From time to time, preparations from plants have achieved reputations as cures for the ubiquitous malaria. Some active constituents with diverse chemical structures from plants were reported to have significant antimalarial activity. Most of the compounds that were used as antimalarials have the nitrogen-containing heterocyclic ring system.

The bark of the cinchona tree was used in South America by the indigenous people for the control of fevers. The active principle, quinine, was isolated by Pelletier and Caventou in 1820 and found to be more palatable than the nauseating powdered cinchona bark. The chemical structure of quinine **(Fig. 3-1-b)** was elucidated in 1908 and key steps in its total synthesis were achieved by Woodward and Doering in 1944.

During the 1920s a synthetic quinoline derivative, pamaquin **(Fig. 3-1-c)** was found to be more effective than quinine in killing malarial parasites lodged in the liver. Also mepacrine **(Fig. 3-1-d)** was developed as a synthetic alternative to quinine. Further research led to the production of chloroquine which has fewer side effects and does not turn the patient yellow. Primaquine **(Fig. 3-1-e)** is another quinoline derivative with antimalarial properties

particularly effective against P. viva, the cause of benign tertian fever. A biguanidine compound proguanil (Fig. 3-1-f) also has powerful antimalarial properties but is more generally used as a prophylactic. A pyrimidine derivative, pyrimethamine (Fig. 3-1-g), by itself is used for suppression only. For treatment it is used in combination.

Most drugs for the treatment of malaria are derivatives of quinoline and acridine and, until recently, there was no alternative chemotherapy. Today, the most important are 4-aminoquinolines (e.g. chloroquine), 8-aminoquinolines (e.g. primaquine), dihydrofolate reductase inhibitors (e.g. pyrimethamine), dihydrofolate synthetase inhibitors (e.g. sulfadoxine) as well as quinine[5]. Chloroquine accounts for about 80 to 90% of all antimalarial drugs used in control programs and is probably the third most widely consumed drug in the world after Aspirin and Paracetamol. Unfortunately, since 1960 two alarming trends have become evident. The incidence of P. falciparum is increasing and new strains are evolving which are resistant to chloroquine and its chemical relatives. The sulfadoxine-pyrimethamine combination which is deployed as a second line treatment when chloroquine fails is no longer recommended for prophylaxis because of severe side effects. Consequently, there is an urgent need for new drugs. Fortunately a new lead compound has appeared and early prospects are very promising.

3-3: Artemisinin and its derivatives as antimalarial drugs

An important part of traditional medicine in China is the use of herbs for the treatment of diseases. The classical remedy for malaria in traditional Chinese medicine is the root of Dichroa febrifuga Loureiro (changshan in Chinese). This material was investigated as part of the effort during World War II to find alternatives to quinine. An alkaloid, febrifugine (Fig. 3-1-h),

was extracted from the root and found to be 100 times more effective against P. cynomolgi than quinine. However, even at subtoxic levels, febrifugine is a powerful emetic and this has effectively precluded its general clinical use in the treatment of malaria.

Another traditional cure for fever, first mentioned in the bencao nearly 2000 years ago and many times subsequently, is the herb qinghao (sweet wormwood or annual wormwood), a weedlike plant growing over large parts of China. In Bencao Gangmu it is stated rather concisely that qinghao "can cure malaria, fever and cold". The use of qinghao for the treatment of malaria is also described in 'The Barefoot Doctor's Manual', a manual which did much to improve primary health care in China. It was to this traditional herbal remedy that Chinese scientists turned in an effort to fight the resurgence of malaria.

Extraction of the dried leaves of qinghao with petroleum ether at low temperature and chromatography on silica gel with subsequent recrystallization gave fine, colorless crystals, named qinghaosu (extract of qinghao) in Chinese but also given the Western name artemisinin. The formula $C_{15}H_{22}O_5$ suggested the compound to be a sesquiterpene and reaction with triphenylphosphine to give the phosphine oxide was consistent with the presence of a peroxide group. The lactone ring has a trans configuration. The most unusual feature of the chemical structure is the 1,2,4-trioxane ring which may also be viewed as a bridging peroxide group. Artemisinin is the only known 1,2,4-trioxane occurring in nature, although compounds with peroxide bridges are common, particularly in marine organisms. In extensive clinical trials in China artemisinin showed promise in the treatment of otherwise drug-resistant forms of malaria, notably P. falciparum.

3-4: The properties of artemisinin

Artemisinin (Fig. 3-2-a) was isolated in 1971 from a Chinese herbal remedy which had been used in the treatment of fevers for over 2000 years. Both artemisinin and its derivatives, particularly artemether, the methyl ether of dihydroartemisinin (Fig. 3-2-b), have been widely used in Asia where over 2 million doses have been given in China alone. Other artemisinin derivatives are currently undergoing Phase I and Phase II clinical testing[6].

The structure of this interesting sesquiterpene lactone endoperoxide has been fully confirmed by various methods. The most interesting aspect of artemisinin's chemistry is the stability of the peroxide bridge. Artemisinin is labile to acidic or basic treatment, but unexpectedly stable in neutral solvents heated up to 150 ^{0}C. Artemisinin is unaffected by heating for about 2.5 min at 200 ^{0}C, i.e. about 50 ^{0}C above its melting point. Artemisinin is poorly soluble in water (0.46 mg/ml at 37 ^{0}C) and but soluble in most aprotic solvents. This unusual compound has a peroxide grouping but lacks a nitrogen containing heterocyclic ring system which is found in most antimalarial compounds.

The absolute configuration has also been ascertained as the trans configuration of the lactone ring. X-ray analysis of artemisinin showed that all the five oxygen atoms present in it are crowded on the same side of the molecule, and all the carbon-oxygen bond distances lying well within the ranges of a normal single bond or a partial double bond. Probably, the lone pair of electrons of oxygen are no longer confined only on the oxygen atom and a variation of bond type has occurred. This may tend to make the entire molecule more stable[7].

FTIR and Raman spectra of artemisinin

Both IR and Raman spectra can provide structural information about molecules. The IR spectrum of solid artemisinin shows an intense peak at 1745 cm^{-1} (δ-lactone) and peaks at 831, 881, 1115 cm^{-1} (peroxide) The IR spectrum of artemisinin in aqueous solution is not available because of the strong absorption of water.

Raman spectroscopy is a suitable method for use in investigating biochemical problems, largely because the study of molecules in their normal environment--aqueous solutions of low concentration--is possible. This is not so in the case of infrared spectra because of the strong absorption bands of water.

The Raman and infrared spectra show clearly their complementary nature. The O-O grouping in peroxides, peracids, and peresters gives rise to a strong Raman band (stretching vibrations) in the range 700-900 cm^{-1} (the υ(O-O) in the region 900-845 cm^{-1} and the intensity is strong (s)[17-19]).

UV-VIS *spectra of hemin*

Hemin and heme show different maximum absorbances. The oxidized form occurs at 404 nm while that of the reduced form is at 424 nm in DMSO.

There is no absorption peak in artemisinin from UV-VIS because there are no unsaturated bonds in the structure.

3-5: Synthetic antimalarial drugs

The combination of interesting biological activity, novel chemical structure and low yield of artemisinin from natural sources prompted the scientists all over the world to search for new synthetic routes of artemisinin and related compounds. The first total syntheses of artemisinin were reported by Schimd and Hofheinz[8] and Zhou et al[9].

The demand for the antimalarial drug to combat malaria infected with P. vivax and P. falciparum exceeds the potential supply from plant source and synthesis of artemisinin. Thus the search for other antimalarial drugs related to the artemisinin is being continued vigorously. It is found that a necessary requirement for potent antimalarial activity is the cyclic peroxide linkage found in artemisinin, but the peroxide linkage alone is insufficient for activity. Some of the trioxanes synthesized by Jefford et al[10] were tested for antimalarial activity (against the sensitive N-strains of P. berghei in mice) and found to be moderately active in comparison to artemisinin and dihydroartemisinin. The general lack of high activity indicates that the 1,2,4-trioxane ring system alone is not sufficient for antimalarial activity.

In most cases the trioxane ring has been formed by addition of singlet oxygen to an olefin in the presence of a photosensitizer followed by protonation and reaction with a carbonyl compound **(Fig. 3-3 The formation of trioxane ring scheme)**. This approach to the synthesis of trioxanes has been fully explored by Jefford and his co-workers[11-15].

3-6: Hemin and its catalysis by artemisinin and peroxide compounds

Artemisinin's antimalarial activity has been shown to be mediated by activated oxygen (i.e., superoxide, hydrogen peroxide, and/or hydroxyl radicals)[16]. Evidence has been found that the malarial parasites are rich in hemin which is derived from the digestion of host hemoglobin. Artemisinin may react with hemin within the parasite to generate toxic activated oxygen byproducts. The reaction between artemisinin and hemin, when carried out in the presence of red cell membranes, leads to the oxidation of protein thiols. Artemisinin's reactivity toward hemin may explain its selective toxicity to malarial parasites.

Hemin (Fig. 3-2-c) has been known for a long time as a catalyst of peroxide compounds. Study of the catalysis of hemin to artemisinin and its derivatives can help us to understand the reaction mechanism of artemisinin in the treatment of malaria.

Part 2

Chapter 4: Electrochemical study of artemisinin and its derivatives

4-1: Introduction

Many reactions involve electron transfer. The intraparasitic hemin may mediate the antimalarial activity of artemisinin and its derivatives by generating organic free radicals. In this reaction, electron(s) may transfer from reduced hemin to artemisinin and break down the oxygen-oxygen bridging bond. Electrochemistry is a very useful tool for this study. It can tell us what is the redox potential of artemisinin and can provide kinetic information, i.e., the number of electrons involved in the reduction, the electron transfer rate constant, the following chemical rate constant, etc.

4-2: Experimental section

Solution of bovine hemin also named chloroprotoporphyrin IX iron(III), FW 651.96, (Sigma Chemical Co., St. Louis, MO) were first prepared in a small volume of 0.25 M NaOH (<10%). Different portions of dehydrated ethanol (AAPER Alcohol and Chemical Co., Shelbyville, KY) and aqueous buffers were added daily. Hemin solutions aggregate after about a week. Tris-hydroxymethyl aminomethane (TRIS), $(HOCH_2)_3CNH_2$, FW 121.14, 99.9+%, ultra-pure grade was from Aldrich and Sigma. Phosphate-buffered saline (PBS), pH=7.2, was also purchased from Aldrich Chemical Co., Milwaukee, WI. Artemisinin, FW 282.34, from Aldrich Chemical Co. was first dissolved in various volumes of ethanol and then diluted with aqueous buffers. Because the TRIS buffer has a very large resistance, 0.1-0.2 M NaCl or KCl was added to the buffer. TBAP (tetrabutylammonium perchlorate) was obtained from Sigma (St. Louis, MO). All aqueous solutions were made from deionized-distilled water which was passed through a carbon filter, a

multiple-ion exchange system, and then is distilled.

Electrochemical experiments were performed using a BAS-100A electrochemical analyzer (BAS) and a home built instrument[1]. Potentials were measured vs. a Ag/AgCl (sat. KCl) reference electrode.

The experimental results were transferred to a PC-XT computer, then converted and analyzed. The electrochemical cell (5 to 10 ml capacity) contained a working electrode, a Ag/ AgCl with saturated KCl reference electrode and a Pt wire, 99.95% pure, 0.64 mm in diameter (Fisher Scientific Co., Springfield, NJ) as the auxiliary electrode. The working electrodes were polished to a bright surface with 0.05-μm Micropolish II alumina powder (Buehler Ltd., Lake Bluff, IL) at the beginning of each experiment and then washed with distilled-deionized water to remove any trace of alumina. All solutions were degassed with prepurified nitrogen for 10 to 15 minutes before taking data. Experiments were conducted at room temperature (ca. 25 ^{0}C).

Various working electrodes were used. They were obtained from BAS (Bioanalytical Systems, Inc.), Cypress Cypress Systems, Inc., (P.O. Box 3931, 2500 West 31st Street, Suite D, Lawrence, Kansas 66047) and some were home made. Microelectrodes were obtained from BAS and Cypress system. Cypress microelectrodes (glassy carbon, gold, and platinum) are 10 μm in diameter. The BAS glassy carbon microelectrode is 33 μm in diameter and the silver microelectrode is 25 μm in diameter. BAS minielectrodes (silver, platinum, gold) are 1.6 mm in diameter and the glassy carbon electrode is 3 mm in diameter. All Cypress minielectrodes are 1 mm in diameter. Several different sizes of silver electrodes (250 and 500 μm in diameters) made in our lab were used in the double potential step and differential pulse experiments.

4-3: Results and discussion

4-3-1: Results of cyclic voltammetry (CV) on carbon electrode

Cyclic voltammetry is perhaps most widely used by chemists as a method to determine the standard reduction potential of a redox couple, E^0. Actually, CV can provide information not only on the thermodynamics of redox processes but also on the kinetics of heterogeneous electron transfer reactions and coupled chemical reactions. The characteristic shapes of the voltammetric waves and their unequivocal position on the potential scale virtually fingerprint the individual electrochemical properties of redox systems.

Different electrode materials show different responses to artemisinin with CV. Among the commonly used electrodes, glassy carbon and carbon paste electrodes show similar responses[2]. Silver electrode shows a very nice cyclic voltammogram of artemisinin which is significantly different from that using carbon electrodes. Other metallic electrodes, i.e., Pt, Au, Hg and amalgam electrodes have poor CV responses to artemisinin and were not further considered in this project.

Reduction of artemisinin and dihydroartemisinin:

In 40/60 of ethanol/PBS (v/v) with a glassy carbon electrode, 1 mM artemisinin showed a reduction peak at potentials from -0.873 V to -1.054 V at scan rates from 0.03 V/s to 5 V/s. No reverse oxidation peak was obtained at any scan rate, indicating an irreversible chemical reaction following the reduction which is faster than the time scale of the experiment. Dihydroartemisinin showed a similar irreversible reduction, but the peak potential was 50-100 mV more negative than artemisinin. **(Fig. 4-1 & Fig. 4-2 show both the CV of artemisinin and dihydroartemisinin).** The cyclic voltammograms of both artemisinin and dihydroartemisinin with

background subtraction showed a diffusion process. For comparison, 1 mM hydrogen peroxide in PBS buffer showed a well defined irreversible diffusion controlled reduction peak from -1.015 to -1.332 V at the same scan rate range as above. This reduction of hydrogen peroxide had been well studied and assigned as a two-electron reduction process corresponding to the reduction of hydrogen peroxide to oxygen[3-4].

Artemisinin (Qinghaosu) showed an irreversible reduction peak at ca. -1.2 V in the 85/15 ethanol/TRIS solvent. As we will show later, higher proportion of water favor the reduction at this potential. Because some of the synthetic drugs are insoluble in solvent mixture containing more than 15% aqueous, the 85/15 ratio is the best we can do to dissolve them. The normalized reduction peak height became less with increasing scan rate which indicates that this is a slow electron transfer process.

Reduction of hemin:

1 mM of hemin solution (pH = 7-8) showed a reversible reduction peak at potential from -0.38 to -0.39 V at scan rates from 0.03 V/s to 5 V/s on the glassy carbon electrode. The reduction and oxidation peaks occurred at nearly the same potential, indicative of reversible reduction of an adsorbed species **(Fig. 4-3 CV of hemin)** . A linear relationship between the reduction peak current and the scan rate was further evidence for the reduction of adsorbed species on the electrode surface.

The change in reversibility of the hemin redox peaks is a very significant indicator of reactions between the antimalarial drugs and hemin. In chapter 5, I will describe the change in the hemin's reversible oxidation peak when it is mixed with various synthetic drugs in the electrode solution, which can tell us whether the drugs are active or not. I will demonstrate that

the biologically active drugs react with hemin (or be catalyzed by) and show an irreversible peak at -0.38 V at relative slow scan rates (less than 10 V/s). The non-active drugs show a reversible peak at -0.38 V at all scan rates from 0.1 V/s to 50 V/s or faster, just like the pure hemin solution itself.

Reductions of artemisinin and dihydroartemisinin in the presence of hemin

The reduction peak of artemisinin (1 mM) at around -1.0 V completely disappeared in the presence of hemin at concentration of 10^{-5} M or higher, and a new reduction peak appeared at -0.435 to -0.460 V close to the same peak current as the original peak in 40/60 of ethanol/PBS solution (**Fig. 4-4 CV of artemisinin with hemin at 1 mM**).

When the concentration of hemin was between $5x10^{-8}$ and $1x10^{-5}$ M, the new peak current was larger at slow scan rates (< 0.3 V/s) than at fast scan rates (> 0.3 V/s) and the peak potential shifted to the positive potentials with increasing concentration of hemin.

Comparing the new reduction peak and the artemisinin reduction peak with hemin concentrations below $1x10^{-5}$ M, the two reduction processes compete with each other which can be seen from the CV at different scan rates. When the scan rate was fast (5 V/s), the reduction process corresponding to the new peak was not as fast as the scan rate, so artemisinin has reacted only partially with heme (assuming the reduction of hemin to heme is extremely fast) and the artemisinin left on the electrode gave a clear reduction peak. When scan rate was slow (0.03 V/s), all artemisinin on the electrode reacted with adsorbed heme and in the mean time there was enough time for artemisinin to diffuse from the bulk solution to the electrode surface. This CV again showed a clear artemisinin peak with a more significant peak at . When the scan rate was equivalent to the diffusion rate of

artemisinin (0.7 V/s), the artemisinin peak totally disappeared at hemin concentrations as low as $2x10^{-7}$ M. **(Fig. 4-5 show 3 CV at different scan rates).**

For hemin concentrations above $1x10^{-5}$ M in the 1 mM artemisinin solution, the artemisinin reduction peak was totally lost and only the new peak was left. This means that all artemisinin reacted with adsorbed heme on the electrode surface and there may be more hemin adsorbed on the electrode. The new peak was more significant at slow scan rates (< 0.3 V/s), because a slow scan rate (or long time) allows artemisinin to diffuse from bulk solution to the electrode surface and react with extra surface heme. Another way to explain this is that the regeneration of the heme catalyst after the catalysis of the artemisinin reaction can react with more artemisinin if the reaction rate is fast enough to catch the scan rate.

From the cyclic voltammetric study of the reaction of hemin and artemisinin, I can qualitatively conclude that the reduction of artemisinin and the reduction of hemin-artemisinin product are both not very fast.

Because the reduction peak potentials of adsorbed hemin and the new peak are separated by only 0.1 V, the observed peak results from a combination of the two. The contribution in the new peak from the adsorbed hemin can be identified in the cyclic voltammogram from the growing oxidation peak at -0.30 to -0.40 V when the concentration of hemin increases. When the concentration ratio of artemisinin to hemin is large (>100 to 1000), the interference from hemin is negligible.

The new peak occurred at very low concentration of hemins. It began to show up clearly, especially at slow scan rates, when the concentration of hemin was just $5x10^{-8}$ M **(Fig. 4-6 shows CV of artemisinin with $5x10^{-8}$ M hemin)**. A 50 nM concentration is far below the detection limit of cyclic voltammetry, so the new peak can not be from hemin itself. Because the

concentration ratio of artemisinin to hemin is so large (10^2-$2x10^4$), stoichiometric reaction is unlikely. We assume the new peak is a catalytic peak. Another possibility is that the very low concentration of hemin adsorbs on the electrode surface and accumulates to give high surface coverage which is capable of reacting with artemisinin and forming a hemin-artemisinin adduct[5].

As the concentration of hemin increased, the new peak current continued to increase (Fig. 4-7) and the peak potential shifted to the positive direction. The non-catalytic reduction peak of artemisinin decreased as the hemin concentration increased. The catalytic peak was maximized and the non-catalytic peak disappeared when hemin reached a concentration of $1x10^{-5}$ M.

The new peak potentials shift in the positive direction when the hemin concentration is increased, as predicted by Brdicka for a typical catalysis process[6-7].

When the concentration of hemin was held constant at $1x10^{-4}$ M and the concentration of artemisinin is increased from $1.2x10^{-4}$ M to $1.6x10^{-3}$ M, the new peak current was linearly proportional to the concentration of artemisinin, providing further evidence that hemin is indeed a catalyst for the reduction of artemisinin.

Similar results were obtained for the reduction of dihydroartemisinin in the presence of hemin (**Fig. 4-8 shows CV of dihydroartemisinin with 1 mM hemin**). As for the artemisinin, the dihydroartemisinin catalytic peak current reached its maximum and the non-catalytic peak disappeared when the concentration of hemin was above $1x10^{-5}$ M.

No catalysis of artemisinin by Fe^{3+} and other porphyrins

The reduction of artemisinin (1 mM) was studied in the presence of ferric sulfate. There was no catalysis shown for concentrations of ferric sulfate ranging from $2x10^{-7}$ M to $2.2x10^{-4}$ M.

Meso-tetra-4-sulfonatophenyl-porphine dihydrochloride (MTPD), F.W. 1007.69, (Porphyrin Products, Inc., Utah) (no iron in the molecule) mixed in different proportions ($5x10^{-8}$ M to $1.8x10^{-6}$ M of MTPD) with 5 mM artemisinin in 1 mM SDS (sodium dodecyl sulfate, electrophoresis grade, from Eastman Kodak Co., Rochester, NY) and 0.1 M NaCl showed no new reduction peak except the reduction peak of artemisinin at ca. -1.0 V.

0.224 mM of Fe meso-tetra-4-sulfonatophenyl-porphine chloride (Fe-T), (acid form), F.W. 1026.07, in PBS showed a reversible peak at -0.25 V. The reduction peak moved to negative potential with increasing of the scan rates. Adding Fe-T (2.36 mM) into artemisinin (1.15 mM) in a 50/50 of acetonitrile/PBS solvent, there was no catalytic peak. In the same solvent, 1 mM artemisinin had a reduction peak at -1.1 V to -1.2 V at scan rates 0.05 V/sec to 0.5 V/sec. Addition of 0.56 mM of hemin into the 1 mM artemisinin produced a catalytic reduction at -0.46 V to -0.5 V and the -1.1 V peak totally disappeared.

The reasons for not observing a catalytic peak in these three cases can be explained. First of all, iron is a critical part of the catalysis molecules; and second, the adsorption of the catalyst on the electrode surface is important. In non-iron porphyrin, there is no reduction of Fe(III) to Fe(II) with inorganic Fe(III) salts and water is soluble synthetic porphyrin Fe-T, there is no adsorbed species on the electrode surface. The reduced species may diffuse back into solution and the Fe(II) and artemisinin may not have the chance to react with each other.

4-3-2: Results of cyclic voltammetry on silver electrode

The cyclic voltammogram of artemisinin on silver is different from that on a carbon electrode. Artemisinin (1 mM to 5 mM) in 40/60 of ethanol/TRIS with a 1.6 mm diameter Ag electrode gave an irreversible reduction peak at -0.645 to -0.697 V in the scan rate range from 0.1 V/s to 1 V/s. It is a diffusion controlled process **(Fig. 4-9 CV of artemisinin on Ag electrode)**. With the same the electrode in same solvent, hemin ($2x10^{-4}$ M) had a reversible redox peak with standard potential at ca. -0.5 V. It is again a diffusion controlled process **(Fig. 4-10 CV of hemin)**. On mixing the hemin with 1 mM artemisinin, there was no new peak such as was observed on a glassy carbon electrode. The artemisinin peak totally disappeared and the cyclic voltammogram of the mixture was almost the same as that of pure hemin solution. **(Fig. 4-11 shows CV of artemisinin in the presence of hemin).**

The difference on Ag and carbon electrodes can be explained as follows. First, the hemin is not adsorbed on the Ag electrode, so the possibility of the catalysis is small for a concentration ratio of hemin to artemisinin less than 0.01; Second, the Ag itself seems to catalyze the reduction of artemisinin, we can see the reduction peak potential on Ag is 0.3 V or more positive to that on glassy carbon.

Comparing the cyclic voltammograms of artemisinin on Ag and carbon electrodes, we can see that the quality of the voltammogram on Ag electrode is much better than that on carbon because the reduction peak on carbon is near the potential scanning limit and the background current is very large. The well defined reduction peak of artemisinin on Ag with very little background current can provide good quantitative information.

The differential pulse voltammetry (DPV) on Ag a electrode provides a

good technique for the quantitative determination of artemisinin. In theory the detection limit of DPV is 10-20 ng/ml, It is superior to other analytical methods because of the ease of sample preparation and the lack of interferences from the background.

A wide variety of chromatographic techniques and approaches could be utilized to obtain a specific and sensitive measurement of artemisinin and its synthetic derivatives, but they require selective extraction and cleanup before the analytical measurement can be made.

The distinct advantage of differential pulse voltammetry over cyclic voltammetry is the discrimination against capacitive charging currents which can enhance its sensitivity by several orders. DPV is a fast, sensitive, accurate and relatively inexpensive analytical method which can be used in the routine work.

4-3-3: Solvent and pH effects on the reduction of artemisinin

It has been reported that artemisinin is very stable in neutral solvents but is labile in acids and bases. Artemisinin is slightly soluble in water but is soluble in most aprotic solvents. Artemisinin is very stable in ethanol and was unaffected for months when it was kept at 4 ^{0}C. Is there any solvent effect for the reduction of artemisinin? Can we see the decomposition of artemisinin in different pH value from CV?

When 1 mM artemisinin was dissolved in 100% dehydrated ethanol with 0.1 M of TBAP (non-buffer) electrolyte (pH=6.0), a electrochemical reduction at ca. -1.5 V was shown which became more negative at relatively faster scan rates (>500 mV/sec). The potential limit can reach -2.5 V in this medium. When water is added to the ethanol solution for make a 20% (v/v) water solution, there are two reduction peaks, one was at ca. -1.4 V (which is

the same one in pure ethanol but peak position is changed) and another at -1.1 V. The -1.4 V peak was smaller than in the pure ethanol solution. In a 40% water solution (pH 5.85), there are two reduction peaks at relatively slow scan rates (<500 mV/sec) and the -1.1 V peak dominated at relatively fast scan rates. With higher proportions of mixed solvent aqueous, only the -1.1 V reduction peak showed up but the peak height was smaller because artemisinin was not totally soluble. **(Fig. 4-12 CV of artemisinin with different solvents)**

In most experiments, I observed the peak at ca. -1.1 V in different ethanol/aqueous buffer solutions.

The peak heights in pure ethanol solution (only -1.4 V peak) and in 40/60 water/ethanol solution (only -1.1 V peak at 500 mV/sec or faster) are compatible which tells us that the number of electrons involved in the -1.1 V and -1.4 V reductions are the same.

How do I explain this? It is possible that there are two electrons involved overall. In the first reduction, artemisinin adds one electron to forms a radical anion. Then, another electron can be added to the radical anion to form an anion with -2 charge. Because the repulsion by the radical anion of the electron, the second reduction is more difficult than the first one and the reduction potential is more negative. Because the potential scanning limit in aqueous ethanol is much smaller than in pure ethanol, the second reduction may not be seen in the aqueous ethanol solutions. However, we are more interested in the first reduction of artemisinin anyway.

Another possibility is that the two reduction peaks of artemisinin come from a one electron transfer process but one needs water to assist the reduction at (-1.1 V) but not that at (-1.4 V).

From the other experiments I will describe in next section, I will prove

that the reduction peak of artemisinin at -1.1 V is a one electron transfer process.

The effect of pH was tested using 1 mM artemisinin in 40/60 ethanol/PBS solvent. The original solution had pH 8.61 and had a reduction peak at -1.1 V. Reducing the pH to 4.86 and then increasing to 9.68 by adding HCl or NaOH, there was peak current almost no significant change in the peak potential in the reduction peak. For pH > 11.00, the peak height gradually decreased. For pH < 2, there was a reduction of the proton ($2H^+ + 2e^- \rightarrow H_2$) at peak potential of -1.2 V which was slightly more negative than the artemisinin reduction peak. Because the peak current for proton reduction at this pH was so larger compared to that of artemisinin (concentration ratio of proton to artemisinin is 10 to 100), there is no way to see the artemisinin peak at pH less than 2.0. **(Fig. 4-13 CV of artemisinin at different pH)**

The effect of pH was also tested in 1 mM artemisinin plus 10^{-6} M hemin. The catalytic peak at ca. -0.5 V decreased at the pH was gradually increased to 12.90. Reducing the pH to 7.04, the peak at -0.5 V was much smaller than in the beginning. Adding HCl to bring the pH to 5.13, the peak was totally gone at all scan rates. This indicates that strong base destroys the artemisinin and the decomposition of artemisinin is irreversible. Hemin is not soluble in pH < 5 solution.

In order to prevent the decomposition of artemisinin, the pH was maintained between 6 to 8 in the ethanol/aqueous buffer mixtures There was no difference in cyclic voltammograms using different aqueous buffers (PBS, TRIS and various portions in ethanol).

4-3-4: Evaluation of the electrochemical parameters

The electrochemical parameters (formal reduction potential, heterogeneous rate constant, homogeneous rate constant, transfer coefficient, and number of electrons, etc.) can be determined by various electrochemical methods. Double potential step experiments can provide information on the homogenous rate constant, especially for fast following chemical reactions. Cyclic voltammetry can provide both thermodynamic and kinetic information.

A knowledge of the number of electrons associated with an electrode reaction is essential to the analysis of kinetic data. For an irreversible system, there are two types of electrons involved, one is the number of electron(s) in the rate determination step and another is the total number of electron(s). The two may be the same or may not be.

The number of electrons in the rate determining step (n_a) of the reduction of artemisinin has been tested carefully by cyclic voltammetry[8]. For the irreversible diffusion process

$$E_p = \text{constant} - \frac{RT}{2\alpha n_a F} \ln \upsilon \qquad (1)$$

The slope S_E of E_p against log (υ) is

$$S_E = \frac{-0.059}{2\alpha n_a} \qquad (2)$$

The αn_a is available from S_E data. The data in table 4-1 shows that the $n_a = 1$ and $\alpha = 0.3$ to 0.4, which is slightly dependent on the nature of solvent. ($n_a = 2$ is not likely because the $\alpha < 0.2$ is rare). A value of $\alpha < 0.5$ indicates that the structure of the transition state for reduction is close to the product[1,9], and it suggests that the O-O single bond in artemisinin is broken in the transition state. **Table 4-1** lists the results which proved the CV experimental results in last section.

The total number of electrons (n) may be different from the number of

electrons in the rate determined step (n_a) for an irreversible reduction process. There are several ways to determine n.

Controlled-potential bulk electrolysis (BE) with coulometry can be used to determine the total number of electrons involved in the redox reaction[10-12]. When the electrolysis of the sample is 100% complete, the total charge is used to calculate the amount of material electrolyzed or the number of electrons transferred per molecule by means of Faraday's law

$$Q = nFN = nFCV \qquad (3)$$

Where Q is charge, N is number of moles, V is volume of solution, C is molarity.

However, this method is time consuming and also yields incorrect results when electron transfer is followed by a catalytic reaction or disproportionation. Thin-layer bulk electrolysis with coulometry has also been developed[13-14]. The advantages of the thin-layer cell are the shorter time required and elimination of side-reaction. Problems with IR drop and reaction with the solvent make the use of such a system difficult in nonaqueous media.

Reticulated vitreous carbon (RVC), 100 ppi, a form of glass-like carbon[15-17]; Ag, Pt bulk electrodes (in shapes of rod or plate); and GC, Au, Ag thin layer cells were tested by coulometric methods. Both regular BE and thin-layer BE experiments failed to work on artemisinin with all of the electrodes mentioned. (They worked very well on ferricyanide). The reason for this is the reduction product(s) of artemisinin are re-reduced on the electrodes during the long time scale which causes the BE to be continuous.

Another method reported by Baranski et al[18] shows the potential possibility of determining the total number of electrons in the reduction of artemisinin in seconds. The method involves comparing the parameters of

current against time transients at a microelectrode[19-30] and at a normal size electrode (diameter in millimeters) in the solution on the basis of chronoamperometric (double potential step) experiments.

The current in chronoamperometry at a microelectrode is composed of

$$I = I_p + I_s \tag{4}$$

Where I_p is the planar component and I_s is the spherical one. At times greater than 10 sec. after the potential step, I_p is negligible and the current reaches a steady-state value given by the spherical component

$$I_\infty = I_s = 4mFCD \tag{5}$$

The values of n and D (diffusion coefficient) may be determined separately by employing a technique which relates these parameters in a different way. When a normal size electrode (diameter in millimeters) is used, the current after a potential step to a diffusion controlled process is given by the Cottrell equation

$$I = \frac{nFAD^{1/2}C}{\pi^{1/2}t^{1/2}} \tag{6}$$

The slope S of the plot of I against $t^{-1/2}$ is

$$S = \frac{nFAD^{1/2}C}{\pi^{1/2}} \tag{7}$$

Combining the I_s and S equations, the n and D are determined.

$$D = \frac{1}{\pi} \times \left[\frac{I_s A}{4rS}\right]^2 \tag{8}$$

$$n = \frac{4\pi rS^2}{FCA^2 I_s} \tag{9}$$

The time scale of the chronoamperometry for both electrodes is ca. 10-20 sec. It may be still too long on the millimeter of diameter electrode in the artemisinin case because of the re-reduction of the reduction products. (This is not a serious problem of the microelectrode because the amount of electrolyzed product(s) on the microelectrode are negligible).

CV experiments at different scan rates may be another option. The time

scale of the CV experiments is much less than that of the potential step experiments. For the irreversible system

$$I_p = (2.99\times10^5)n(\alpha n_a)^{1/2}ACD^{1/2}\upsilon^{1/2} \quad (10)$$

The slope S_i of I_p against $\upsilon^{1/2}$ is

$$S_i = (2.99\times10^5)nACD^{1/2}(\alpha n_a)^{1/2} \quad (11)$$

The αn_a was determined by the same CV experiments from S_E (Eq. 2). By combining the S_i and i_s equations, we can get n and D.

$$D = \alpha n_a\left(\frac{2.99\times10^5 I_- A}{4rFS_i}\right)^2 \quad (12)$$

$$n = \frac{4rFS_i^2}{8.94\times10^{10} I_-(\alpha n_a)CA^2} \quad (13)$$

The results from the double potential step experiment are listed in Table 4-2 which shows that n=1 in experiments with GC electrodes.

The following chemical rate constant k_{chem} in the reduction of artemisinin was tested by double potential step experiments on both the BAS-100A and an in-house instrument. The BAS-100A has a time scale limit of 1 msec with 0.1 msec resolution[31]. By estimating, $k_{chem} \times t = \ln(2) = 0.693$, $t = t_{1/2}$ for the first order reaction[32-34], $k_{chem} = 690\ sec^{-1}$ with this instrument is the limit. Our in-house instrument has a time scale limit of 20 μsec, which can give $k_{chem} = 35{,}000\ sec^{-1}$, but in most cases, 50 μsec is the actual limit because of the AC noise, thus, $k_{chem} = 14{,}000\ sec^{-1}$ is the best we can get. The time scale should be t = (3-10) RC of the microelectrode and the concentration of the chemical species should be relatively high (10 mM or higher) in order to get a good S/N ratio[35].

Comparing the experimental data and the simulated data, there is no match between the 1 msec and 50 μsec time scale. The total current is mainly from the charging current. So the $k_{chem} > 14{,}000\ sec^{-1}$ at room temperature. The exact value is not available from our instrument.

The reason why the following chemical rate is so fast after the reduction of artemisinin is discussed by several authors[36].

Electron transfer to molecules is very often accompanied by the breaking of an existing bond and/or the formation of a new bond. The main factor governing the thermodynamics and kinetics of the reductive cleavage is the dissociation energy of the bond that is broken. The electron transfer and bond breaking process can be stepwise or concerted which is a function of the π^* orbital energy to the acceptance of the incoming electron. In the stepwise case, the anion radical is an intermediate, whereas, in the concerted case, the energy of the anion radical is so high that the concerted pathway is energetically more advantageous.

When bond breaking and electron transfer are successive steps, two limiting situations may arise according to which is the rate determining step. If the rate determining step is the bond breaking reaction, the electron transfer step interferes in the overall kinetics solely through its thermodynamic characteristics. If electron transfer is rate determining, the dynamics of the overall reaction is that of an outer-sphere electron transfer.

In the case of a concerted process, the electron transfer possesses an inner-sphere character.

The slope of E_p vs. log(υ) is ca. 30-50 mV and the $E_{p/2}$-E_p = 65 mV typically for an EC reaction scheme with a mixed kinetic control by the E and C steps.

The slope of E_p vs. log(υ) which is much larger (100 mV) indicates that the reduction is governed by the kinetics of an electron transfer step and not, even partly, by that of a follow-up chemical step. In addition to this, the transfer coefficient of the rate-controlling electron transfer step is distinctly lower than 0.5 (ca. 0.3) indicating a situation in which the reduction potential

is clearly negative to the standard potential characterizing the electron transfer rate determining step. This reductive cleavage follows a concerted mechanism.

From the results in **Table 4-3**, the reduction of artemisinin is the rate determining step (α=0.2-0.4 and slope>50 mV on glassy carbon) and the following chemical reaction is much faster than the electron transfer reaction. In artemisinin, the carbon-oxygen distances are close to that in the ground state, the σ^* orbital energy is so high that concerted electron transfer-bond breaking is energetically more favorable. This reason makes it difficult or impossible to measure the chemical rate constant.

Part 2

Chapter 5: Preliminary study of the synthetic trioxane type antimalarial drugs

5-1: Introduction

A variety of endoperoxide-containing compounds are potent antimalarial agents. The study of the reaction mechanism of these compounds may help in the synthesis of more effective antimalarial endoperoxides[1-7].

Cyclic voltammetry has been used to demonstrate hemin's effects on the reductive decomposition of artemisinin[8]. In this chapter, I will use cyclic voltammetry to determine whether hemin has a similar catalytic effect on some synthetic trioxanes.

5-2: Experimental section

Cyclic voltammetry measurements were performed as described in chapter 4 in various buffers (PBS and TRIS) in ethanol solvents with glassy carbon (GC) working electrodes (1 or 3 mm in diameters). The compounds **(Fig. 5-1 shows the structures of the synthetic trioxanes used in this study)** were provided by C. W. Jefford from University of Geneva and Steven Meshnick from University of Michigan. Among the compounds, only Chem 270 (most polar one) was soluble in a 40/60 ethanol/TRIS solvent. Its cyclic voltammograms were compared with that of artemisinin. Many of the compounds tested (seven) were soluble in the 85/15 ethanol/TRIS solvent and some (three) were not soluble because they do not bear polar substituents. Two soluble compounds were antimalarial inactive-placeboes (there is no peroxide bond), and I will show their difference in CV from the other endoperoxide compounds.

5-3: Results and discussion

5-3-1: Cyclic voltammetry of Chem 270

Only one of the compounds tested, Chem 270, was soluble enough to be studied in a predominantly aqueous solvent (40% ethanol and 60% aqueous buffer). It was total soluble in the 40/60 ethanol/TRIS solvent and slight insoluble in the 40/60 ethanol/PBS solvent. All the others were totally insoluble in these solvents. 1 mM Chem 270 had a reduction peak at ca. -1.2 V in 40/60 ethanol/TRIS and ca. -1.0 V in 40/60 ethanol/PBS. The peak heights decreased with increasing scan rates, which means that the reduction is a slow electron transfer process, the same as for artemisinin. The reversible hemin peak occurred at -0.5 V and the irreversible catalytic peak occurred at -0.7 V and both peaks showed up when the concentration of hemin was 10^{-5} M or higher. The reduction peak of Chem 270 totally disappeared in this hemin mixed solution. **(Fig. 5-2 and Fig. 5-3 show CV of Chem 270 alone and with hemin)**. A 0.5 V difference between the reduction peaks in the presence and absence of hemin shows that Chem 270 resembles artemisinin in its interaction with hemin.

When cyclic voltammetry was performed in the presence of a higher concentration of ethanol (85/15 ethanol/TRIS), there is no reduction or oxidation peak from 0 V to the negative limit, ca. -1.8 V. Comparing the result of Chem 270 in the 40/60 ethanol/TRIS solvent, I suspect that increasing the fraction of ethanol in the solvent may push the reduction of trioxanes to a more negative potential which may be beyond the potential scanning limit, so no peak is seen. **(Fig. 5-4)**

5-3-2: CV of trioxanes in the presence of hemin

All the compounds tested (soluble or slightly insoluble) are very sensitive to hemin. The catalytic peak in a 10^{-8} M hemin and 1 mM of compounds mixtures occurred but was not very clear. In a mixture containing 10^{-7} M hemin and 1 mM compound, the biological active compounds showed an irreversible reduction peak at ca. -0.3 V at scan rates less than 5 V/sec, and the inactive compounds showed a reversible redox peak at the same potential at all scan rates. All the compounds (active or inactive) showed a reversible redox peak when the scan rate is very fast (50 V/sec). **(Fig. 5-5 to Fig. 5-6 show CV of active and inactive compounds at two scan rates).**

The biological tests showed there was a wide variation in the antimalarial activity of the tested compounds. From the CV study, there was no systematic difference in the peak current or peak potential of the heme-catalyzed reduction peak, but the reversibility of the heme-catalyzed reduction peak at slow scan rates (< 1 V/sec) is a good qualitative indication of the existence of an endoperoxide bridge in the compounds.

The mechanisms of the reactions between the endoperoxide compounds and hemin are expected to be similar as I had observed in Chem 270, but differed in some ways. First, there is no reduction peak of the compounds themselves (to -1.8 V) in the media I used, Second, the reduction peak in the hemin/compound mixtures occurred ca. -0.3 V, not -0.5 V as I saw in the artemisinin and Chem 270 in 40/60 ethanol/buffer. Third, the inactive compounds showed an reversible redox peak at the same potential, ca. -0.3 V, which is also different from hemin in artemisinin while the hemin showed a reversible peak at ca. -0.4 V. Although the results were somewhat different than what I had expected, I postulate either the low solubility is the problem or the artemisinin and the synthetic compounds have different interaction mechanisms with heme. Factors other than interactions with hemin may

determine the efficacy of in vivo antimalarial activity.

Jefford[1] suggested that the difference between Artemisinin and synthetic compounds is in their structures. Artemisinin is a rigid molecule in which the trioxane ring is fixed in a boat conformation, while the other adopts a chair conformation by X-ray studies. The potency of a particular trioxane is due to its ability to adopt a twisted conformation so that it may efficiently complex with the ferrous ion of heme. These findings show that neither a lactone function nor an artemisinin-like skeleton is required to achieve artemisinin-like activity. Nevertheless, the mode of action of potent trioxanes may be similar to that of artemisinin.

In conclusion, analogs which lack the endoperoxide bridge, also lack antimalarial activity. These compounds are also unreactive in the presence of hemin. Thus, there is a crude correlation between antimalarial activity and interaction with hemin from the CV study.

5-4: Conclusions and Future Prospects

From this study and other biological studies, the crucial structure in artemisinin and other trioxanes which give their antimalarial activity is the peroxide bridge[9-11]. Other parts of the molecule can be modified without loss of antimalarial activity. Many compounds not obviously related to artemisinin but which contain a peroxide group should be antimalarial agents. However, even in compounds closely related to artemisinin the possession of a peroxide bridge is not of itself sufficient condition for antimalarial activity and the rest of the molecule has a profound effect on the antimalarial activity in vitro and in vivo. This suggests that the remainder of the artemisinin molecule is responsible for the delivery of the drug to the infected erythrocyte in a still active form where it can exercise its toxicity

towards the parasite.

The action of artemisinin on the malarial parasite is completely different from that of chloroquine and this may well be why artemisinin is effective against parasites which have become chloroquine-resistant.

The reaction with intraparasitic hemin with the subsequent formation of free radicals plays an important role in mediating the antimalarial activity of artemisinin. Malarial parasites contain large granules of precipitated hemin (known as hemozoin) because they digest host hemoglobin, probably without breaking down hemin. When Plasmodium falciparum-infected red cells are exposed to the radiolabeled drug, this hemin-artemisinin adduct can be isolated, suggesting that this same reaction occurs in situ. Further evidence for the critical role of hemin/hemozoin in the mechanism of action of artemisinin is that artemisinin is >50 times less effective against a chloroquine-resistant P. berghei strain which lacks hemozoin.

The hemin-catalyzed reduction of artemisinin can be accounted for in two ways. First, hemin may cause a decrease in the activation energy for the reduction. In this case, the increased rate of electron transfer to artemisinin will cause a positive shift in observed reduction peak potential. Second, the peak shift might occur as a consequence of the catalysis of a chemical reaction that follows reduction. This reaction could remove the reduced form of artemisinin and thereby increase the net rate of electron transfer to the drug. In either case, the fact that very small amounts of hemin (50 nM) catalyze the reduction of artemisinin argues against a stoichiometric reaction of hemin with artemisinin taking place on the time scale of the present experiments (seconds).

Hemin catalyzes the reduction of artemisinin, dihydroartemisinin and Chem 270 in an almost identical manner, indicating that the structure of the

lactone/lactol ring does not affect the ability of the drug to interact with hemin. Artemisinin, dihydroartemisinin, and other analogs containing the endoperoxide bridge have comparable antimalarial activities. In contrast, derivatives of artemisinin which lack the endoperoxide bridge lack antimalarial activity[12-13] and the difference between active and non-active can be seen easily from our CV experiments qualitatively.

For the hemin-mediated reductive decomposition of artemisinin to occur in situ, there must be a physiologically relevant source of electrons. Electrons could potentially be donated to intraparasitic hemin by thiols such as glutathione, which is present in malarial parasites in millimolar concentrations[14]. Alternately, parasite hemin could catalyze the decomposition of artemisinin in situ by forming an oxene intermediate as has been shown to occur in reactions between iron(III) porphyrins and various peroxides[15-16]. There are indications from prior reports that reduction potential in vivo may well be more favorable than in vitro.

We believe that artemisinin and its derivatives will play a substantial part in the fight against the resurgence of malaria, particularly falciparum malaria, throughout the world. But artemisinin and its derivatives have shortcomings as antimalarial agents. Although partially solved, their low solubility in both oil and water is still a problem. Efficacy by oral administration is very poor and administration by injection is a problem in countries where there are inadequate medical facilities. Thus there is much work still to be done in providing the world with a really successful new antimalarial drug.

Figures and Tables

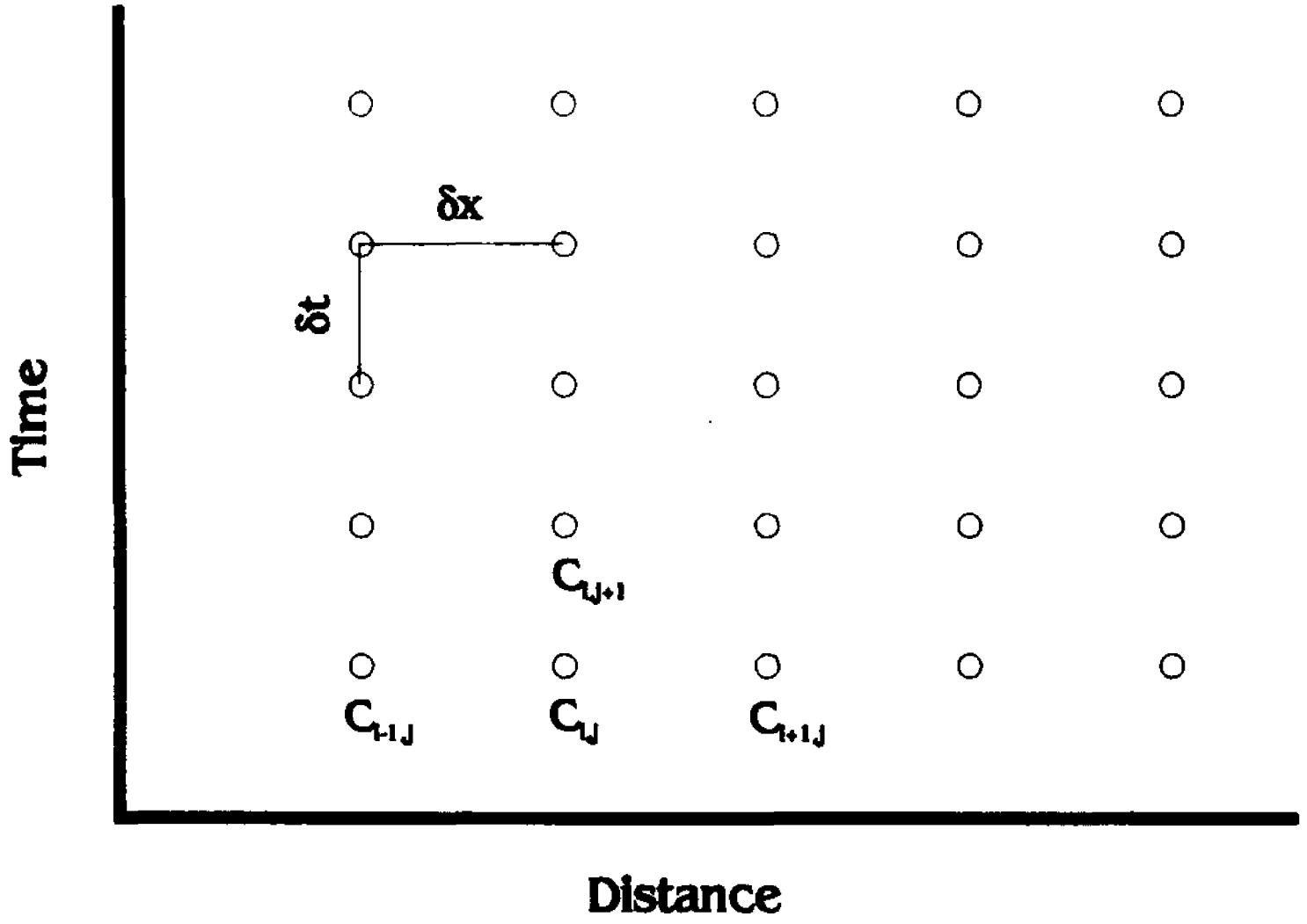

Fig. 1-1 Space-Time grid

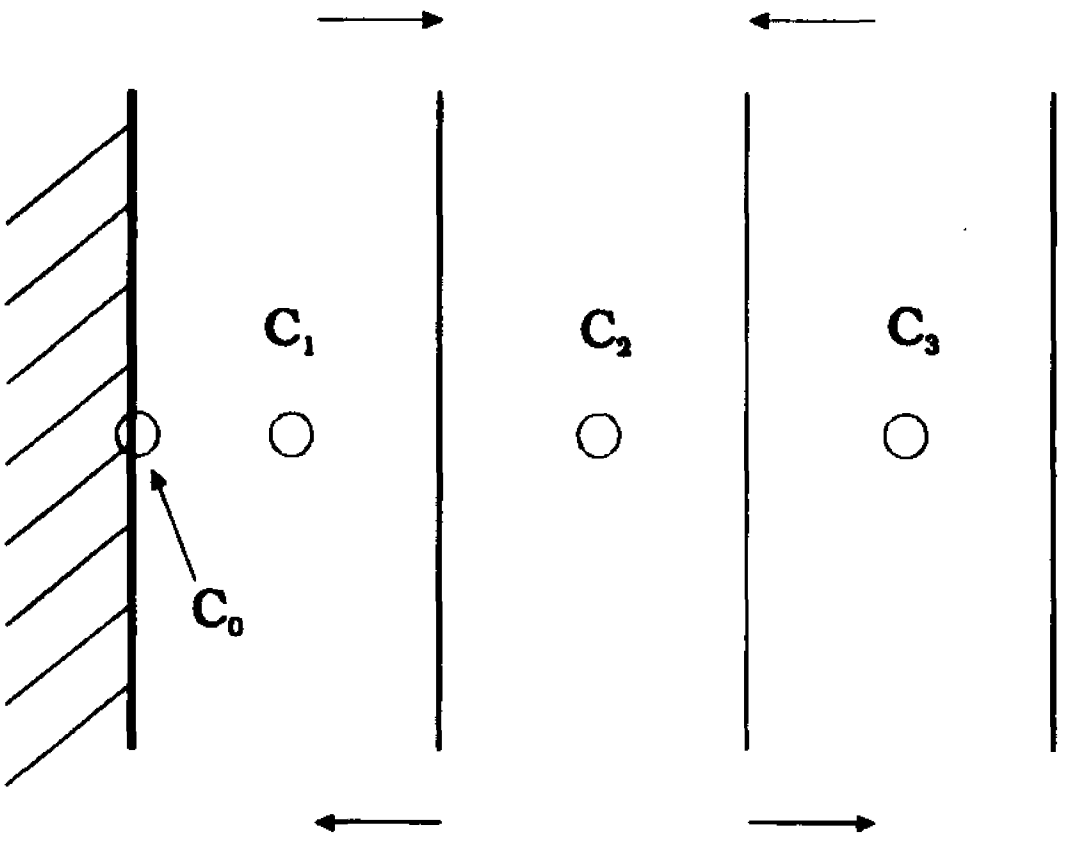

Fig.1-2 Space-Time grid near electrode surface

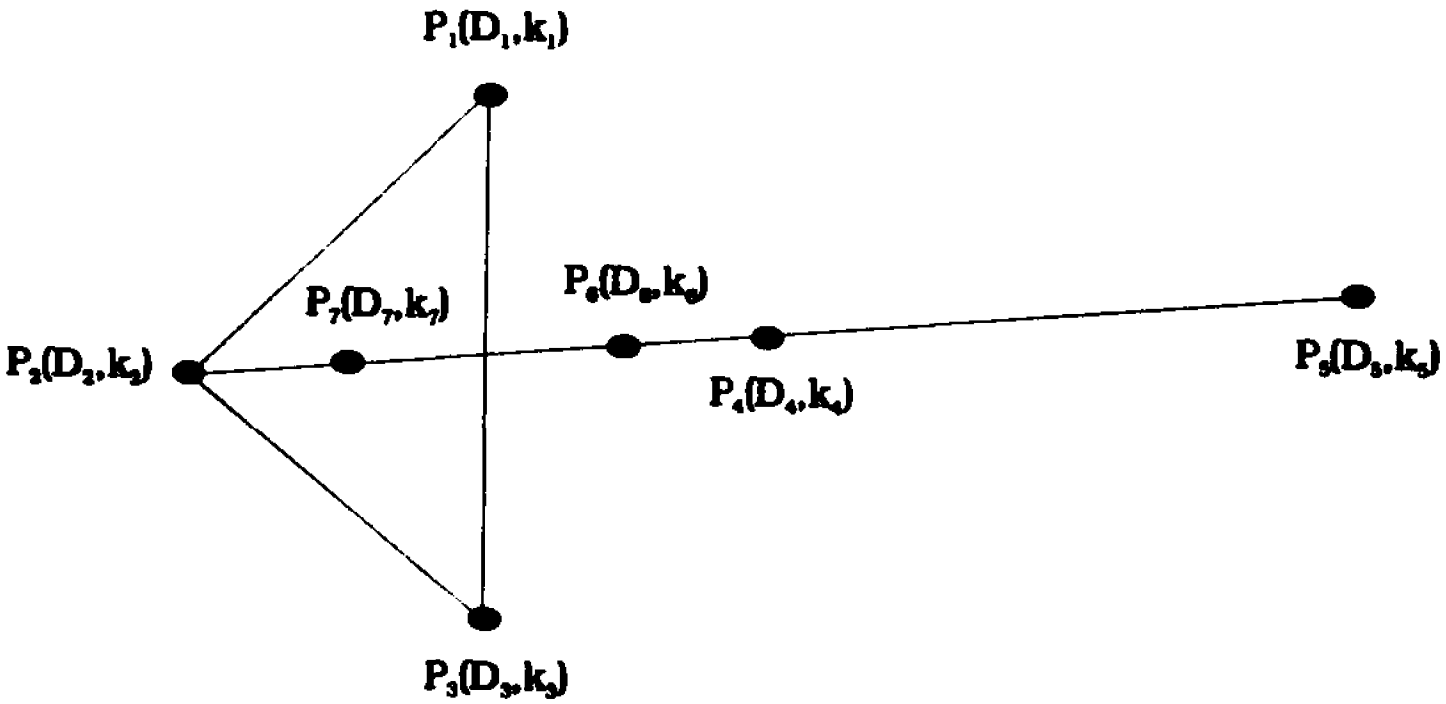

Fig.1-3 The modified simplex procedure

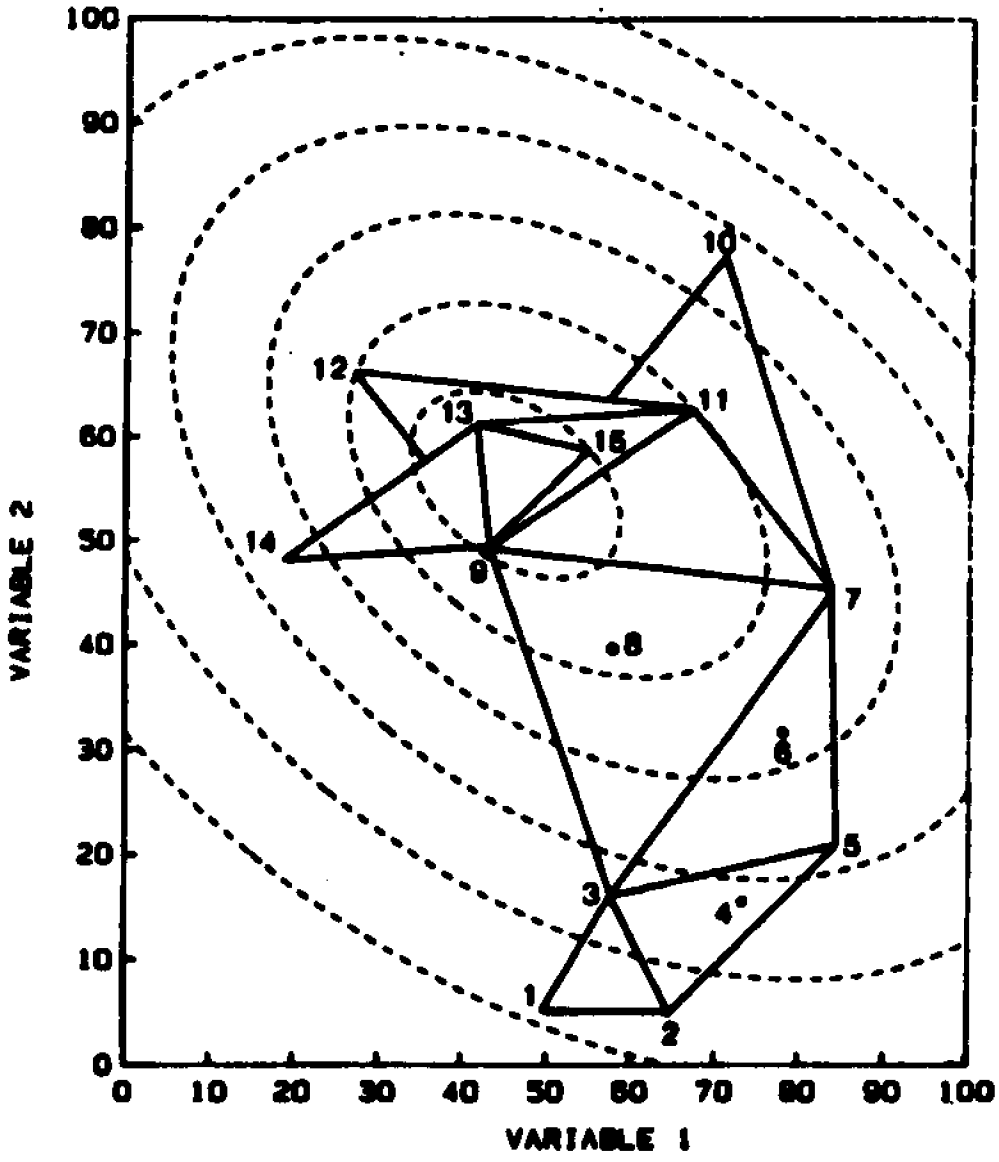

Fig.1-4 Movements of modified simplex procedure

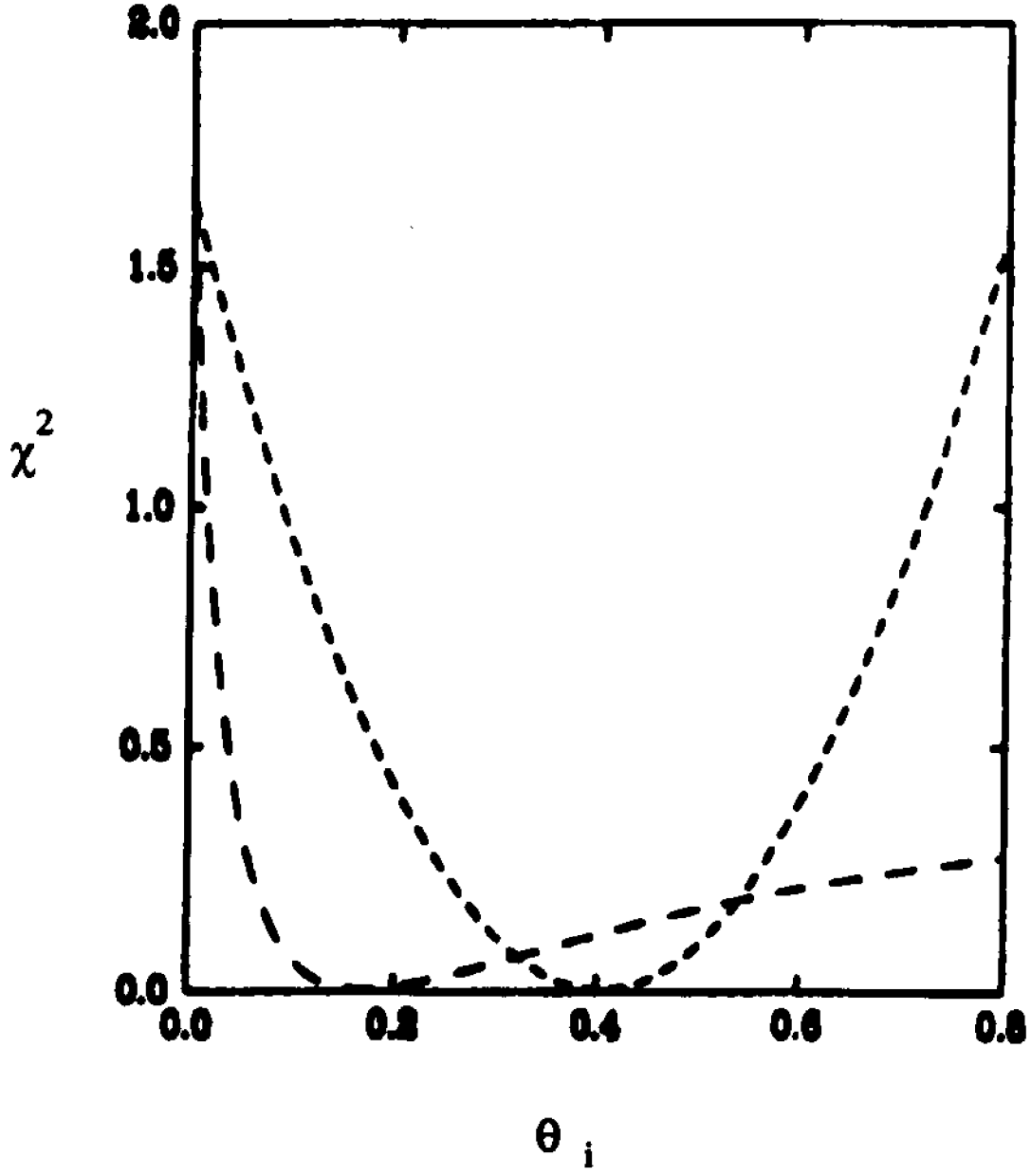

Fig. 1-5 χ^2 vs. θ_i curvature graph

	$C_{A,n}$		
Iteration	**Analytical solution**	**Differential method**	**Modified Euler method**
0	1.000	1.000	1.000
1	0.6065	0.5000	0.5000
2		0.7500	0.6250
3		0.6250	0.5938
4		0.6875	0.6016
5		0.6563	0.5996
6		0.6719	0.6001
7		0.6641	0.6000

Table1-1 Comparison of approximation methods for A→B reaction. $C_{A,0}$=1.0, δt=0.5, $k_{A\to B}$=1.0

		CV simulations of the simplexes			
E (mV)	Experiment current (μA)	Current calc. from P_1	Current calc. from P_2	Current calc. from P_3	Current calc. from P_4
10	0.04	0.06	0.08	0.02	
20	0.08	0.09	0.12	0.03	
30	0.12	0.14	0.24	0.09	
40	0.23	0.27	0.46	0.32	
50	0.57	0.48	0.57	0.63	
60	0.81	0.64	0.86	0.94	
70	0.63	0.77	0.97	0.87	
80	0.54	0.84	0.90	0.73	
90	0.32	0.63	0.82	0.64	
100	0.29	0.52	0.74	0.59	
χ^2		0.29	0.79	0.32	?

Table 1-2 Potential-current chart with calculated χ^2

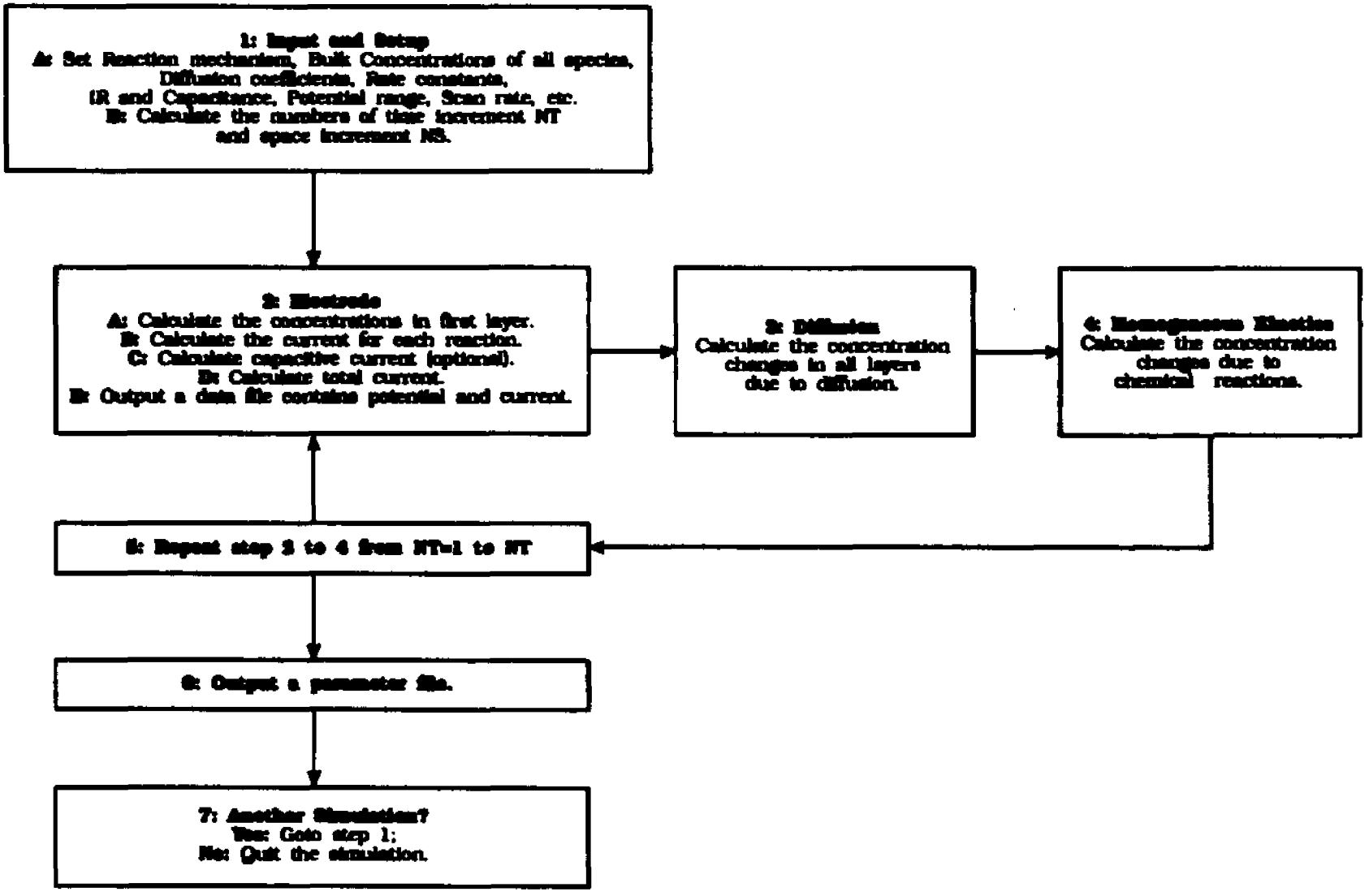

Fig. 2-1 Flowchart of CVSIM program

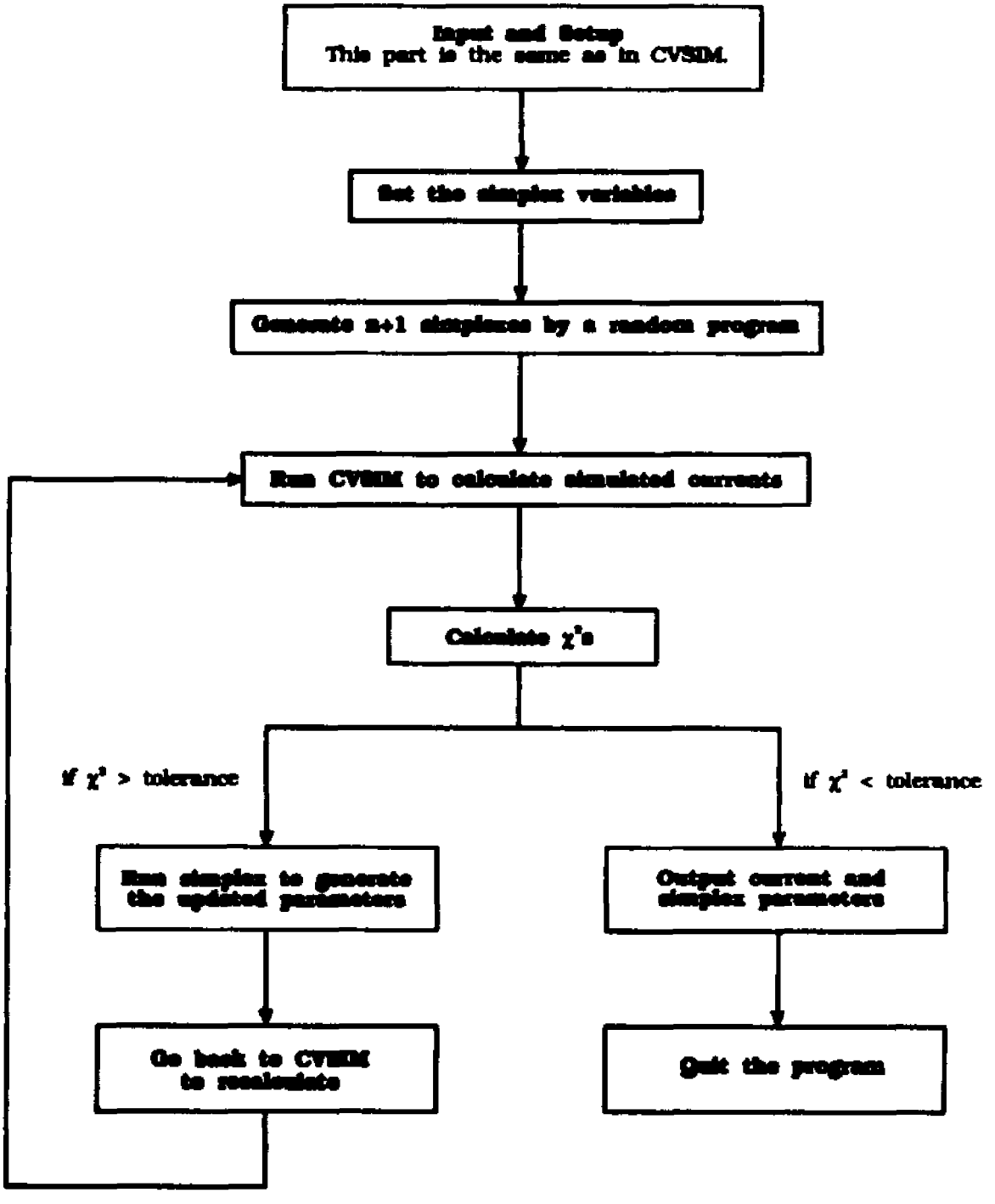

Fig. 2-2 Flowchart of CVFIT program

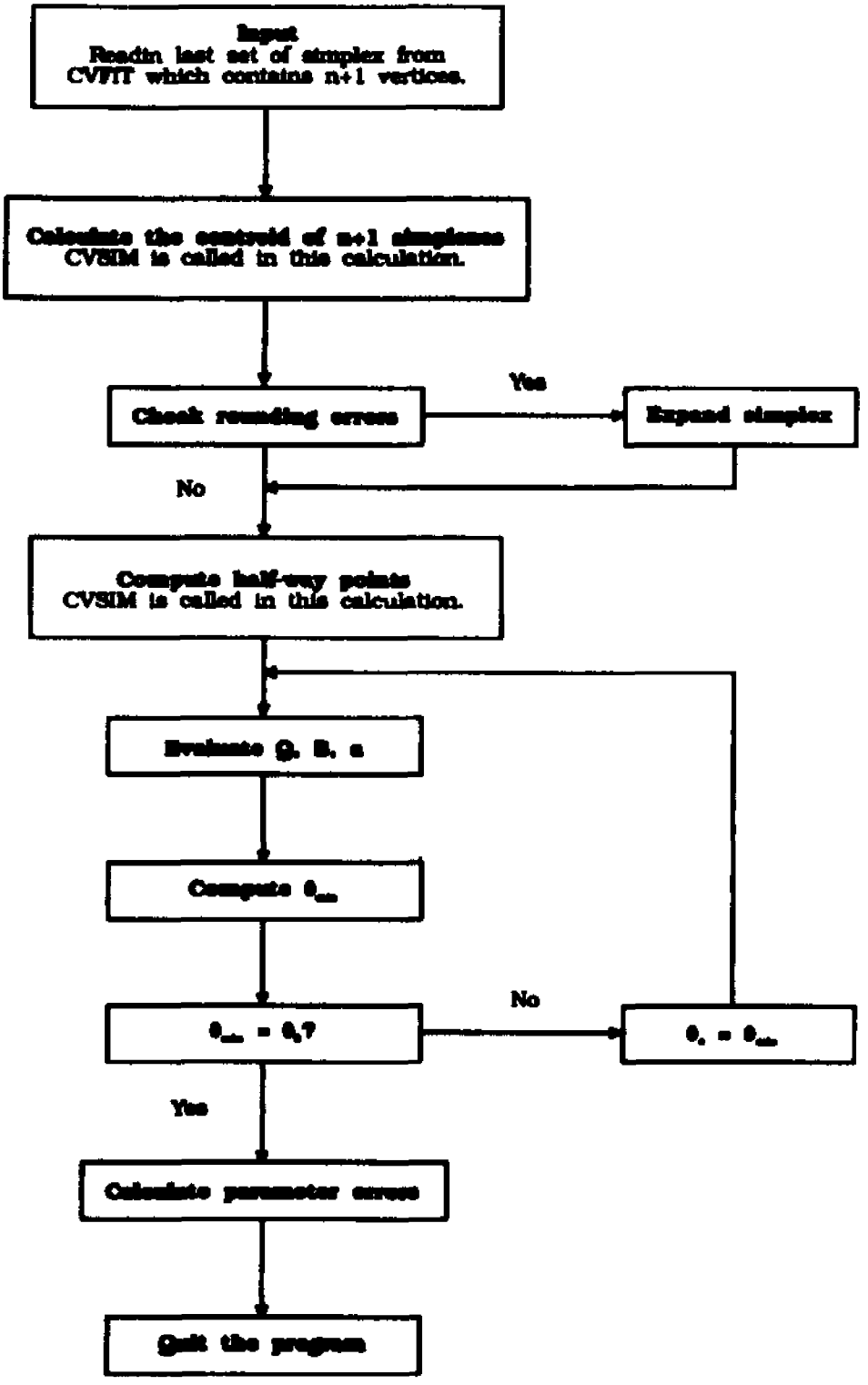

Fig. 2-3 Flowchart of EET program

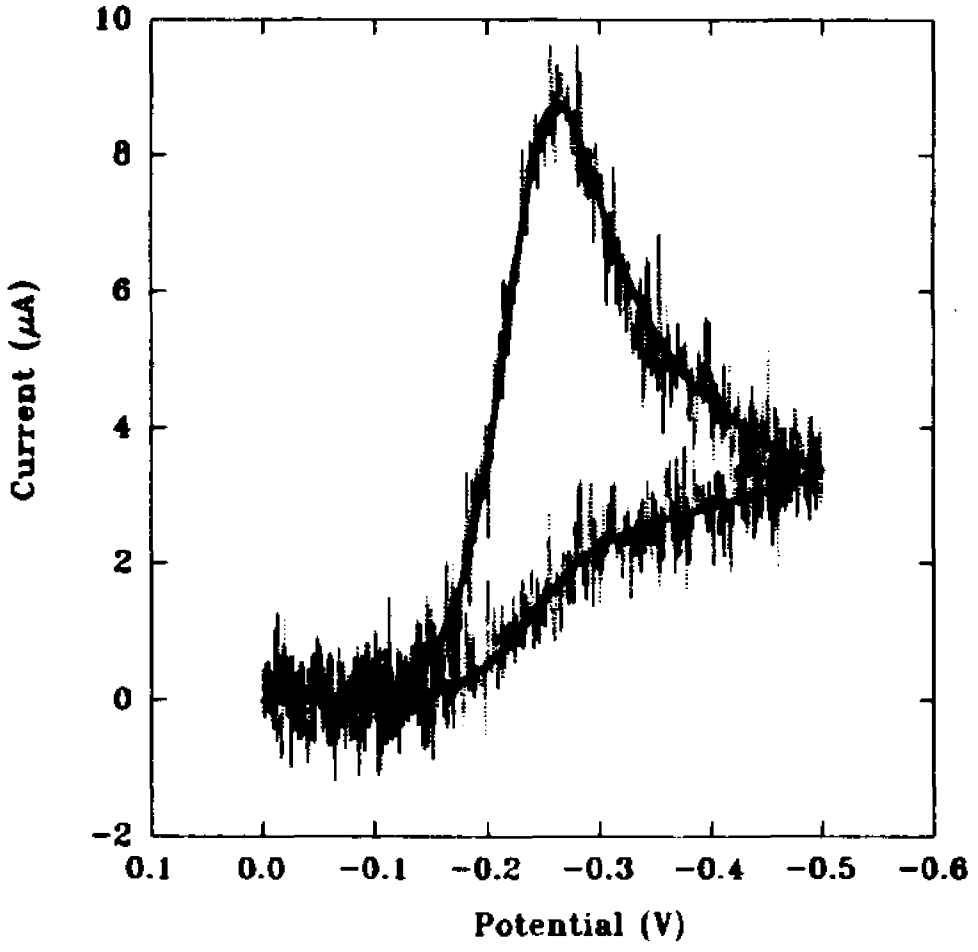

Fig. 2-4 The simulated EC mechanism with 7.0% noise level in the data file. See table2-1 for the details.

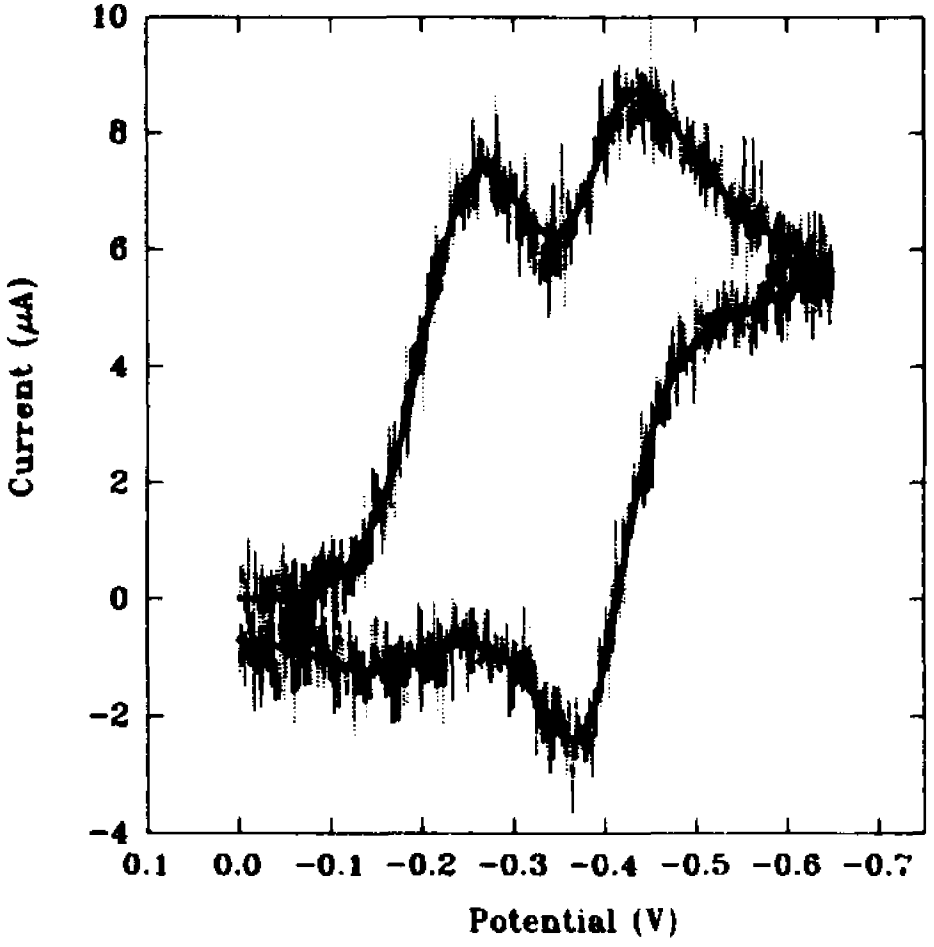

Fig. 2-5 The simulated ECE mechanism with 7.0% noise level in the data file. See table2-2 for the details

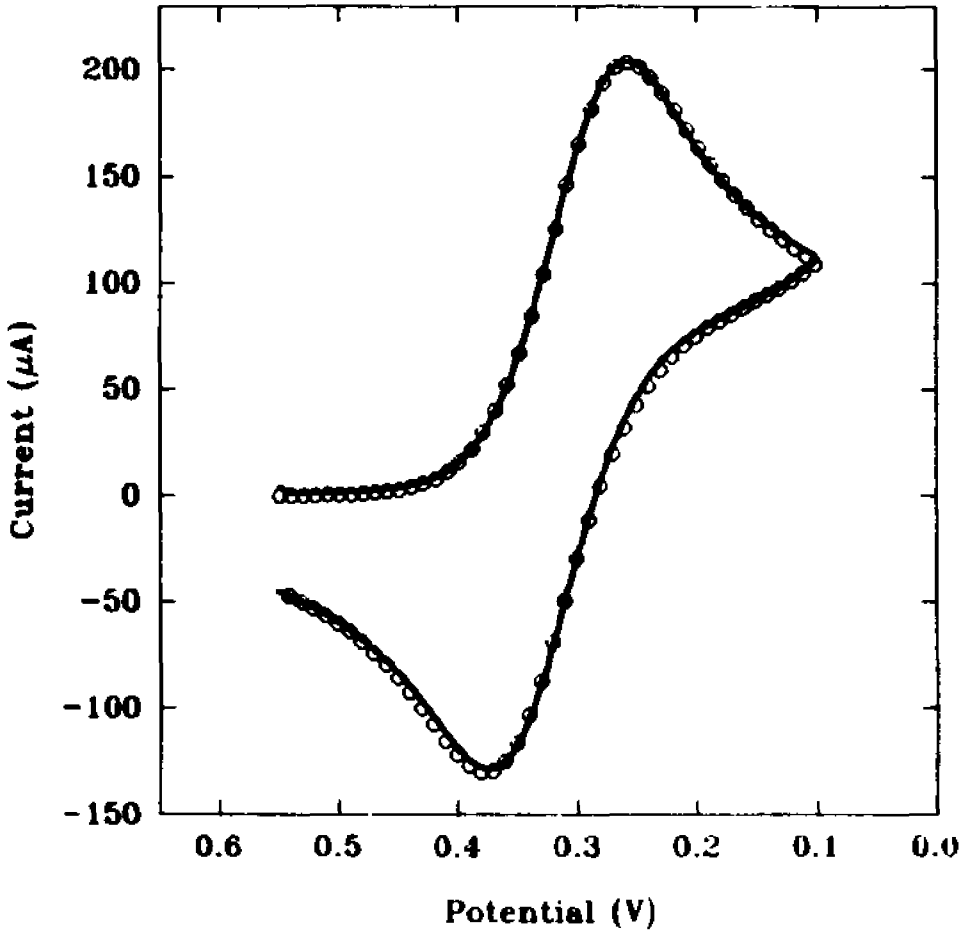

Fig. 2-6 The simulation result for 2 mM ferricyanide at 5 V/sec.

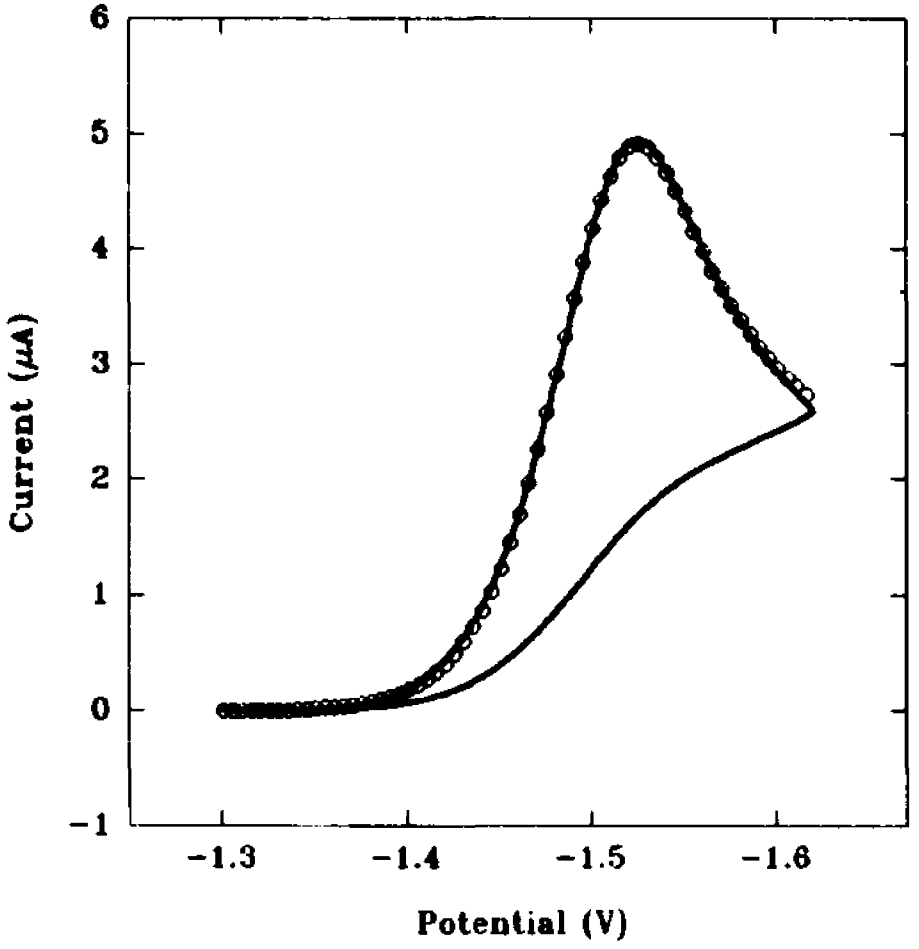

Fig. 2-7 The simulation result for 2 mM methyl-cobalamin at 0.1 V/sec.

Noise Level (%)	E^0 (V)	k^0 (cm/sec)	α	k_{chem} (sec^{-1})	Error ($\times 10^{-10}$)	Iteration
0.0	-0.2500	0.1000	0.4999	100.05	5.6167	261
1.4	-0.2506	0.1011	0.4966	107.43	9.2141×10^{4}	470
7.0	-0.2530	0.1075	0.4786	142.21	2.3024×10^{5}	225
14.0	-0.2535	0.1967	0.5804	115.16	9.2059×10^{5}	176

Table 2-1 Simulation result for an EC mechanism. The input parameters are: E^0 = -0.25 V, k^0 = 0.1 cm/sec, α = 0.5, k_{chem} = 100 sec^{-1}, scan rate = 1 V/sec. The noise level is presented in the percentage to the peak current.

Noise Level (%)	E_1^0	k_1^0	E_2^0	k_2^0	k_{chem}	Error ($\times 10^{-6}$)	Iteration
0.0	-0.2000	0.0100	-0.4000	0.1012	9.9945	7.7020	267
1.4	-0.2001	0.0101	-0.4000	0.1019	9.9703	1.2091×10^{4}	398
7.0	-0.2008	0.0108	-0.3996	0.3147	9.5699	3.0485×10^{5}	214
14.0	-0.2009	0.0113	-0.3997	0.2565	9.5178	1.2121×10^{6}	384

Table 2-2 Simulation result for an ECE mechanism. The input parameters are: $E_1^0 = -0.2$ V, $k_1^0 = 0.01$ cm/sec, $E_2^0 = -0.4$ V, $k_2^0 = 0.1$ cm/sec, $\alpha = 0.5$, $k_{chem} = 10$ sec^{-1}, scan rate = 1 V/sec. The noise level is presented in the percentage to the peak current.

Scan Rate (V/sec)	$E^{0'}$ (V)	k^0 (cm/sec)	α	Area ($\times 10^{-2}$ cm^2)	Error ($\times 10^{-9}$ A^2)	Iteration
5	0.3201	0.025	0.52	6.8	3.0	123
10	0.3195	0.028	0.52	6.7	7.6	142
15	0.3195	0.027	0.51	6.7	39.0	192
Average	0.3197 ±0.0003	0.027 ±0.001	0.52 ±0.003	6.7 ±0.03		
RAD	9.4×10^{-4}	3.7×10^{-2}	5.8×10^{-3}	4.5×10^{-3}		

Table 2-3 The simulation result for ferricyanide.

Scan Rate (mV/sec)	$E^{0'}$ (V)	k^0 (cm/sec)	α	Area ($\times 10^{-2}$ cm^2)	Error ($\times 10^{-13}$ A^2)	Iteration
50	-1.531	0.013	0.77	1.9	1.0	99
100	-1.524	0.010	0.80	2.0	2.1	99
300	-1.531	0.013	0.76	1.9	7.4	110
Average	-1.529 ±0.003	0.012 ±0.001	0.78 ±0.02	1.9 ±0.03		
RAD	2.0×10^{-3}	1.1×10^{-1}	2.1×10^{-2}	1.8×10^{-2}		

Table 2-4 The simulation result for methylcobalamin.

Chloroquine (a)

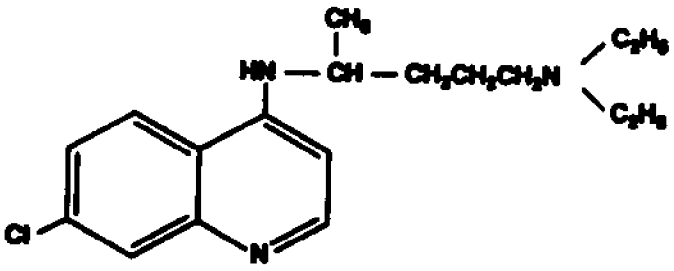

Quinine (b)

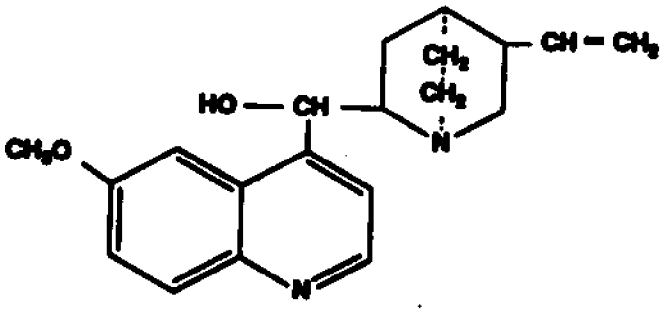

Pamaquine (c)

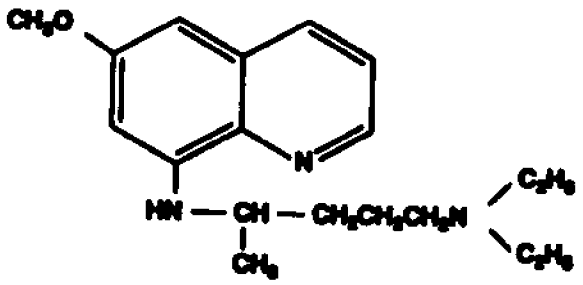

Fig. 3-1: The structures of antimalarial drugs.

Mepacrine (d)

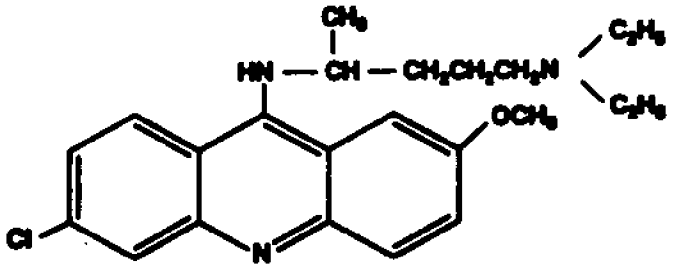

Primaquine (e)

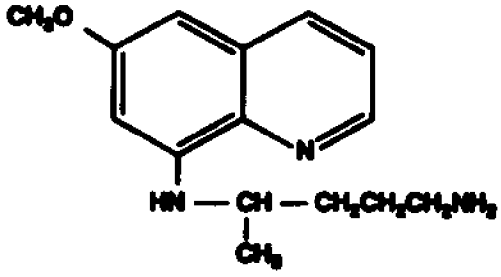

Proguanil (f)

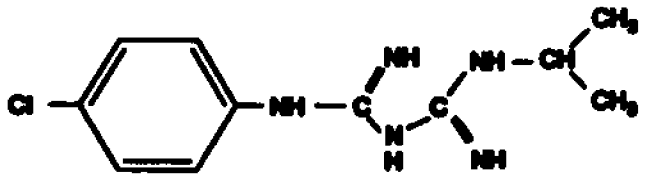

Fig. 3-1: Continued

Pyrimethamine (g)

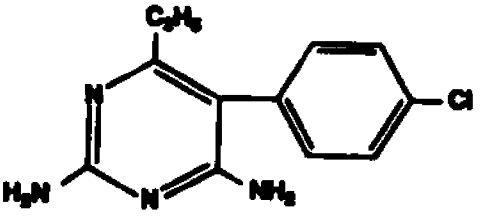

Febrifugine (h)

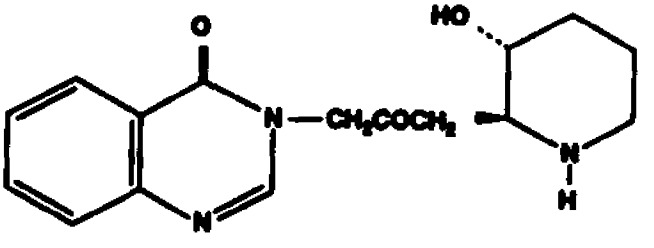

Fig. 3-1: Continued

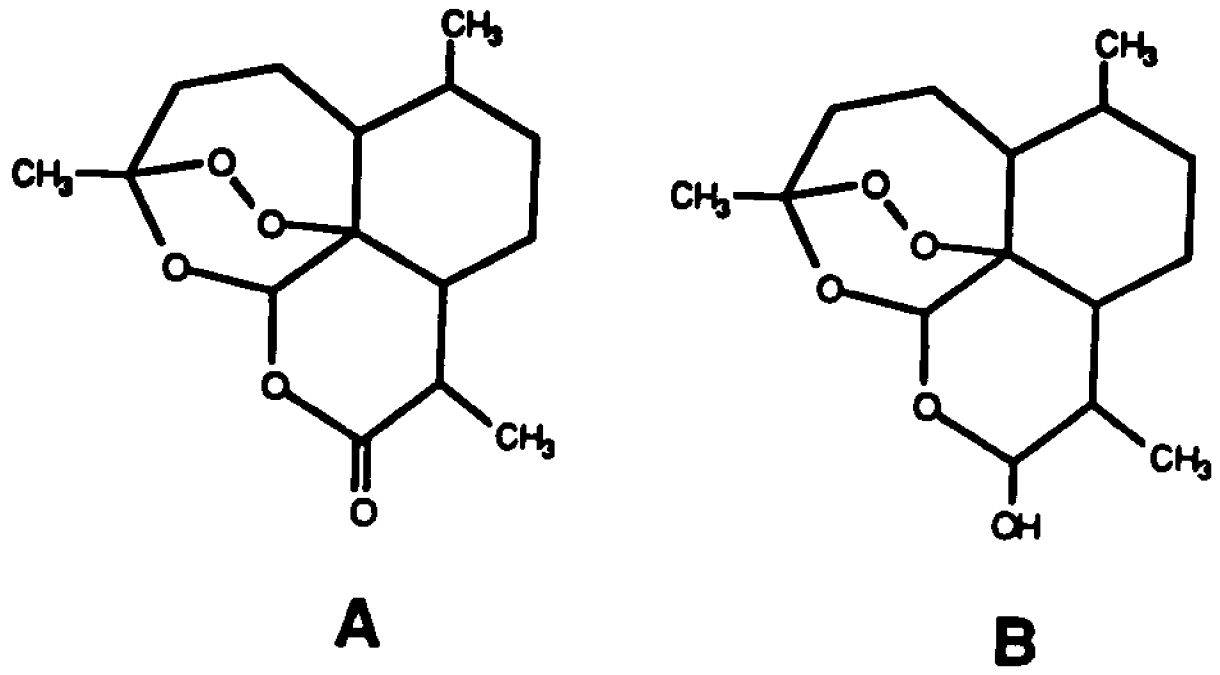

Fig. 3-2: The structures of artemisinin (a) and dihydroartemisinin (b).

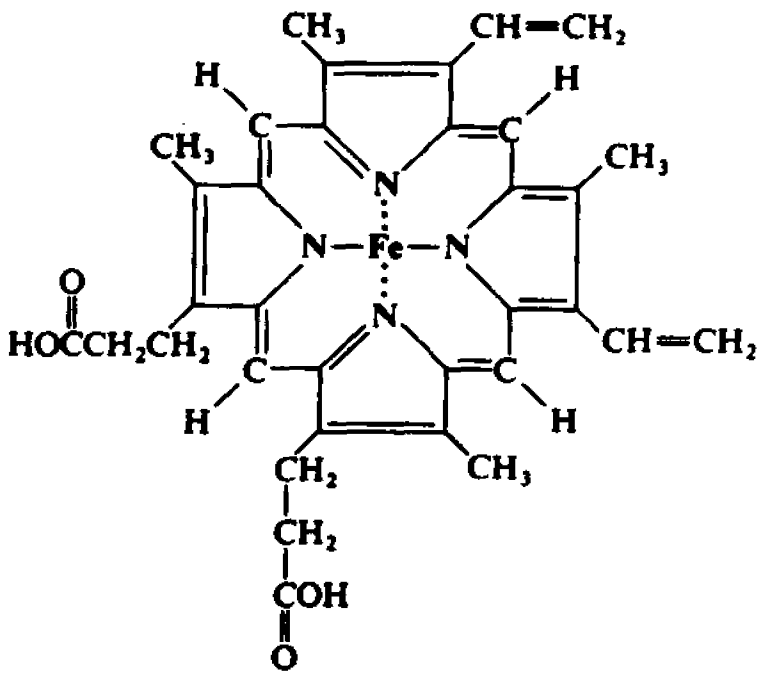

Fig. 3-2c: The structure of hemin.

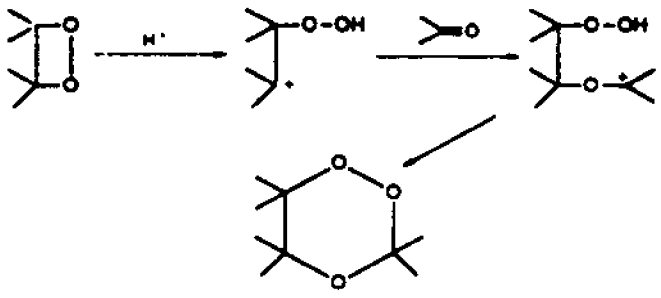

Fig. 3-3: The scheme of trioxane ring formation.

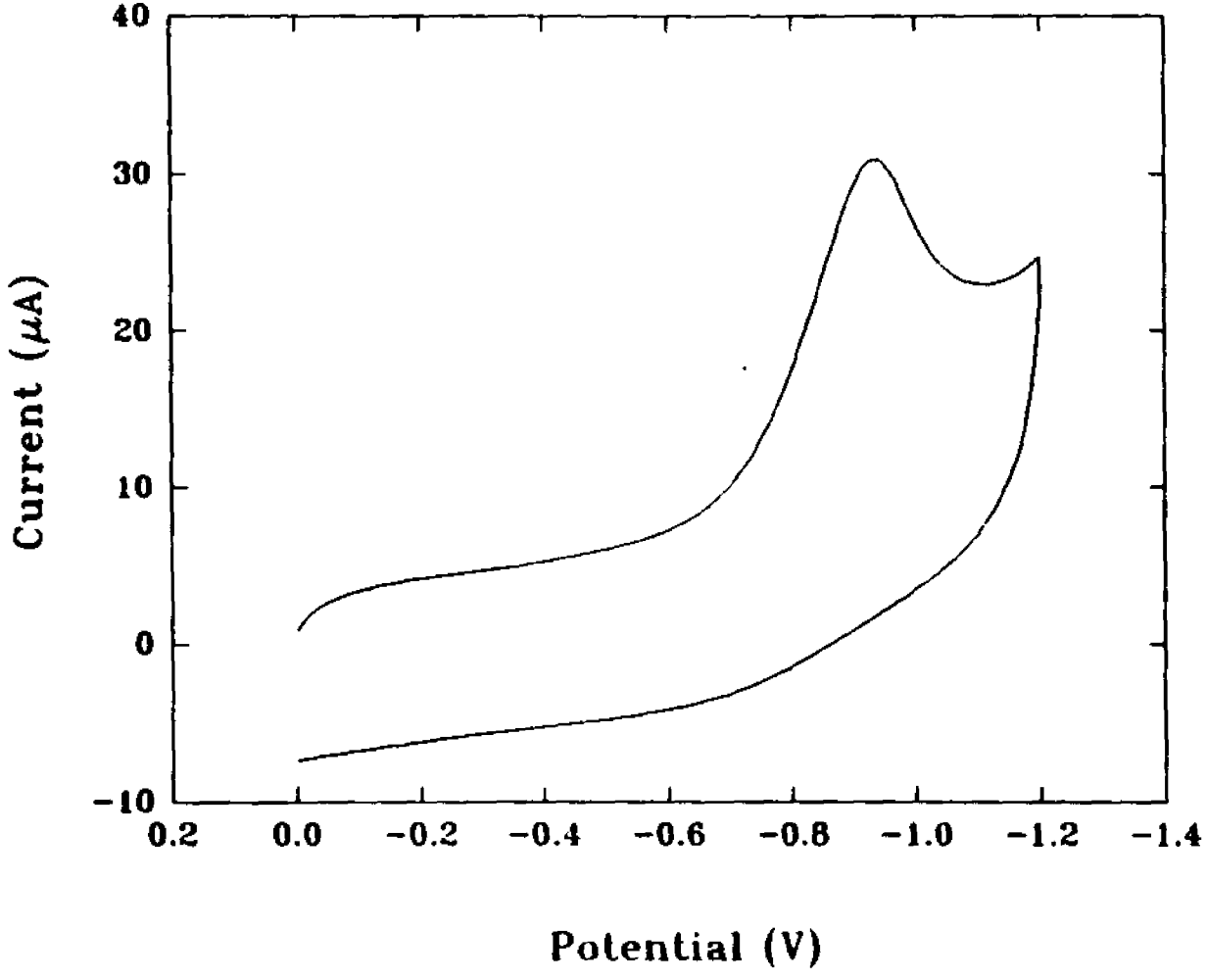

Fig. 4-1: Cyclic Voltammogram of artemisinin (1 mM) at scan rate of 300 mV/sec on GC working electrode.

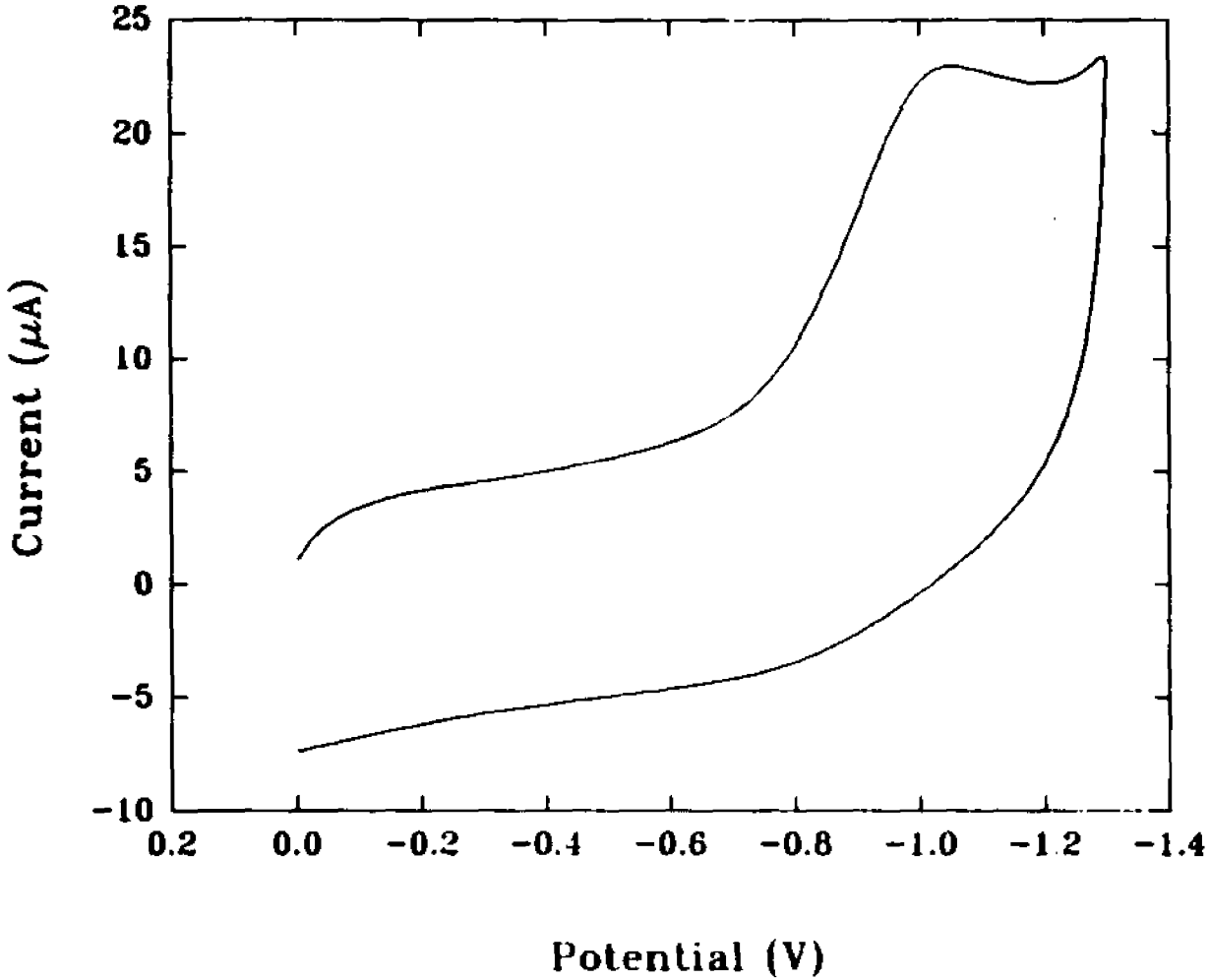

Fig. 4-2: CV of dihydroartemisinin (1 mM) at 300 mV/sec on GC electrode.

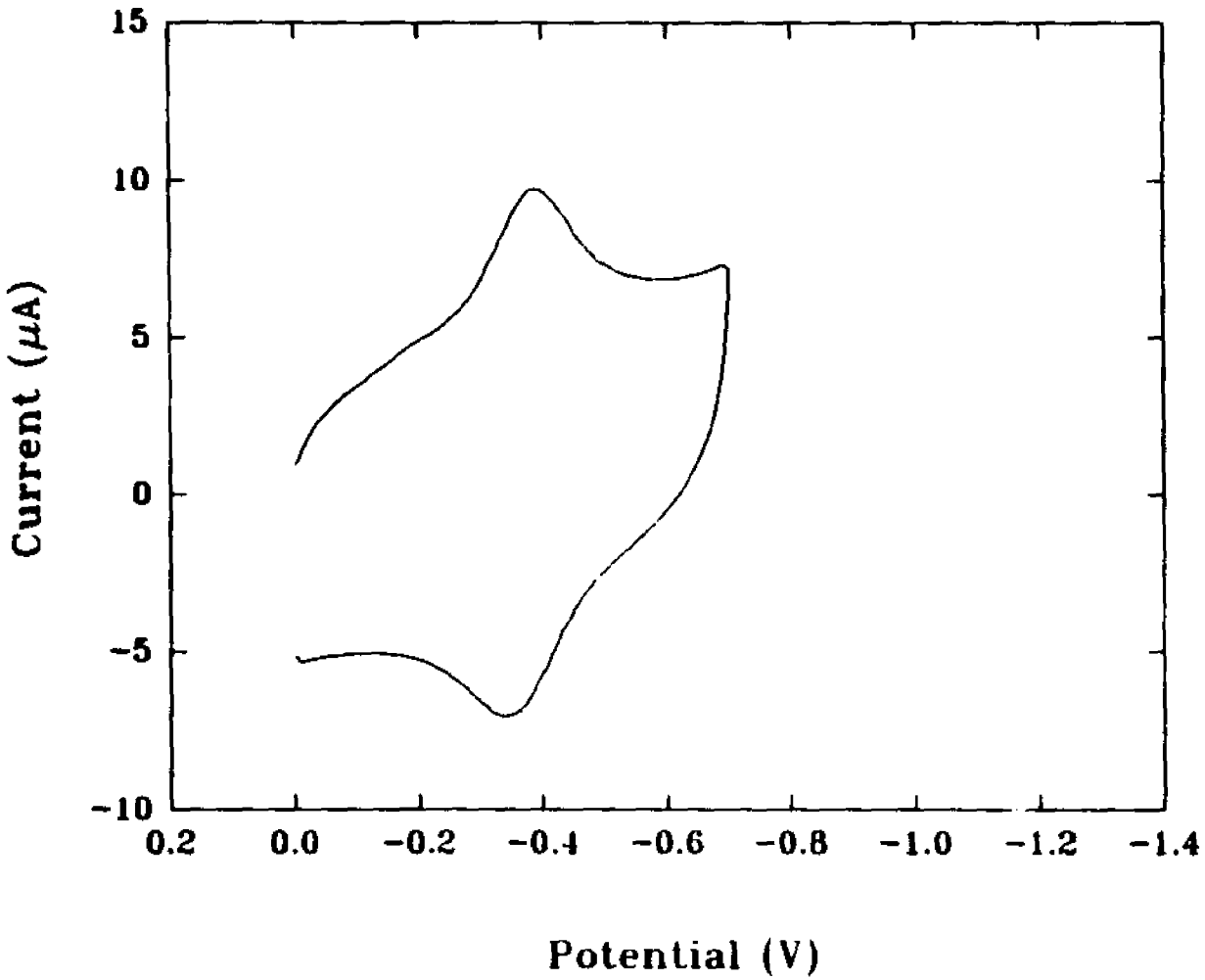

Fig. 4-3: CV of hemin (1 mM) at 300 mV/sec on GC electrode.

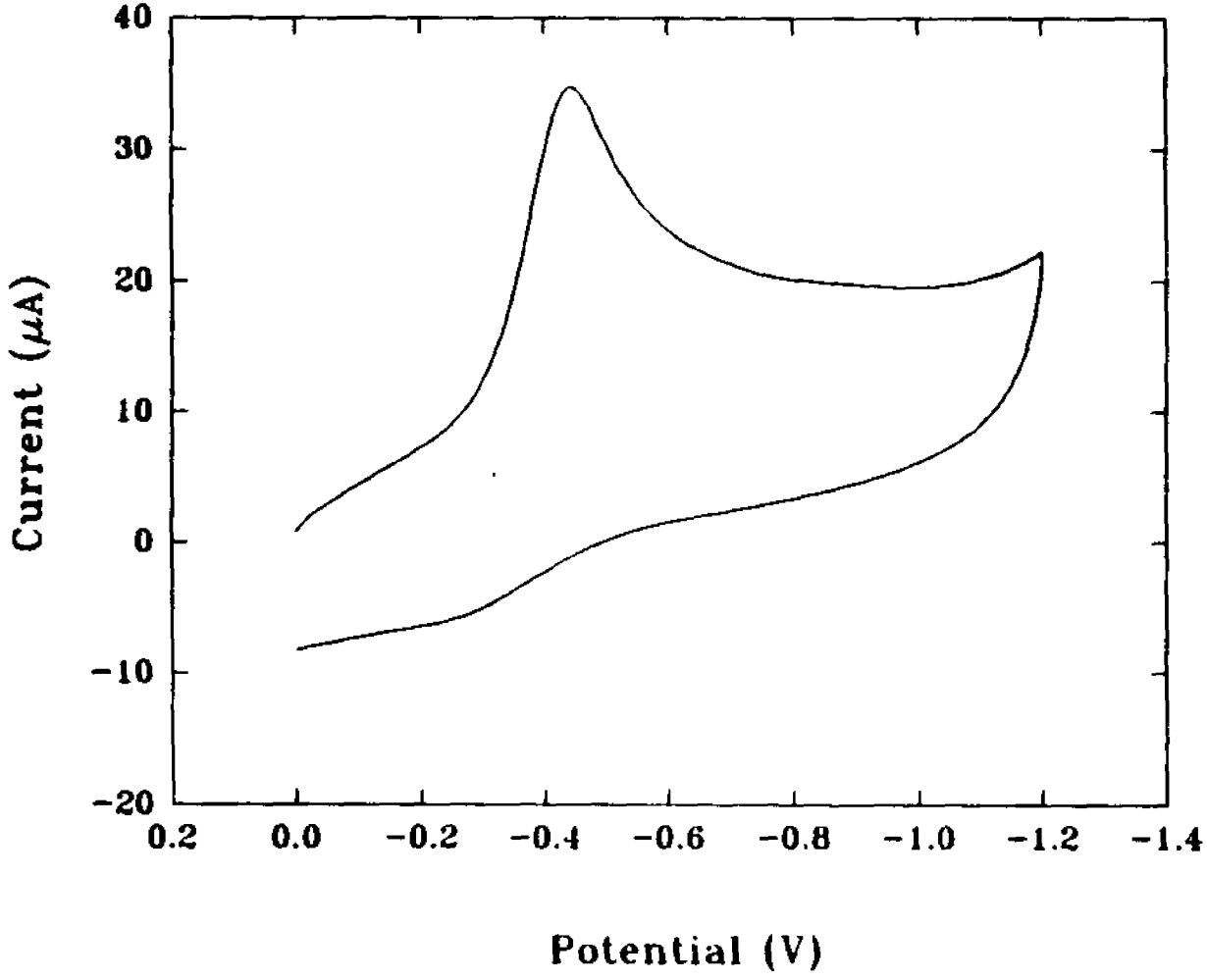

Fig. 4-4: CV of artemisinin (1 mM) in the presence of hemin (0.01 mM) at 300 mV/sec on GC electrode.

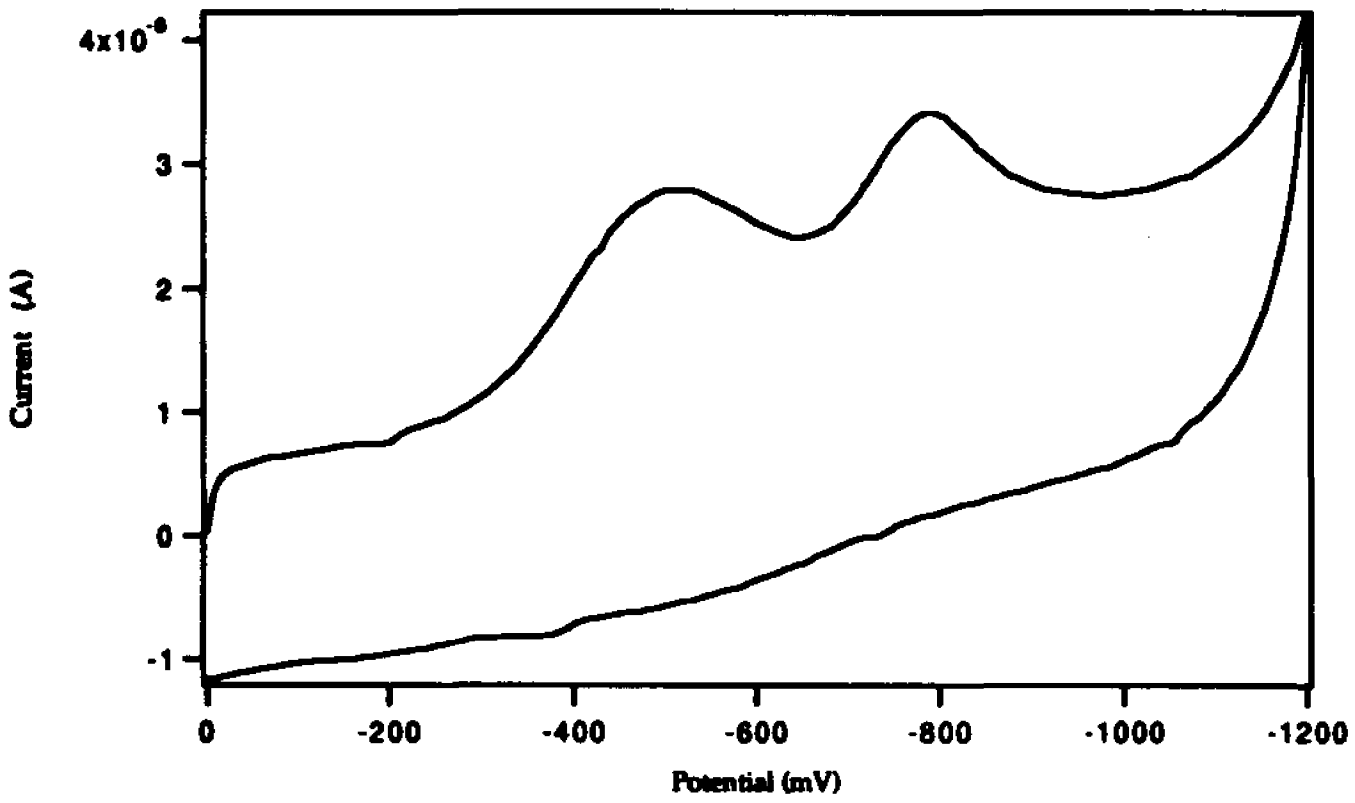

Fig. 4-5a: CV of artemisinin (1 mM) in the presence of hemin (9.0×10^{-7} M) in 40/60 of ethanol/PBS with GC electrode at 30 mV/sec.

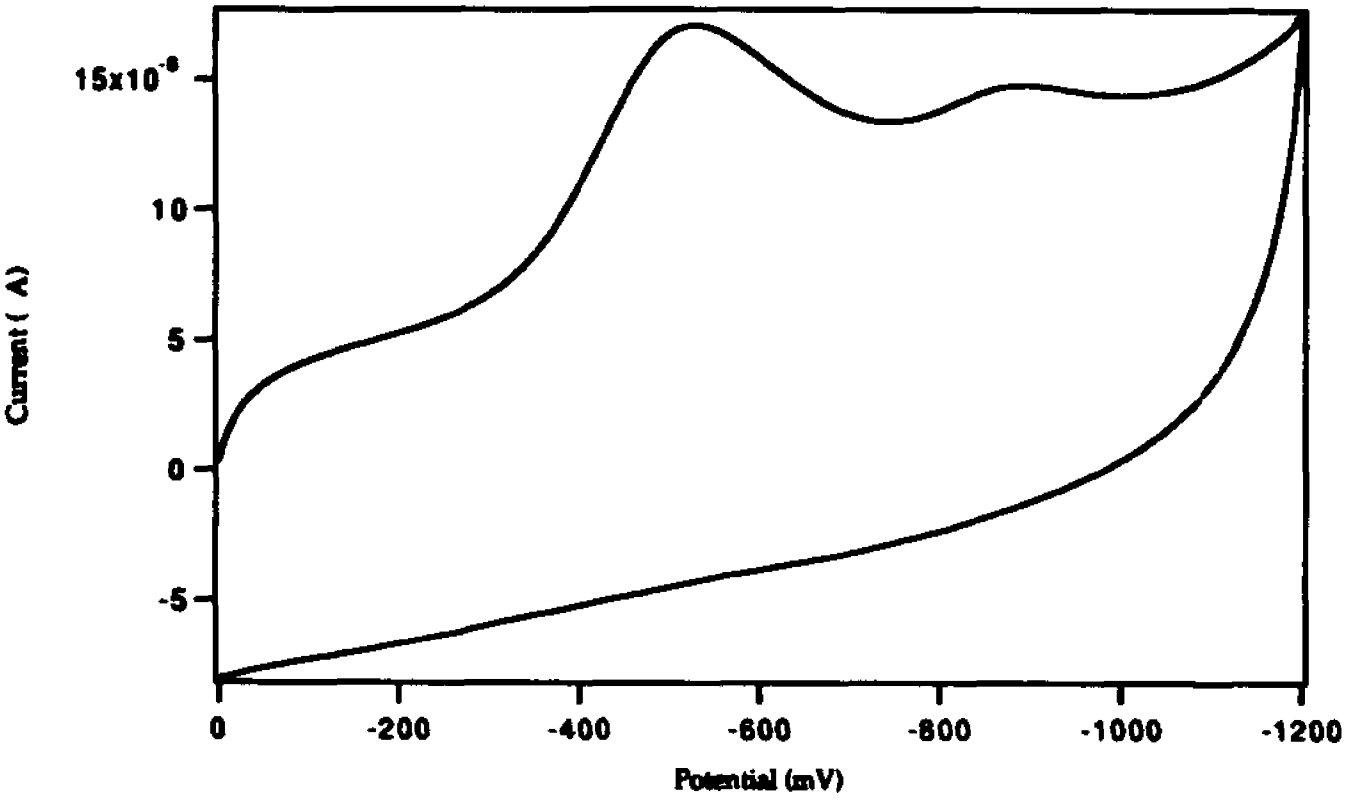

Fig. 4-5b: CV of artemisinin (1 mM) in the presence of hemin (9.0×10^{-7} M) in 40/60 ethanol/PBS with GC electrode at 300 mV/sec.

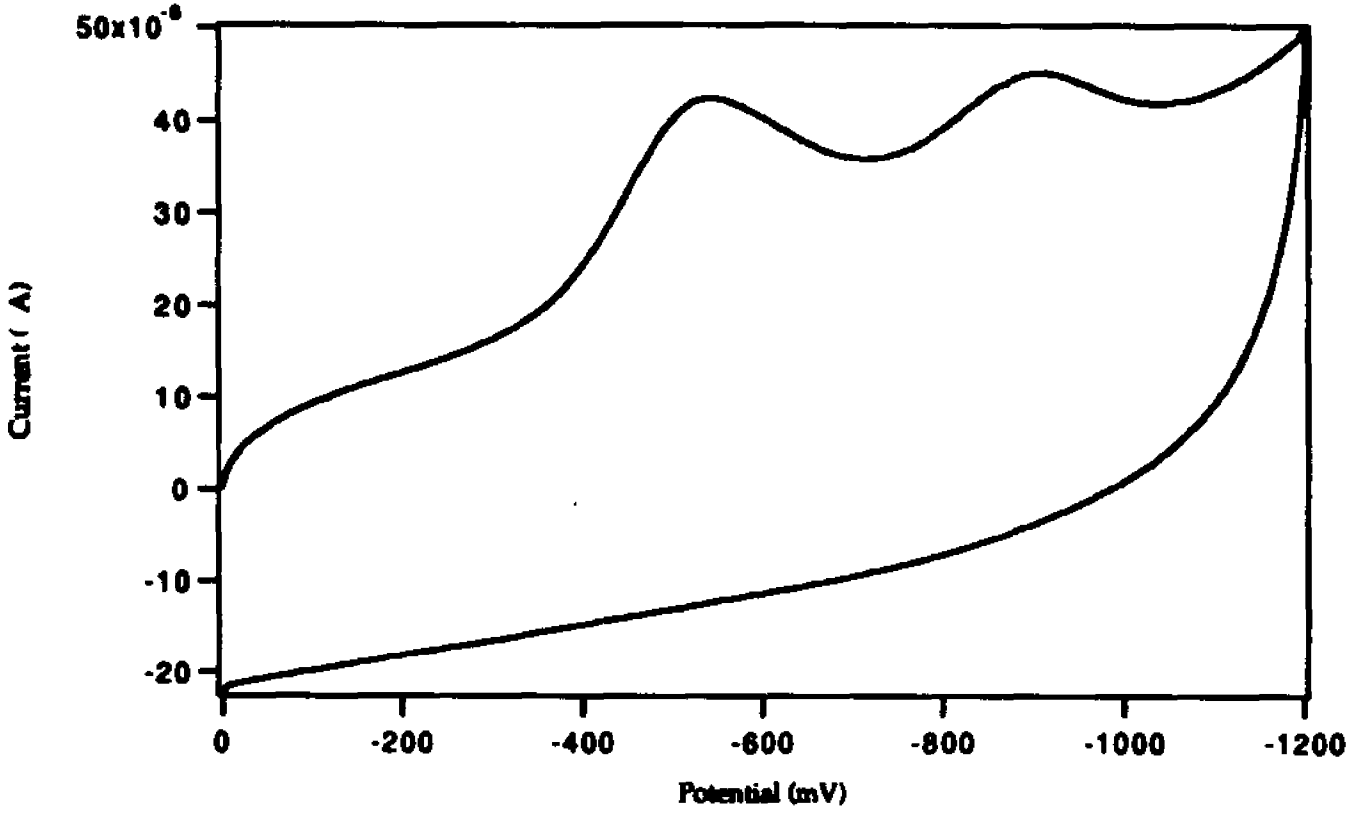

Fig. 4-5c: CV of artemisinin (1 mM) in the presence of hemin (9.0×10^{-7} M) in 40/60 ethanol/PBS with GC electrode at 1000 mV/sec.

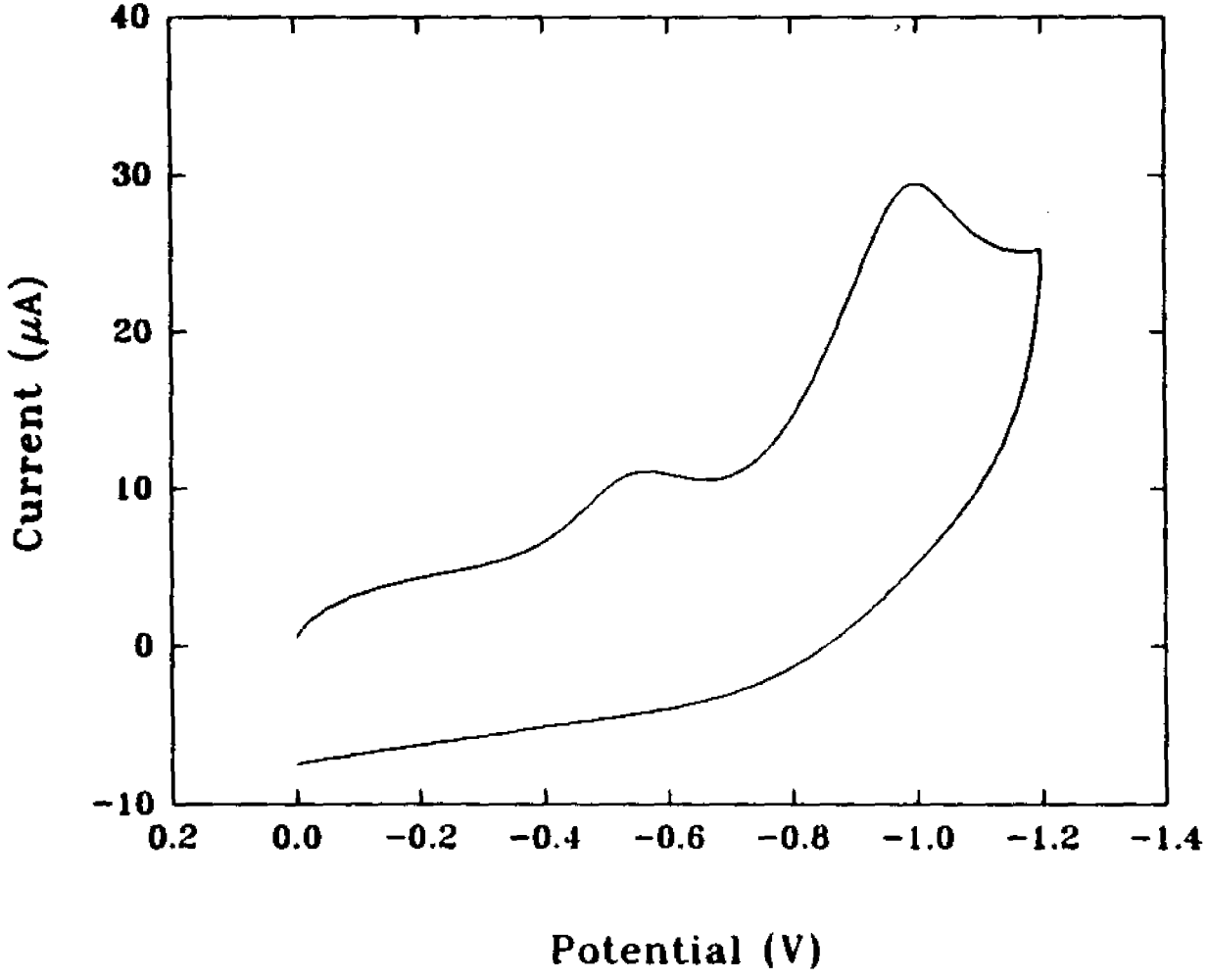

Fig. 4-6: CV of artemisinin (1 mM) in the presence of extreme low concentration of hemin ($5x10^{-8}$ M) at 300 mV/sec on GC electrode.

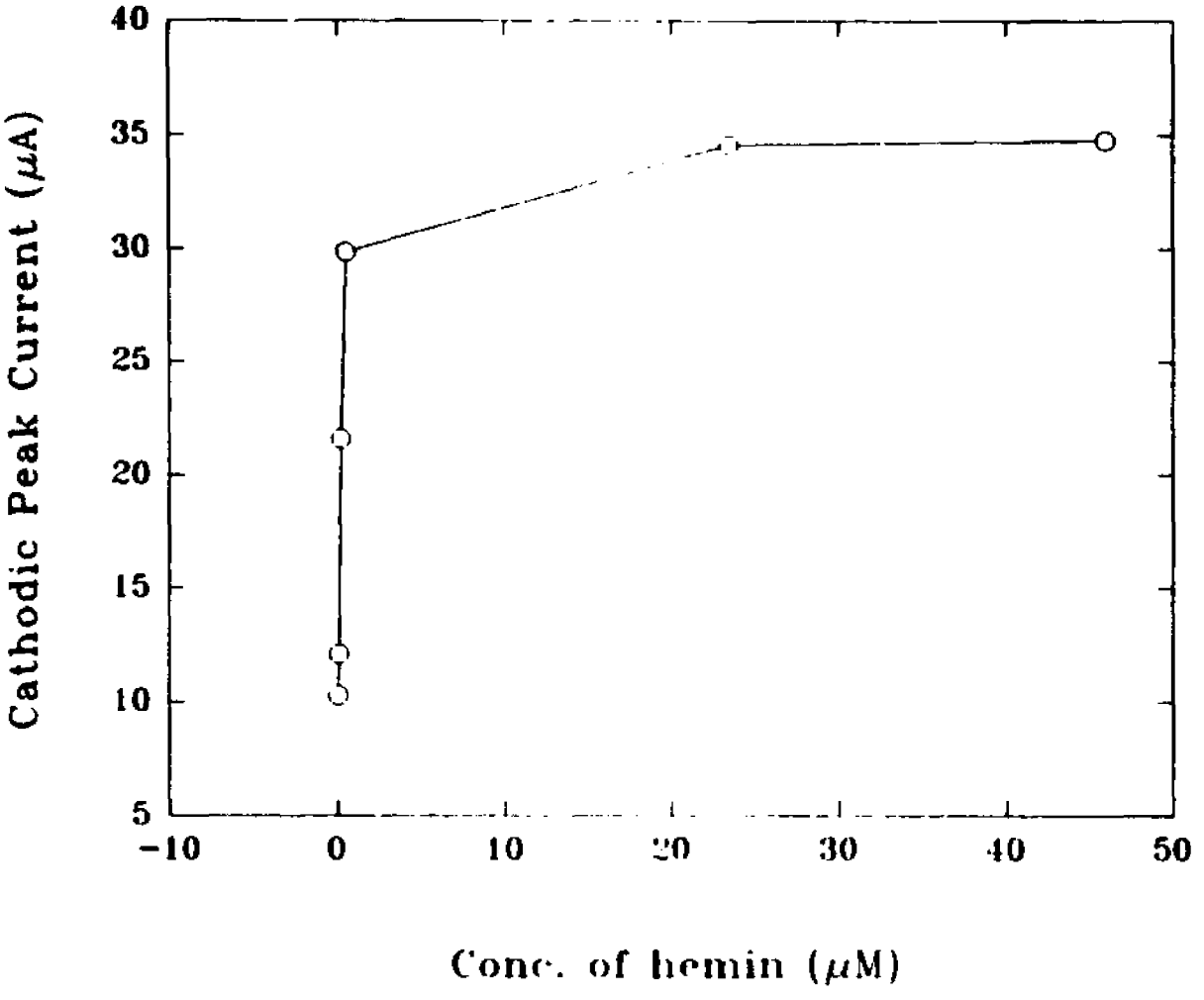

Fig. 4-7: Artemisinin reduction peak current vs. concentration curve.

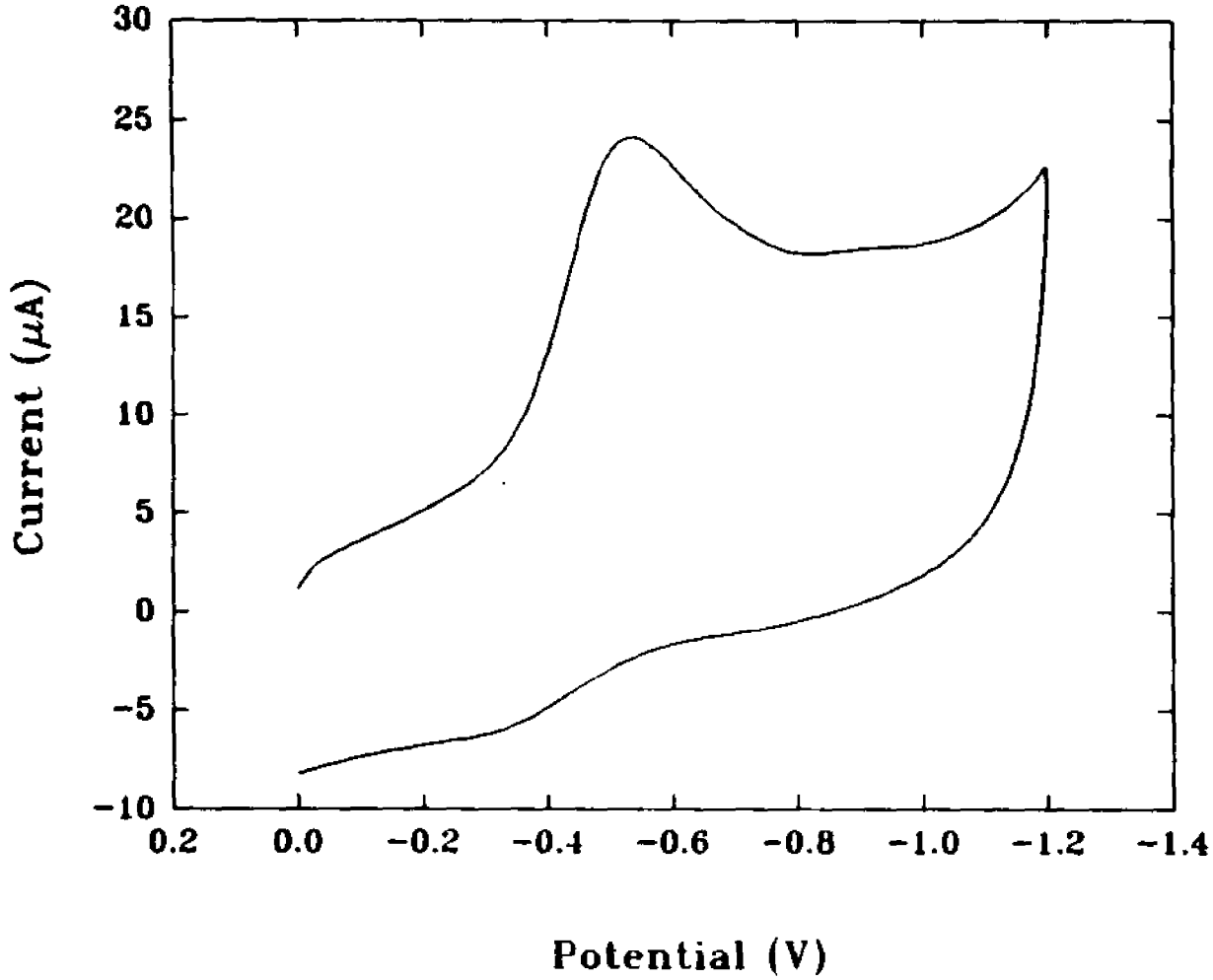

Fig. 4-8: Dihydroartemisinin (1 mM) in the presence of 0.01 M of hemin at 300 mV/sec on GC electrode.

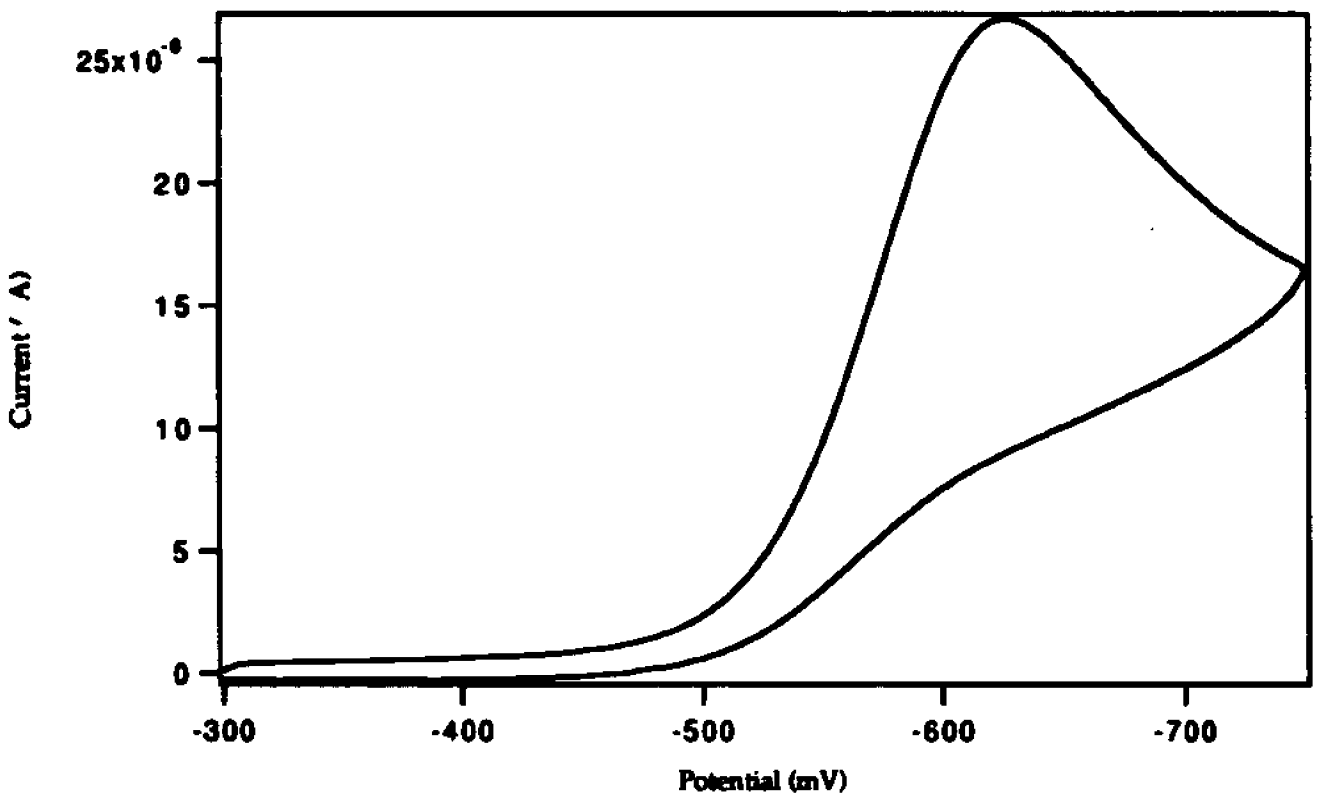

Fig. 4-9: CV of artemisinin (5.1 mM) in 40/60 ethanol/TRIS with Ag electrode (1.6 mm in diameter) at 100 mV/sec.

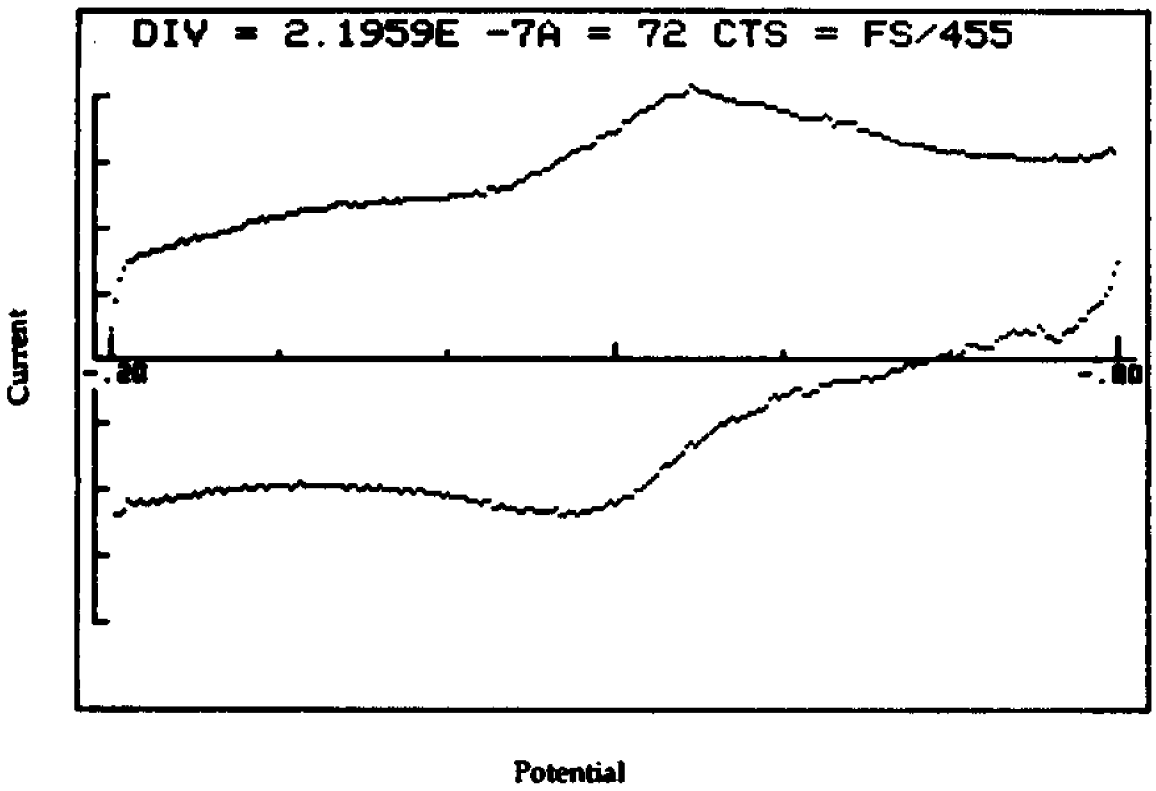

Fig. 4-10: CV of hemin (0.2 mM) in 40/60 ethanol/TRIS with Ag electrode (1.6 mm in diameter).

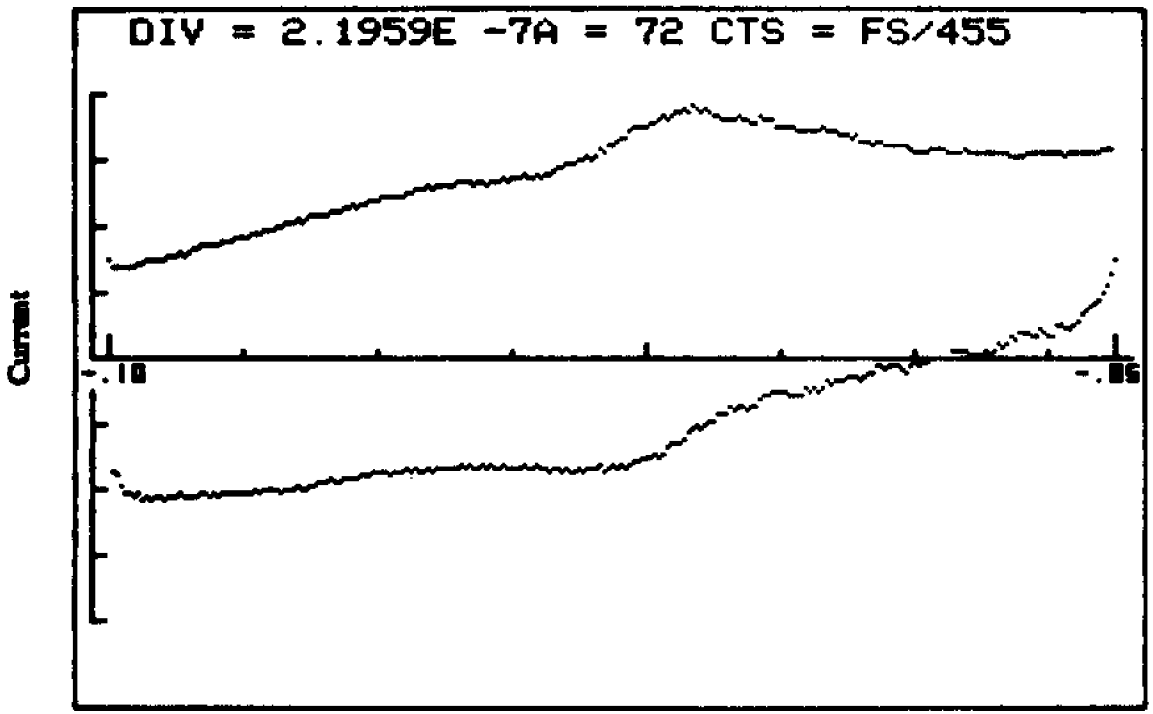

Fig. 4-11: CV of artemisinin (1 mM) in the presence of hemin (0.2 mM) with Ag electrode.

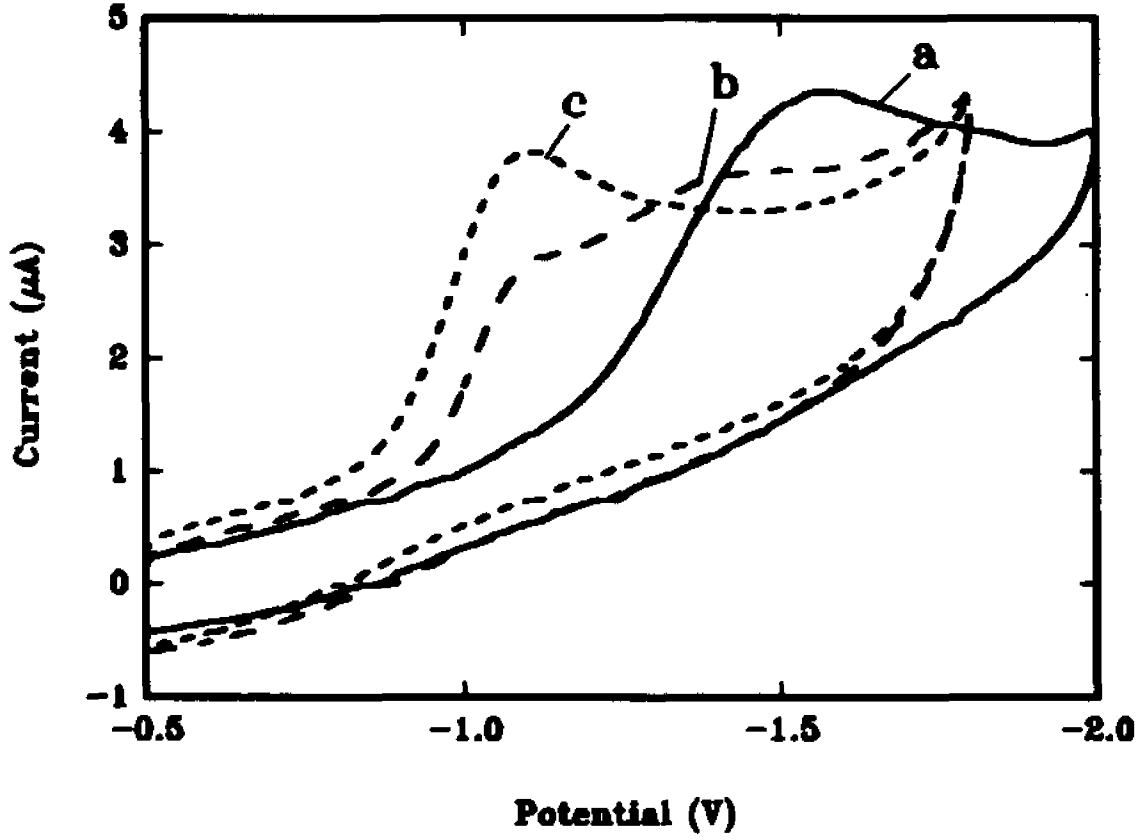

Fig. 4-12: CV of artemisinin (1 mM) in different portions of water/ethanol solvents. (a) 100% ethanol; (b) 80%; (c) 60%

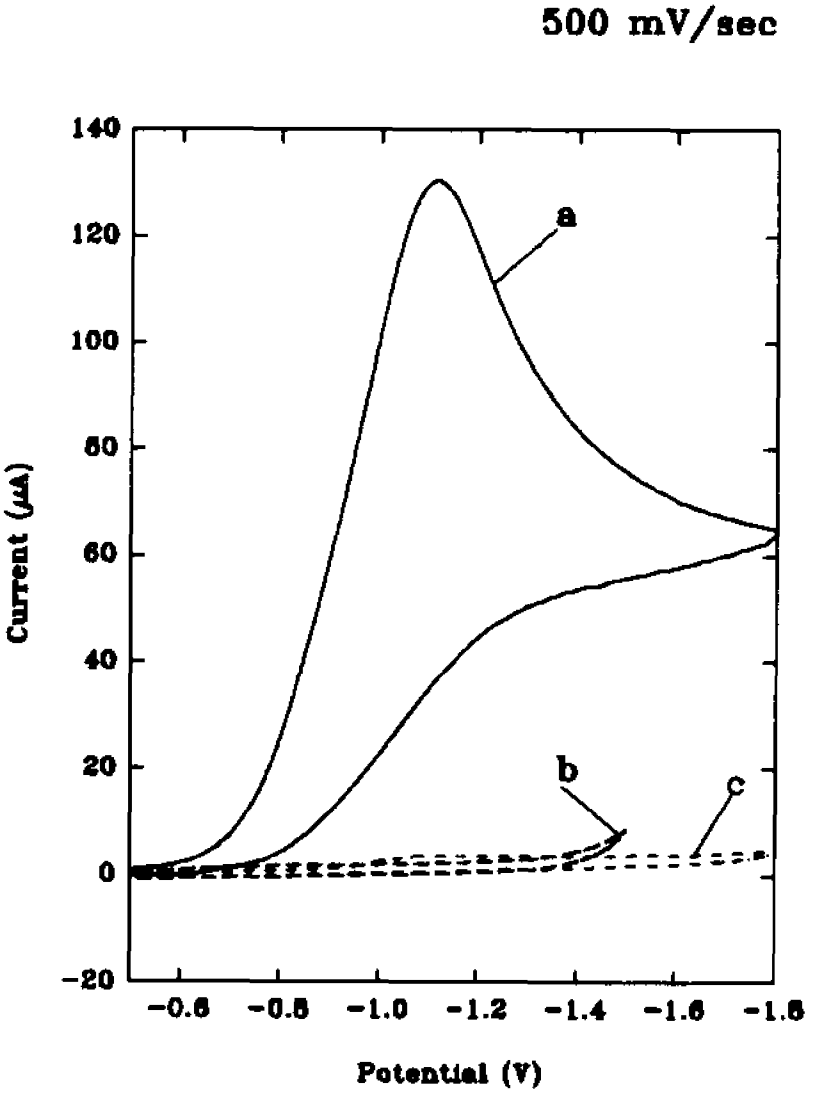

Fig. 4-13: CV of artemisinin (1 mM) at different pH in 60/40 ethanol/water. (a) pH=1.65; (b) pH=13.60; (c) pH=5.85.

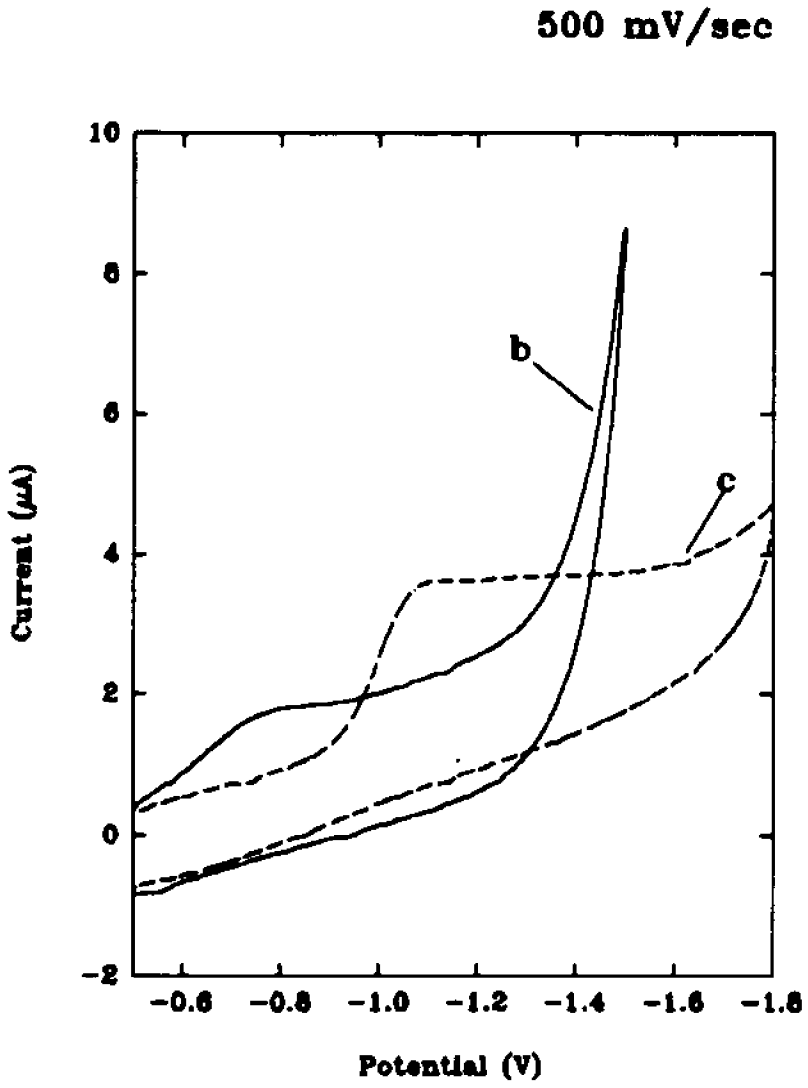

Fig. 4-13: Enlarged CV of (b) and (c).

Sample Number	Concentration of Artemisinin (in mM)	Solvent	αn_a Value
1	1.204	40/60 ethanol/PBS	0.406
2	1.000	40/60 ethanol/PBS	0.337
3	1.098	40/60 ethanol/TRIS	0.290
4	5.000	40/60 ethanol/TRIS	0.312

Table 4-1: Determination of the transfer coefficient in the reduction of artemisinin from the experimental results (3 mm in diameter GC working electrode used).

Sample Number	1	2
Concentration of Artemisinin with Microelectrode (in mM)	7.143	7.143
Diameter of Microelectrode (in μM)	GC (33 μm)	Ag (25 μm)
Concentration of Artemisinin with Minielectrode (in mM)	8.320	8.320
Diameter of Minielectrode (in mm)	GC (3.0 mm)	Ag (1.6 mm)
Slope of Current vs. time $^{-1/2}$	98.295	31.883
Limiting Current (in nA)	45	25
Number of Electron (n)	0.971	1.707
Diffusion Coefficient (D)	1.01×10^{-5}	4.24×10^{-6}

Table 4-2: Experimental results of the total number electron and diffusion coefficient in the reduction of artemisinin.

Sample Number	Concentration of Artemisinin (in mM)	Working Electrode	Solvent	Slope of E_p vs. log (υ) (in mV)	αn_a value
1	8.320	GC (3 mm in diameter)	50/50 ethanol/TRIS	121	0.24
2	7.143	GC (3 mm)	80/60 ethanol/TRIS	74.5	0.40
3	8.320	Ag (1.6 mm)	50/50 ethanol/TRIS	41	0.71
4	7.143	Ag (1.6 mm)	80/60 ethanol/TRIS	54	0.55

Table 4-3: The slope of the artemisinin reduction peak potential vs. logarithm of scan rate from CV experiments.

Fig. 5-1: The structures of soluble synthetic trioxanes used in this study.

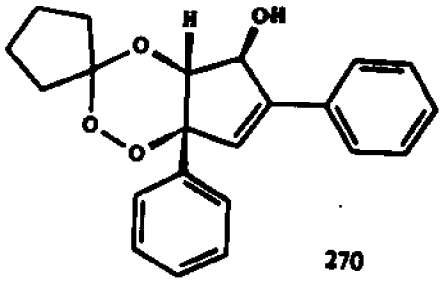

270

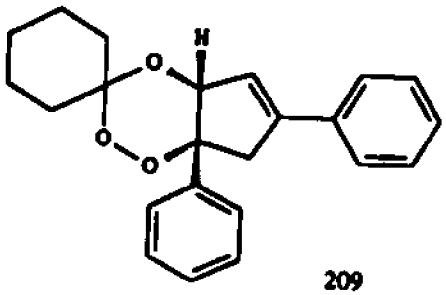

209

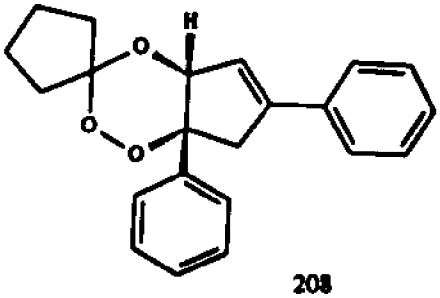

208

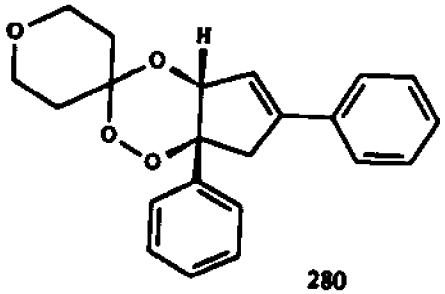

280

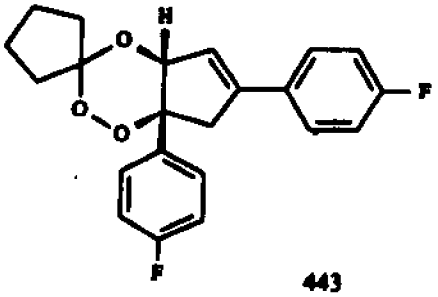

443

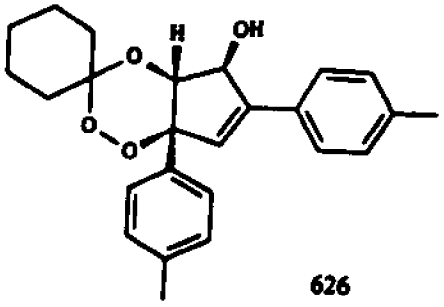

626

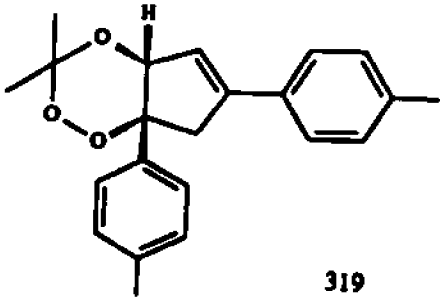

319

Fig. 5-1: The structures of insoluble synthetic trioxanes used in this study.

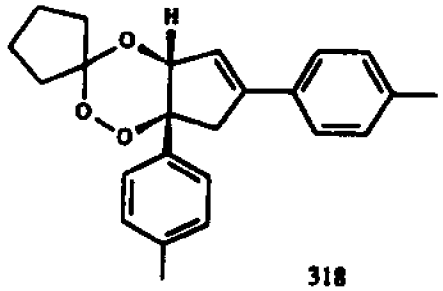

318

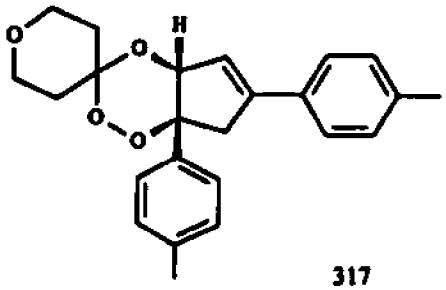

317

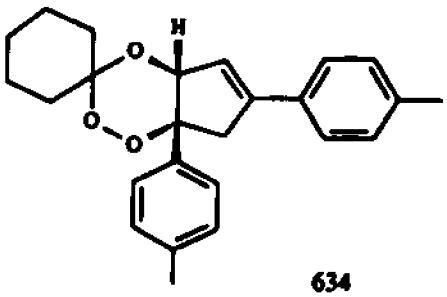

634

Fig. 5-1: The structures of placeboes used in this study.

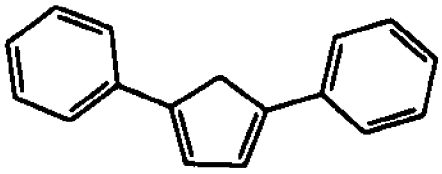

284

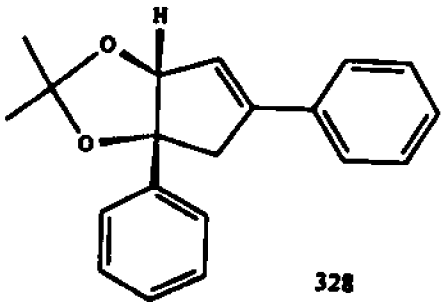

328

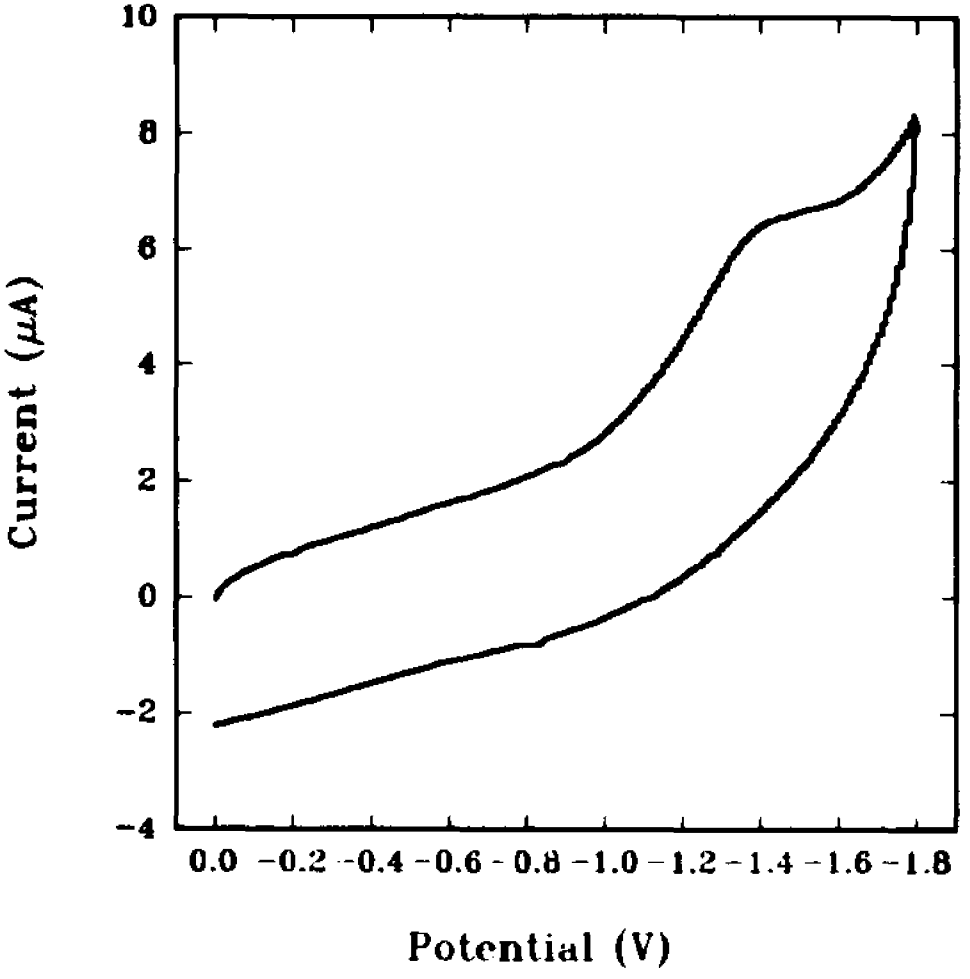

Fig. 5-2: CV of Chem 270 (1 mM) at 300 mV/sec on GC electrode (1 mm in diameter) in 40/60 ethanol/PBS.

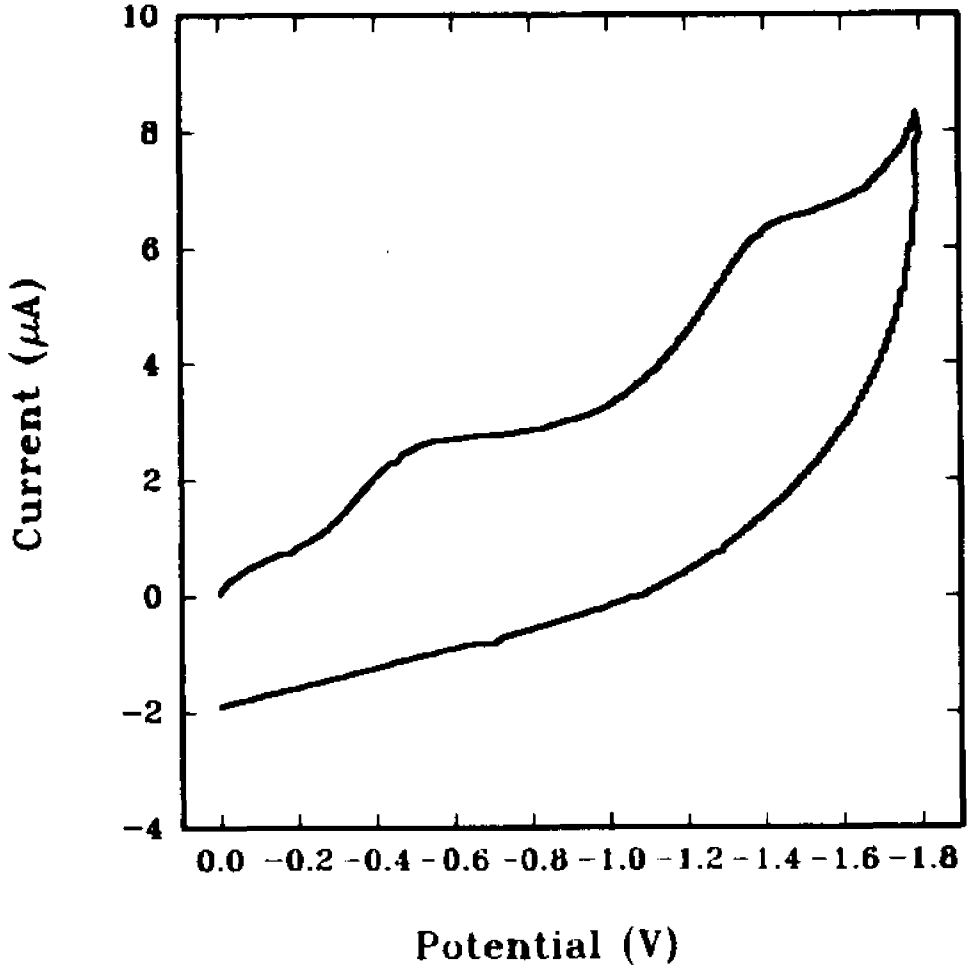

Fig. 5-3: CV of Chem 270 (1 mM) in the presence of hemin (0.01 mM) at 300 mV/sec on GC electrode in 40/60 ethanol/PBS.

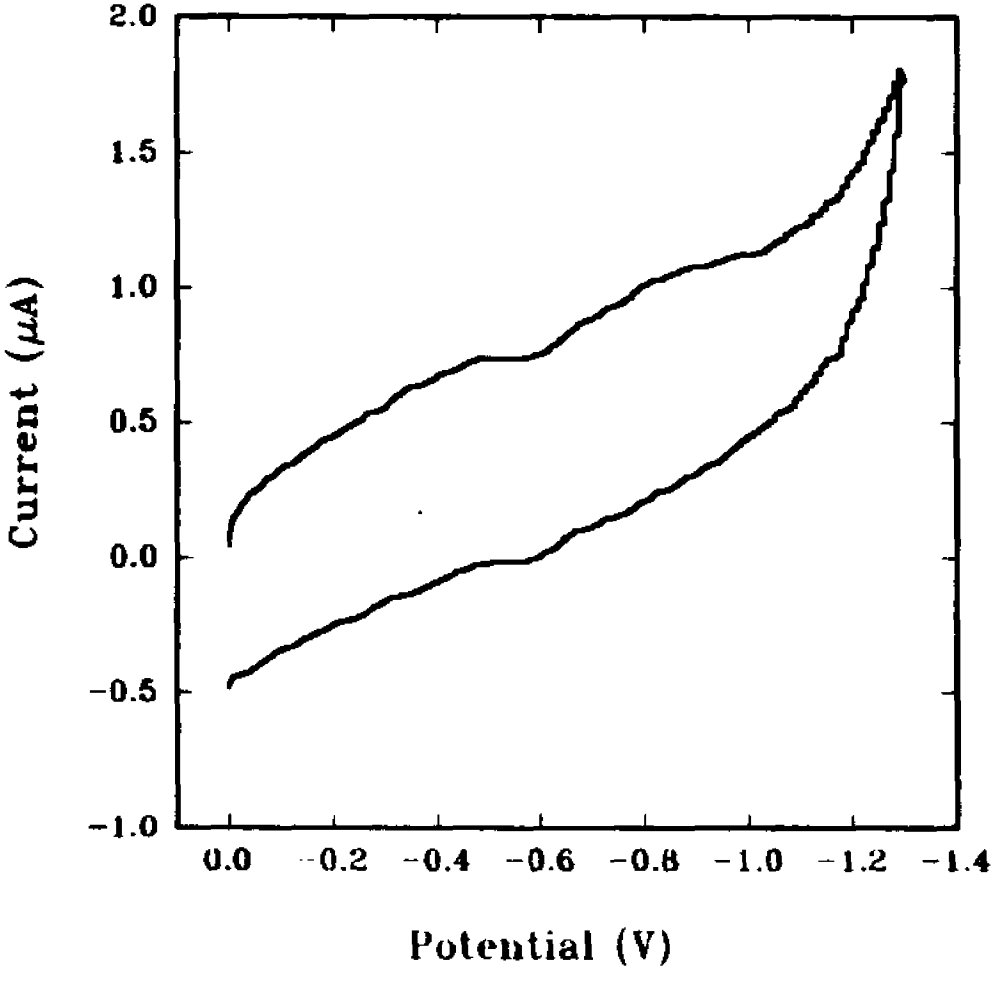

Fig. 5-4: CV of Chem 270 (1 mM) at 100 mV/sec on GC electrode in 85/15 ethanol/TRIS.

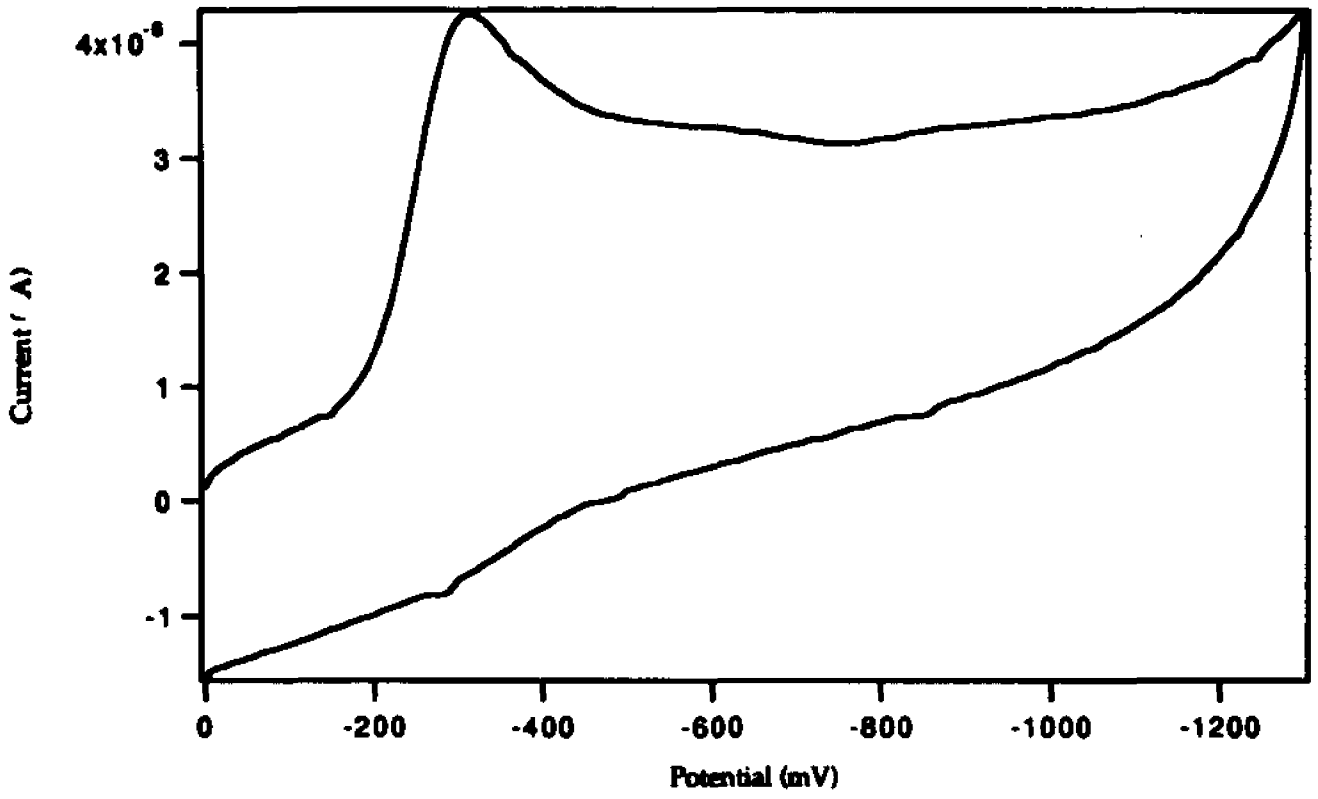

Fig. 5-5a: CV of Chem 270 (1 mM) in the presence of hemin ($1x10^{-5}$ M) in 85/15 ethanol/TRIS with GC electrode at 0.5 V/sec.

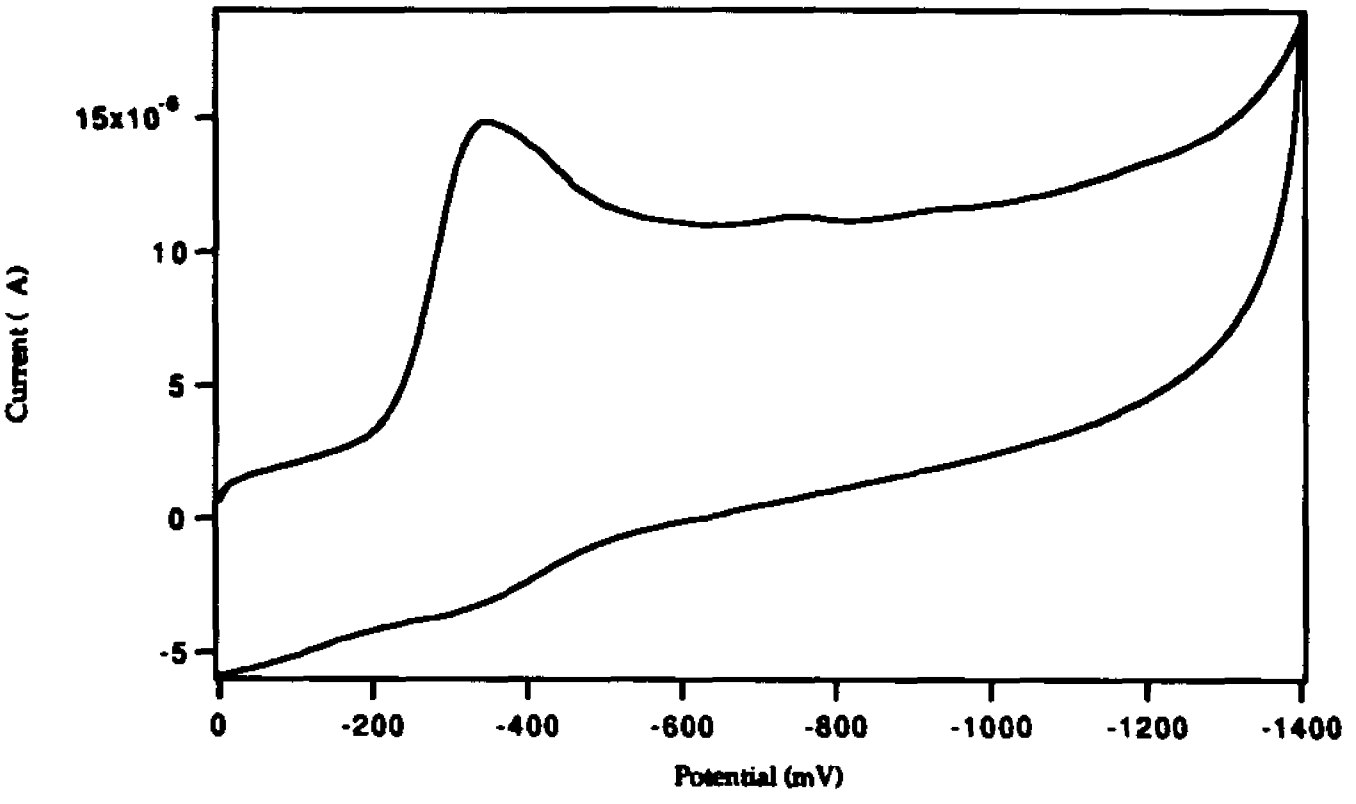

Fig. 5-5b: CV of Chem 270 (1 mM) in the presence of hemin ($1x10^{-5}$ M) in 85/15 ethanol/TRIS with GC electrode at 5 V/sec.

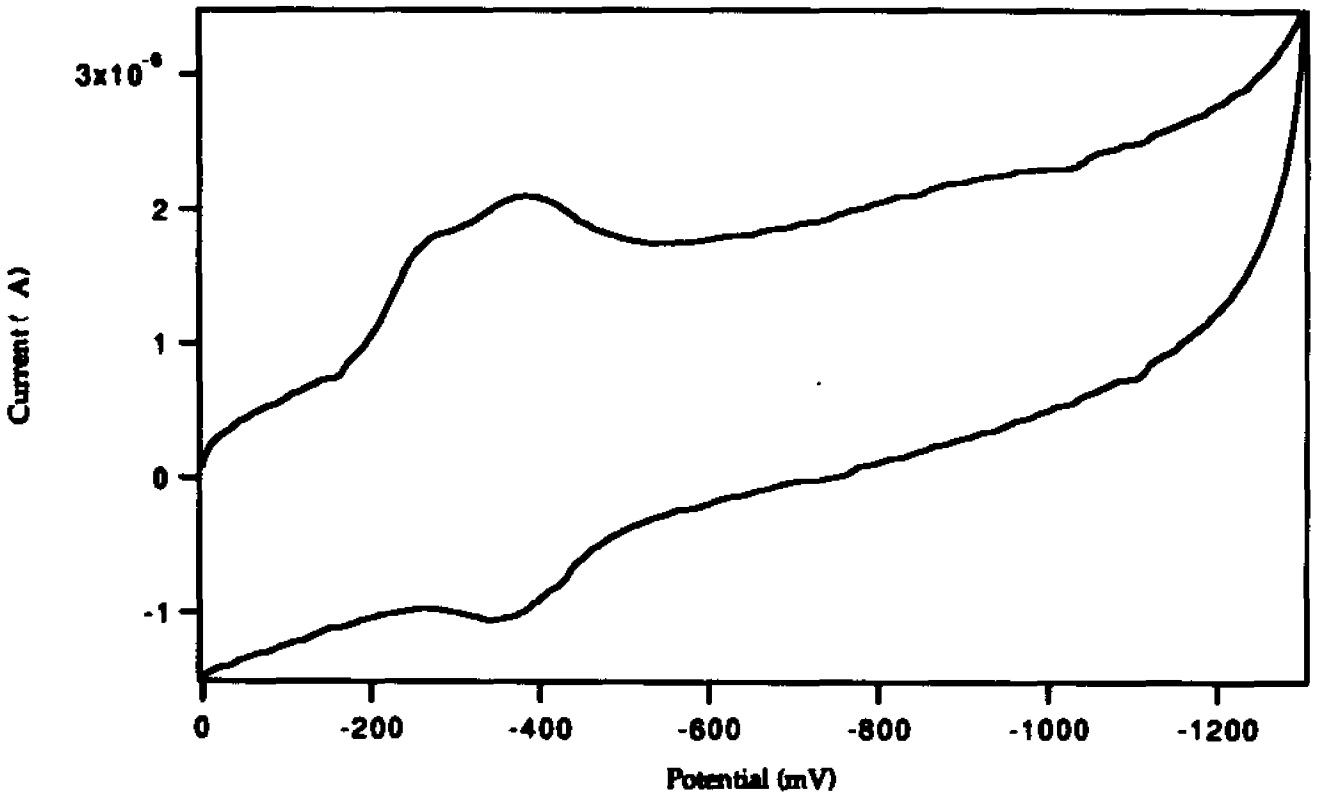

Fig. 5-6a: CV of Chem 328 (1 mM) in the presence of hemin ($1x10^{-5}$ M) in 85/15 of ethanol/TRIS with GC electrode at 0.5 V/sec.

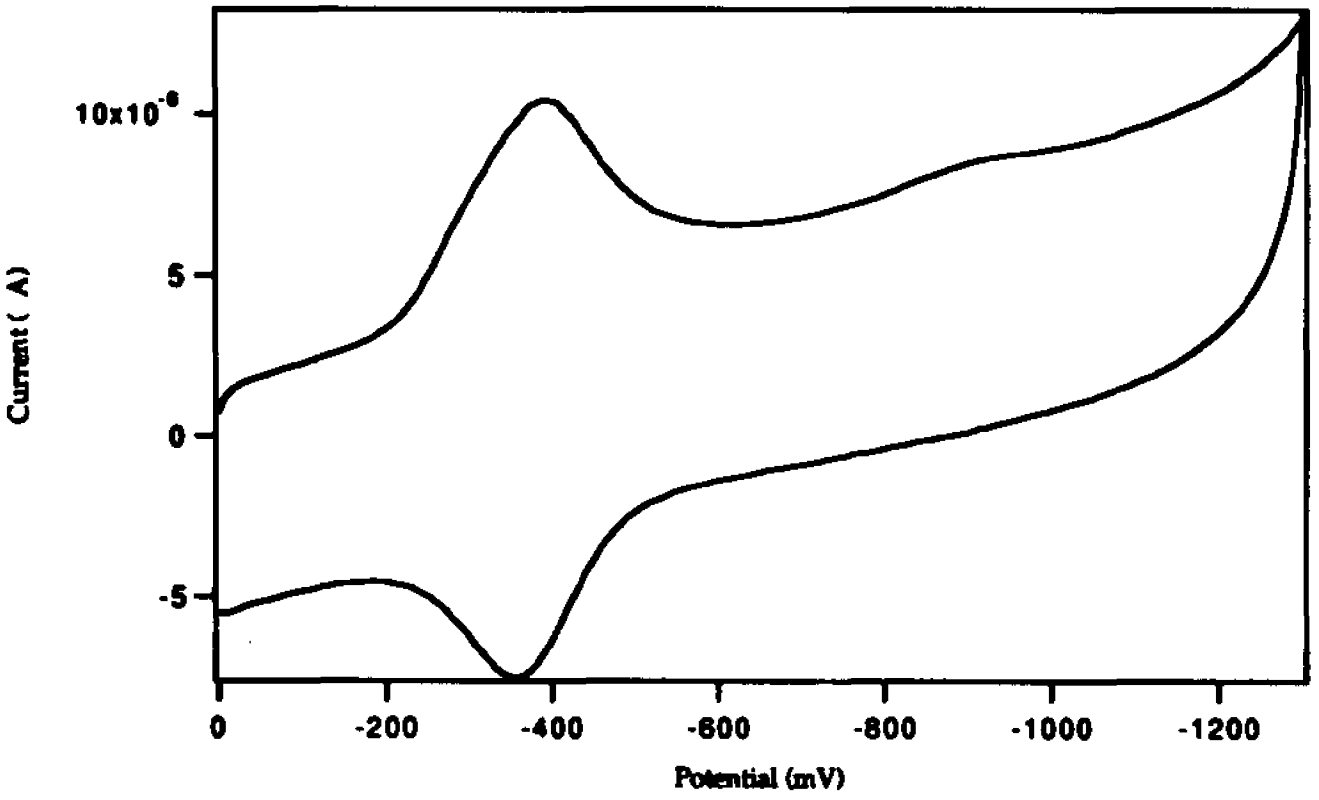

Fig. 5-6b: CV of Chem 328 (1 mM) in the presence of hemin ($1x10^{-5}$ M) in 85/15 ethanol/TRIS with GC electrode at 5 V/sec.

Appendices

Appendix 1: Program CVFIT (Simplex procedure only)

```
{*****************************************************************}
{*            A GENERALIZED SIMULATION PROGRAM                   *}
{*                 FOR CYCLIC VOLTAMMETRY                        *}
{*                                                               *}
{*****************************************************************}

Program runall;    {including inputz.exe and cvrunz.exe}
                   {Version 92 - fits all mechanisms}
                   {flag fitting parameters in same order as flagged before}
                   {Area,Diff,E,Khet,alfa,rkf,rkr}

{Procedures func, input1, input2, output1, output2 are not included}

Procedure amy; {Simplex routine}
label 99;
begin
 outq2name:= 'frstdata.pas';
 assign (outq2,outq2name);
 rewrite(outq2);
 iter := 0;
 while true do begin
 gotoxy(4,8);  writeln('***iteration is: ',iter); {keep track of simplex}

 gotoxy(1,10);
 for ccc := 1 to mp do begin
 for eee := 1 to np do begin
  write(p[ccc,eee]:13,' ');
  write(outq2,p[ccc,eee]:18,'  ');
 end;
  writeln;
  writeln(outq2);
  writeln('  ',y[ccc]:15);
  writeln(outq2,'  ',y[ccc]:20);
 end;
 writeln(outq2);    {readin simplex parameters}
 delay(10000);

 ilo := 1;
 if (y[1] > y[2]) then begin
  ihi := 1;  inhi := 2  end
 else begin
```

```
 ihi := 2;  inhi := 1  end;

for i := 1 to mp do begin    {have to define mp}
 if (y[i] < y[ilo]) then  ilo := i;
 if (y[i] > y[ihi]) then begin
   inhi := ihi;  ihi := i  end
 else if (y[i] > y[inhi]) then
   if (i <> ihi) then inhi := i       {look for the minimun simplex}
 end;

 rtol :=abs(y[ihi]-y[ilo]);
 if (rtol < ftol) then goto 99;
 if (iter = itmax) then begin
    writeln('!too many iterations!');
  exit;                 {stop running simplex}
 end;

 iter := iter+1;
 for j := 1 to np do pbar[j] := 0.0;
 for i := 1 to mp do
   if (i <> ihi) then
   for j := 1 to np do
    pbar[j] := pbar[j]+p[i,j];
 for j := 1 to np do begin
  pbar[j] := pbar[j]/np;
   pr[j] := (1.0+alpha)*pbar[j]-alpha*p[ihi,j]     {simplex reflection}
 end;

 {write out to paramtr.pas}
 {flag fitting parameters in same order as flagged before}
 {Area,Diff,E,Khet,alfa,rkf,rkr}

 letp := 1;

 if Ar[2] > 0.5 then begin
   Ar[1] := pr[letp];  letp := letp + 1;
 end;

 for BB := 1 to nspec do begin
  If Q[bb,2] > 0.5 then begin
    Q[bb,1] := pr[letp]; letp := letp + 1;
  end
 end;

 for BB := 1 to ncoup do begin
  If E[bb,2] > 0.5 then begin
```

```
  E[bb,1] := pr[letp]; letp := letp + 1;
 end;
 if Khet[bb,2] > 0.5 then begin
  Khet[bb,1] := pr[letp]; letp := letp +1;
 end;
 if alfa[bb,2] > 0.5 then begin
  alfa[bb,1] := pr[letp]; letp := letp + 1;
 end;
end;

for bb := 1 to nreact do begin
 if rkf[bb,2] > 0.5 then begin
  rkf[bb,1] := pr[letp]; letp := letp +1;
 end;
 if rkr[bb,2] > 0.5 then begin
  rkr[bb,1] := pr[letp]; letp := letp + 1;
 end;
end;

{Ar := pr[1]; E[1] := pr[2]; khet[1] := pr[3]; alfa[1] := pr[4];}
{rkf[1] := pr[5]; Cap := pr[6];}
output1; func; input3;
ypr := value;       {first func call}

if (ypr <= y[ilo]) then begin      {simplex expansion}
  for j := 1 to np do prr[j] := gamma*pr[j]+(1.0-gamma)*pbar[j];
  {write out to paramtr.pas}

 letp := 1;
 if Ar[2] > 0.5 then begin
  Ar[1] := prr[letp]; letp := letp + 1;
 end;

 for BB := 1 to nspec do begin
  if Q[bb,2] > 0.5 then begin
   Q[bb,1] := prr[letp]; letp := letp + 1;
  end
 end;

 for BB := 1 to ncoup do begin
  if E[bb,2] > 0.5 then begin
   E[bb,1] := prr[letp]; letp := letp + 1;
  end;
  if Khet[bb,2] > 0.5 then begin
   Khet[bb,1] := prr[letp]; letp := letp +1;
  end;
```

```
 if alfa[bb,2] > 0.5 then begin
  alfa[bb,1] := prr[letp]; letp := letp + 1;
 end;
end;

for bb := 1 to nreact do begin
 if rkf[bb,2] > 0.5 then begin
  rkf[bb,1] := prr[letp]; letp := letp +1;
 end;
 if rkr[bb,2] > 0.5 then begin
  rkr[bb,1] := prr[letp]; letp := letp + 1;
 end;
end;

{Ar := prr[1]; E[1] := prr[2]; khet[1] := prr[3]; alfa[1] := prr[4];}
{rkf[1] := prr[5]; Cap := prr[6];}
 output1; func; input3;
 yprr := value; {seocnd func call}

if (yprr < y[ilo]) then begin
 for j := 1 to np do p[ihi,j] := prr[j];
 y[ihi] := yprr end
else begin
 for j := 1 to np do p[ihi,j] := pr[j];
 y[ihi] := ypr end end
else if (ypr >= y[inhi]) then begin
if (ypr < y[ihi]) then begin
 for j := 1 to np do p[ihi,j] := pr[j];
 y[ihi] := ypr end;

for j := 1 to np do prr[j] := beta*p[ihi,j]+(1.0-beta)*pbar[j];

{write out to paramtr.pas }    {simplex contraction}

letp := 1;

if Ar[2] > 0.5 then begin
 Ar[1] := prr[letp]; letp := letp + 1;
end;

for BB := 1 to nspec do begin
 if Q[bb,2] > 0.5 then begin
  Q[bb,1] := prr[letp]; letp := letp + 1;
 end
end;
```

```
for BB := 1 to ncoup do begin
 if E[bb,2] > 0.5 then begin
  E[bb,1] := prr[letp]; letp := letp + 1;
 end;
 If Khet[bb,2] > 0.5 then begin
  Khet[bb,1] := prr[letp];  letp := letp +1;
 end;
 if alfa[bb,2] > 0.5 then begin
  alfa[bb,1] := prr[letp]; letp := letp + 1;
 end;
end;

for bb := 1 to nreact do begin
 if rkf[bb,2] > 0.5 then begin
  rkf[bb,1] := prr[letp]; letp := letp +1;
 end;
 if rkr[bb,2] > 0.5 then begin
  rkr[bb,1] := prr[letp]; letp := letp + 1;
 end;
end;

{Ar := prr[1];  E[1] := prr[2];  khet[1] :=  prr[3];  alfa[1] := prr[4];}
{rkf[1] := prr[5];  Cap := prr[6];}
 output1;  Func;  input3;
 yprr := value;  {third func call}

if (yprr < y[ihi]) then begin
  for j := 1 to np do p[ihi,j] := prr[j];
 y[ihi] := yprr  end
else begin
  for i := 1 to mp do
    if (i <> ilo) then begin
     for j := 1 to np do begin
      pr[j] := 0.5*(p[i,j]+p[ilo,j]);
      p[i,j] := pr[j]
     end;

 {write out to paramtr.pas}

letp := 1;

if Ar[2] > 0.5 then begin
  Ar[1] := pr[letp];  letp := letp + 1;
end;

for BB := 1 to nspec do begin
```

```
      if Q[bb,2] > 0.5 then begin
       Q[bb,1] := pr[letp]; letp := letp + 1;
      end
     end;

     for BB := 1 to ncoup do begin
      if E[bb,2] > 0.5 then begin
       E[bb,1] := pr[letp]; letp := letp + 1;
      end;
      If Khet[bb,2] > 0.5 then begin
       Khet[bb,1] := pr[letp];  letp := letp +1;
      end;
      if alfa[bb,2] > 0.5 then begin
       alfa[bb,1] := pr[letp]; letp := letp + 1;
      end;
     end;
     for bb := 1 to nreact do begin
      if rkf[bb,2] > 0.5 then begin
       rkf[bb,1] := pr[letp]; letp := letp +1;
      end;
      if rkr[bb,2] > 0.5 then begin
       rkr[bb,1] := pr[letp]; letp := letp + 1;
      end;
     end;

     {Ar := pr[1]; E[1] := pr[2]; khet[1] := pr[3]; alfa[1] := pr[4];}
     {rkf[1] := pr[5]; Cap := pr[6];}
      output1; func; input3;
      y[i] := value; {4th func call} end end end
      else begin
       for j := 1 to np do p[ihi,j] := pr[j];
       y[ihi] := ypr
      end end;
99:
  writeln('===> error criterion satisfied !');
  writeln(outq2,iter);
  close(outq2);
end;

{********************** MAIN PROGRAM **********************}

Begin
 alpha :=1.0; beta :=0.5; gamma :=2.0; itmax := 10000;
 {ftol := 10E-12;}
 textcolor(yellow);
 textbackground(blue);
```

```
  swapvectors;
   exec('inputz.exe',");
  swapvectors;

  func;    {run cvrunz, calc sumofsq. it uses new diffusion constsnt}
  input1;  {read the paramtr.pas file} np := par; mp := par +1;
  input2;  {read the sumofsq file -- sumof.pas }
  amy;
End.
```

Appendix 2: Program of EET for 5 fitting parameters

```
program errorestimation;
                              {this program uses the simplex results to calculate}
{$N+}                         {the error estimation of the fitting parameters.}
{$G+}
{$M 1024,0,0}
uses Dos,Crt;
const
  np = 5;  n = np;  mp = np + 1;  round = 1.0e-9;
type
  glindx = array [1..np] of longint;
  glnarray = array [1..np] of extended;
  glnpbynp = array [1..np,1..np] of extended;
var
  b: glnarray;
  a,y: glnpbynp;  { a is B matrix }
  indx: glindx;
  d,r: extended;

  (*$I ludcmp.pas *)
  (*$I lubksb.pas *)
var
  error : array[1..mp] of extended;
  p : array[1..mp,1..mp] of extended;
  halfp : array[1..mp,1..mp,1..mp] of extended;
  er : array[1..mp,1..mp] of extended;
  w : array[1..mp] of extended;
  rd : array[1..mp] of extended;
  cntr : array[1..mp] of extended;  { centroid of all np+1 }
  av : array[1..np] of extended;  { A vector }
  qm : array[1..np,1..np] of extended;  { Q matrix }
  t : array[1..np] of extended;
  h : array[1..np] of extended;
  v : array[1..np,1..np] of extended;
```

```
  pmin : array[1..np] of extended;
  ematx : array[1..np,1..np] of extended;
  sdp : array[1..np] of extended;

  infname : string[12]; {sumofdat.pas : this file is part of frstdata.pas}
  inf1 : text;
  outfname : string[12];  { rsltdata.pas }
  outrd : text;

  i,j,l,k,npo,bb,count,ilo : integer;
  sumofsq,emin,ase,x1,x2,ext1,ext2,ecntr: double;

  code,par,nspec,ncoup,ns,nreact,ncyc : integer;
  ipot,spot,spot2,fpot,scanr,te,Ar,Cap,Res,Cstar : extended;
  nt : longint;
  ansC, ansI : char;
  Q : array[1..8] of extended;
  C : array[1..8,1..50] of extended;
  E : array[1..6] of extended;
  Ired : array[1..2,1..6] of longint;
  khet : array[1..6] of extended;
  alfa : array[1..6] of extended;
  IR : array[1..2,1..6] of longint;
  IP : array[1..2,1..6] of longint;
  rkf : array[1..6] of extended;
  rkr : array[1..6] of extended;

  inq1name   : string[12];  {paramtr.pas}
  inq1       : text;
  inq3name   : string[12];
  inq3       : text;
  outq1name : string[12];
  outq1      : text;

procedure input1;
begin
  inq1name := 'paramtr.pas';
  assign(inq1,inq1name);
  reset(inq1);

  readln(inq1,ansC);
  readln(inq1,ansI);
  readln(inq1,code);
  readln(inq1,par);

  read(inq1,Ar,Cstar);
```

```
 if ansC = 'y' then  begin
  read(inq1,Cap,Res);
 end else begin
    if ansI = 'y' then  read(inq1,Res);
 end;
 readln(inq1);

 readln(inq1,te);
 readln(inq1,nspec);

 For bb := 1 to nspec do begin
  readln(inq1,C[bb,1]);
 end;

 Readln(inq1,ncyc);
 if ncyc = 1 then Read(inq1,ipot,fpot,scanr);
 if ncyc = 2 then Read(inq1,ipot,spot,fpot,scanr);
 if ncyc = 3 then read(inq1,ipot,spot,spot2,fpot,scanr);
 Readln(inq1);

 For bb := 1 to nspec do begin
  Readln(inq1,q[bb]);
 end;

 Readln(inq1,ncoup);
 For bb := 1 to ncoup do begin
  read(inq1,Ired[1,bb],Ired[2,bb],E[bb],khet[bb],alfa[bb]);
   readln(inq1);
 end;

 readln(inq1,nreact);
 if nreact > 0 then begin
  for bb := 1 to nreact do begin
   read(inq1,ir[1,bb],ir[2,bb],ip[1,bb],ip[2,bb],rkf[bb],rkr[bb]);
    readln(inq1);
  end;
 end;
 close(inq1);
end;

procedure output1;  {output a single set of parameters}
            {overwrite param1.pas code 20}
begin
 outq1name := 'paramtr.pas';
 assign(outq1,outq1name);
 rewrite(outq1);
```

```
writeln(outq1,ansC);
writeln(outq1,ansI);
writeln(outq1,20);
writeln(outq1,par);

write(outq1,Ar:18,'  ',Cstar:18,'  ');
if ansC = 'y' then  begin
  write(outq1,Cap:18,'  ',Res:18);
end else begin
  if ansI = 'y' then  write(outq1,Res:18);
end;
writeln(outq1);

writeln(outq1,Te:7:3);
writeln(outq1,nspec);

For bb := 1 to nspec do begin
 writeln(outq1,C[bb,1]:7:3);
end;

writeln(outq1,ncyc);
write(outq1,ipot:8:3,'    ');

if ncyc = 2 then write(outq1,spot:8:3,'    ');
if ncyc = 3 then begin
                   write(outq1,spot:8:3,'    ');
                   write(outq1,spot2:8:3,'    ');
                 end;

write(outq1,fpot:8:3,'    ');
write(outq1,scanr:8:4);
writeln(outq1);

for bb := 1 to nspec do begin
 writeln(outq1,q[bb]:7:3);
end;

writeln(outq1,ncoup);
For bb := 1 to ncoup do begin
  write(outq1,'  ',Ired[1,bb],'  ',Ired[2,bb],'  ',E[bb]:18,'  '
     ,khet[bb]:18,'  ',alfa[bb]:18);
  writeln(outq1);
end;

writeln(outq1,nreact);
```

```
  For bb := 1 to nreact do begin
   write(outq1,' ',Ir[1,bb],' ',Ir[2,bb],' ',Ip[1,bb],' ',Ip[2,bb],
   ' ',rkf[bb]:18,' ',rkr[bb]:18);
    writeln(outq1);
  end;
  close(outq1);
end;

procedure func;
begin
  swapvectors;
   exec('cvrun1.exe','');
  swapvectors;
end;

procedure input3; {read a single sum of square }
begin
  inq3name := 'tsum.pas';
  assign(inq3,inq3name);
  reset(inq3);
  readln(inq3,sumofsq,npo);
  close(inq3);
end;

procedure errest;
begin
  infname := 'sumofdat.pas';  assign(inf1,infname);  reset(inf1);
  write(outrd, '* the rounding error is:    ');
  writeln(outrd, round:0);
  {read in data from simplex program}
  writeln(outrd, '* the parameters and errors from the last simplex are:');
  for i :=1 to mp do begin
   for j :=1 to np do begin
    read(inf1, p[i,j]);
     write(outrd,p[i,j]:18,'  ');
   end;
   readln(inf1);
   writeln(outrd);
   readln(inf1,error[i]);
   error[i] := error[i] * 1.0e-6;
   writeln(outrd,error[i]:20);
  end;

  {calculate the centroid of all np+1 vertices}
  for j := 1 to np do begin
   cntr[j] := 0.0;
```

```
  for i := 1 to mp do begin
   cntr[j] := cntr[j] + p[i,j];
  end;
  cntr[j] := cntr[j]/mp;
end;
Ar := cntr[1]; {Cap := cntr[2];} E[1] := cntr[2];
khet[1] := cntr[3]; alfa[1] := cntr[4]; rkf[1] := cntr[5];
output1; func; input3;
ecntr := sumofsq * 1.0e-6; {first call cvrun1}

writeln(outrd, '* the centroid and it''s error are:');
for j := 1 to np do begin
  write(outrd,cntr[j]:18,' ');
end;
writeln(outrd);
writeln(outrd,ecntr:20);

{calculate the rounding errors}
count := 0;
for i :=1 to mp do begin
if ((error[i]-ecntr)/ecntr < round) then begin
  count :=count + 1;
  for j :=1 to np do begin
   p[i,j] := p[i,j] + ( p[i,j] - cntr[j] );
   rd[j] := p[i,j];
  end;
  Ar := rd[1]; {Cap := rd[2];} E[1] := rd[2];
  khet[1] := rd[3]; alfa[1] := rd[4]; rkf[1] := rd[5];
  output1; func; input3;
  error[i] := sumofsq * 1.0e-6; {second call cvrun1}
end; end;

writeln(outrd, '* expand simplex''s parameters & errors: ');
for i := 1 to mp do begin
  for j := 1 to np do begin
    write(outrd,p[i,j]:18,' ');
  end;
  writeln(outrd);
  writeln(outrd,error[i]:20);
end;

{calculate the minimum error function}
ilo := mp;
for i := 1 to mp do begin
if (error[i] < error[ilo]) then begin
  ext1 := error[ilo];
```

```
 error[ilo] := error[i];
 error[i] := ext1;
 for j := 1 to np do begin
  ext2 := p[ilo,j];
  p[ilo,j] := p[i,j];
  p[i,j] := ext2;
 end;
end; end;

 writeln(outrd,'* the minimum error function data are: ');
 write(outrd,ilo);
for j := 1 to np do begin
  write( outrd,' ', p[ilo,j]:18,'  ');
end;
 writeln(outrd,error[ilo]:20);

{calculate the half-way points and errors};
for j := 1 to np do begin
for i := 1 to np do begin
for k := i + 1 to mp do begin
 halfp[j,i,k] := (p[i,j] + p[k,j])/2;
 halfp[j,k,i] := halfp[j,i,k];
end; end; end;

for i := 1 to np do begin
for k := i+1 to mp do begin
for j := 1 to np do begin
 w[j] := halfp[j,i,k];
end;
 Ar := w[1]; {Cap := w[2];} E[1] := w[2];
 khet[1] := w[3]; alfa[1] := w[4]; rkf[1] := w[5];
  output1; func; input3;
 er[i,k] := sumofsq * 1.0e-6;
 er[k,i] := er[i,k]; {third call cvrun1}
end; end;

 writeln(outrd, '* the half-way points" data and errors: ');
for i := 1 to np do begin
for k := i + 1 to mp do begin
  write(outrd,i,' ',k,' ');
 for j := 1 to np do begin
   write(outrd, halfp[j,i,k]:18,'  ');
 end;
  writeln(outrd);
  writeln(outrd,er[i,k]:20);
end; end;
```

```
{calculate the a vector, B and Q matrixes};
for i := 1 to np do begin
  av[i] := 2 * er[ilo,i] - (error[i] + 3 * error[ilo])/2;
  a[i,i] := 2 * (error[i] + error[ilo] - 2 * er[ilo,i]);
end;

for i := 1 to np do begin
for k := i + 1 to mp do begin
if ( k <> ilo ) then begin
  a[i,k] := 2 * ( er[i,k] + error[ilo] -er[ilo,i] -er[ilo,k] );
  a[k,i] := a[i,k];
end; end; end;

for j := 1 to np do begin
for i := 1 to np do begin
  qm[i,j] := p[i,j] - p[ilo,j];
end; end;

 writeln(outrd, '* the a vector is composed by :  ');
for i := 1 to np do begin
  write(outrd,av[i]:18,'  ');
end;
 writeln(outrd);

 writeln(outrd, '* the B symmetric matrix is: ');
for i := 1 to np do begin
for k := 1 to np do begin
  write(outrd,a[i,k]:18,'  ');
end;
 writeln(outrd);
end;

 writeln(outrd, '* the Q matrix is:');
for i := 1 to np do begin
for j := 1 to np do begin
  write(outrd,qm[i,j]:18,'  ');
end;
 writeln(outrd);
end;
 close(inf1);
end;
procedure result;  {this part is for calculate the error result}
begin
     writeln(outrd,'************************************************************');
```

```
{begin to calculate the inverse of matrix a[i,j]=B matrix}
ludcmp(a,n,np,indx,d);
for j := 1 to np do begin
for i := 1 to np do b[i] := 0.0;
 b[j] := 1.0;
  lubksb(a,n,np,indx,b);
 for i := 1 to np do y[i,j] := b[i];
end;

{multiply (y[i,j]=B-1)*(av=A vector)}
for i := 1 to np do begin
 t[i] := 0.0;
 for j := 1 to np do begin
  t[i] := t[i] + y[i,j] * av[j];
 end;
end;

{calculate the t[i]*t[i] = A*B-1*B-1*At and Q*B-1*At}
for i := 1 to np do begin
 r := 0.0;
 h[i] := 0.0;
 for j := 1 to np do begin
  r := r + t[j] * t[j];
  h[i] := h[i] + qm[i,j] *t[j];
 end;
end;

writeln(outrd, '* the (Q*B-1*At) = MCAD x.prn is:  ');
for i := 1 to np do begin
  write(outrd,h[i]:18,'  ');
end;
writeln(outrd);
writeln(outrd, '* the (A*B-1*B-1*At) = MCAD y.prn is:  ');
writeln(outrd,r:18);

{calculate the qm[i,j]*y[i,j]*qm[i,j]t = Q*B-1*Qt}
writeln(outrd, '* the (Q*B-1*Qt) = MCAD z.prn is:  ');
for i := 1 to np do begin
for j := 1 to np do begin
 x1 := 0.0;
 for k := 1 to np do begin
  x2 := 0.0;
  for l := 1 to np do begin
   x2 := x2 + y[k,l] * qm[j,l];
  end;
  x1 := x1 + qm[i,k] *x2;
```

```
 end;
 v[i,j] := x1;
  write(outrd,v[i,j]:18,'  ');
end;
 writeln(outrd);
end;

{begin to calculate the parameter error results}
if r > 1.0 then begin
  writeln('  * the y inequality is not satisfied!');
  writeln(outrd,'* the y inequality is not satisfied!');
 exit;
end else begin
 for j := 1 to np do begin
  pmin[j] := p[ilo,j];
 end;
 emin := error[ilo];
end;

 writeln(outrd, '* the minimum parameters and function error:');
for j := 1 to np do begin
  write(outrd,pmin[j]:18,'  ');
end;
 writeln(outrd);
 writeln(outrd,emin:20);

ase := emin/(npo-np);
 writeln(outrd, '* the number of data points and the mean square error is:');
 writeln(outrd,npo:10,'    ',ase:18);

for i := 1 to np do begin
for j := 1 to np do begin
 ematx[i,j] := ase * v[i,j];
end; end;
 writeln(outrd, '* the error matrix or variance-covariance matrix is:');
for i := 1 to np do begin
for j := 1 to np do begin
  write(outrd,ematx[i,j]:18,'  ');
end;
 writeln(outrd);
end;

 writeln(outrd, '* the estimated standard deviation of the ith parameters:');
for i := 1 to np do
for j := 1 to np do
if (i=j) then begin
```

```
   sdp[i] := sqrt(ematx[i,j]);
  end;
  for i := 1 to np do begin
   writeln(outrd,sdp[i]:18);
  end;
end;

        {*******************MAIN  PROGRAM*******************}

begin
  textbackground( blue );
  textcolor( yellow );
  clrscr;
  input1;
  input3;

  outfname := 'rsltdata.pas';
  assign(outrd,outfname);
  rewrite(outrd);

  errest;
  result;
  close(outrd);
end.
```

Appendix 3: Program of random noise generator

```
Program Random;
        {This program is used to produce a file of gaussian random noise}
        {of number points = npts}

Uses Crt;

Const  n = 20;

Var
  infile : string[12];
  rfile : text;

  i, idum, iset, k, klim, npts : integer;
  j, gset, glgset : real;

  gliset, glinext, glinextp : integer;
  glma : Array[1..55] of real;
```

```
 (*$I MODFILE.PAS *)
 (*$I RAN3.PAS *)
 (*$I GASDEV.PAS *)

Begin
 textcolor(yellow);
 textbackground(blue);
 clrscr;

 writeln('How many data points ?'); readln(npts);
 writeln('Noise file will be named (noise.pas)?'); readln(infile);
 assign(rfile,infile);
 rewrite(rfile);

 gliset := 0;
 idum := -13;
 For i:= 1 to npts do
 Begin
  j := gasdev(idum)*0.2*1e-3;
       { 0.2 can be changed for different amplitude of noise }
  writeln(rfile,j);
 end;
 close(rfile);
End.
```

Appendix 4: Program of creating a linear background data file

```
Program Backgroundintheory;  {background of an CV experimental data is }
                             {expressed in y = a*x. }
                             {the Cap and IR are not deducted.}
{$N+}
{$G+}
Uses Crt;
Var
 iexp,current,y,slope,pot,ipot,spot,fpot : extended;
 i : integer;
 infname,outfname : string[12];
 infile,outfile : text;

Begin
 textcolor(yellow);
 textbackground(blue);
 clrscr;

 gotoxy(12,5); writeln('what is the input expt. data name (d.pas)? ');
```

```
  gotoxy(12,7);  writeln('what is the slope of the background line (amperes/V)?
');
  gotoxy(12,9);  writeln('what is the initial potential(V)? ');
  gotoxy(12,11); writeln('what is the switch potential(V)? ');
  gotoxy(12,13); writeln('what is the final potential(V)? ');
 gotoxy(12,16);
  writeln('what is the output expt. file with added background line (data.pas)?
');

  gotoxy(12,6);  readln(infname);

  gotoxy(12,8);  readln(slope);
  gotoxy(12,10); readln(ipot);
  gotoxy(12,12); readln(spot);
  gotoxy(12,14); readln(fpot);
  gotoxy(12,17); readln(outfname);

  assign(infile,infname);      reset(infile);
  assign(outfile,outfname);    rewrite(outfile);

  while not eof(infile) do  begin
    readln(infile,pot,iexp);
   y := slope * (pot-ipot);
   current := iexp + y;
    writeln(outfile,pot:10:15,'    ',current:18);
  end;
close(infile);
close(outfile);
end.
```

Appendix 5: Program of data addition to 1 mV per point for fast scan experiments

```
Program Adddatato1mvperpoint;
                              {This program is used to convert expt data}
                              {to 1 mv/point when scan rate is fast in order}
                              {to fit in the simulation program which requires}
                              {1 mv/point in the calculation}
{$N+}
{$G+}
Uses Crt;
Var
  vstep,npoint : integer;
  i,j : integer;
  iexp : array[1..302] of real;
  current : array[1..1205,1..4] of real;
```

```
 Eexp : array[1..302] of real;
 potential : array[1..1205,1..4] of real;
 infname,outfname : string[12];
 infile,outfile : text;

Begin
 textcolor(yellow);
 textbackground(blue);
 clrscr;

 gotoxy(12,6);  writeln('what is the input expt. data name (d.pas)? ');
 gotoxy(12,8);  writeln('how many data points? ');
 gotoxy(12,10); writeln('what is the potential steps(mv)? ');
 gotoxy(12,12); writeln('what is the output expt. data file (data.pas)? ');

 gotoxy(12,7);  readln(infname);
 gotoxy(12,9);  readln(npoint);
 gotoxy(12,11); readln(vstep);
 gotoxy(12,13); readln(outfname);

 assign(infile,infname);     reset(infile);
 assign(outfile,outfname);   rewrite(outfile);

 for i := 1 to npoint do  begin
  readln(infile,Eexp[i],iexp[i]);
 end;

 for i := 1 to npoint-1 do  begin
  for j := 0 to vstep-1 do begin
   potential[i,j] := Eexp[i] +((Eexp[i+1] - Eexp[i]) * j) / vstep;
   current[i,j] := iexp[i] + ((iexp[i+1] - iexp[i]) * j) / vstep ;
    writeln(outfile,potential[i,j]:10:5,'    ',current[i,j]:15);
  end;
 end;
 writeln(outfile,Eexp[npoint]:10:5,'    ',iexp[npoint]:15);
 close(infile);
 close(outfile);
End.
```

References cited in chapter 1

1: Stephen W. Feldberg, *"Electroanalytical Chemistry"*, Vol.3, 1969, 199-296, edited by Allen J. Bard.

2: Stephen W. Feldberg, *"Computers in Chemistry"*, 1972, chap.7.

3: David K. Gosser and Philip H. Reiger, *Anal. Chem.*, 1988, 60, 1159-1167.

4: Allen J. Bard and Larry R. Faulkner, *"Electrochemical Methods"*, Wiley, 1980, Appendix B.

5: David K. Gosser and Feng Zhang, *Talanta*, 1991, 38(7), 715-722.

6: Jean-Michel Saveant, *J. Phys. Chem.*, 1988, 92, 5992-5995.

7: Dennis H. Evans, *J. Electroanal. Chem.*, 1989, 262, 67-82.

8: W. J. Boyer and Dennis H. Evans, *J. Electroanal. Chem.*, 1989, 67, 262.

9: David K. Gosser, *"Cyclic Voltammetry-Simulation and Analysis of Reaction Mechanisms"*, VCH, New York, 1993.

10: D. Britz, *"Digital Simulation in Electrochemistry"*, 2nd ed., Springer Verlag, Berlin, 1988.

11: James F. Rusling, *Critical Reviews in Analytical Chemistry*, 1989, 21, 49-81.

12: Stanley N. Deming and Stephen L. Morgan, *Anal. Chem.*, 1973, 45, 278A-283A.

13: Philip R. Bevington, *"Data Reduction and Error Analysis for the Physical Sciences"*, McGraw-Hill, 1969.

14: W. H. Press, B. P. Flannery, S. A. Teukolsky and W. T. Vetterling, *"Numerical Recipes"*, Cambridge University Press, Cambridge, 1985.

15: Gregory R. Philips and Edward M. Eyring, *Anal. Chem.*, 1988, 60, 738-741.

16: Gregory R. Philips and Edward M. Eyring, *Anal. Chem.*, 1988, 60, 2656.

17: Steven Brumby, *Anal. Chem.*, 1989, 61, 1783-1787.

References cited in chapter 2

1: Gregory R. Philips and Edward M. Eyring, *Anal. Chem.*, 1988, 60, 738-741.

2: David K. Gosser, *"Cyclic Voltammetry-Simulation and Analysis of Reaction Mechanisms"*, VCH, New York, 1993.

3: *BAS 100A Electrochemical Analyzer Manual*, Bioanalytical Systems Inc. 1987.

4: R. N. Adams, *Electrochemistry at Solid Electrodes*, p. 219. Dekker, New York, 1969.

5: B. B. Damaskin, *"The Principles of Current Methods for the Study of Electrochemical Reactions"*, McGraw-Hill, New York, 1967.

6: Qingdong Huang and David K. Gosser Jr., *Talanta*, 1992, 39, 1155-1161.

References cited in chapter 3

1: Feng Zhang, David K. Gosser Jr. and Steven R. Meshnick, *Biochemical Pharmacology*, 1992, 43(8), 1805-1809.

2: Gary H. Posner and Chang Ho Oh, *J. Am. Chem. Soc.*, 1992, 114, 8328-8329.

3: Syed S. Zaman and Ram P. Sharma, *Heterocycles*, 1991, 32(8), 1593-1638.

4: Anthony R. Butler and Yu-Lin Wu, *Chemical Society Reviews*, 1992, 85-90.

5: Charles W. Jefford, Feng Zhang, David K. Gosser and Steven R. Meshnick, et al, *Perspectives in Medicinal Chemistry*, Chapter 29, Ed. by Bernard Testa et al., VCH, 1993.

6: There are total 3 Phases testing of a drug required by the FDA as a New Drug Application (NDA) for approval of the drug as a marketable product.

Four kinds of pharmaceutical formulations were tested (because artemisinin is not soluble in water and we need to determine which

way is the most suitable route): tablets, in oil, as an oil suspension, and as an water suspension. Artemisinin were administered orally or by intramuscular injection.

7: W. S. Zhou, *Pure & Appl. Chem.*, 1986, 58(5), 817-824.

8: G. Schmid and W. Hofheinz, *J. Am. Chem. Soc.*, 1983, 105, 624.

9: X. X. Xu, J. Zhu, D. Z. Huang and W. S. Zhou, *Tetrahedron*, 1986, 42, 819.

10: C. W. Jefford, et al, *Helv. Chim. Acta.*, 1986, 69, 1778.

11: Charles W. Jefford, Yun Li, Amer Jaber and John Boukouvalas, *Synthetic Communications*, 1990, 20 (17), 2589-2596.

12: Gary H. Ponsner, Chang Ho Oh and Wilbur K. Milhous, *Tetrahedron Letters*, 1991, 32 (34), 4235-4238.

13: Charles W. Jefford, Javier Velarde and Gerald Bernardinelli, *Tetrahedron Letters*, 1989, 30 (34), 4485-4488.

14: P. Groth, *Acta Chemica Scandinavica A*, 1975, 29, 840-842.

15: V. L. Antonovskii, A. F. Nesterov and O. K. Lyashenko, *J. Appl. Chem. USSR*, 1967, 40, 2443.

16: Steven R. Meshnick, Abraham Thomas, Allen Ranz, Cai-Min Xu & Hua-Zhen Pan, *Molecular and Biochemical Parasitology*, 1990, 49, 181-190.

17: Bernhard Schrader, *Angew. Chem. Internat. Edit.*, 1973, 12(11), 884-908.

18: Ronald L. Birke and John R. Lombardi, *Spectroelectrochemistry, Chap. 6 "Surface-enhanced Raman Scattering"*, Ed. by Robert James Gale, Plenum Publishing Co. 1988.

19: J. J. McMabon, S. Baer and C. A. Melendres, *J. Phys. Chem.*, 1986, 90, 1572-1577.

References cited in chapter 4

1: Qingdong Huang, *Ph.D. thesis*, City University of New York, 1993.

2: Feng Zhang, David K. Gosser and Steven R. Meshnick, *Biochemical*

Pharmacology, 1992, 43, 1805-1809.

3: M. Brezina and A. Hofmanova, *Collect. Czech. Chem. Commun.*, 1973, 38, 985-993.

4: M. Brezina and A. Hofmanova-Matejkova, *Collect. Czech. Chem. Commun.*, 1973, 38, 3024-3031.

5: Robert S. Tieman, William R. Heineman, et al, *J. Electroanal. Chem.*, 1990, 281, 133-145.

6: R. Brdicka and K. Wiesner, *Collect. Czech. Chem. Commun.*, 1947, 12, 39-63.

7: C. F. Kolpin and H. S. Swofford, *Anal. Chem.* 1978, 50, 916-920, 920-929.

8: Kjetil Fossdal and Einar Jacobson, *Anal. Chim. Acta*, 1971, 56, 105-115.

9: Allen J. Bard and Larry R. Faulkner, *Electrochemical Methods*, 1980, Wiley, New York.

10: G. W. C. Milner and G. Phillips, *Coulometry in Analytical Chemistry*, 1967, Pergamon Press.

11: Garry A. Rechnitz, *Controlled Potential Analysis*, 1963, Pergamon Press.

12: G. C. Goode and J. Herrington, *Anal. Chim. Acta*, 1967, 38, 369-375.

13: V. E. Norvell and Gleb Mamantov, *Anal. Chem.*, 1977, 49 (9), 1470-1472.

14: Thomas P. DeAngelis and William R. Heineman, *J. Chem. Edu.*, 1976, 53 (9), 594-597.

15: Janet Weiss Sorrels and Howard D. Dewald, *Anal. Chem.*, 1990, 62 (15), 1640-1643.

16: S. Zamponi, M. Dimarino and R. Marassi, *J. Electroanal. Chem.*, 1988, 248, 341-348.

17: Theodore Kuwana and William R. Heineman, *Acc. Chem. Res.*, 1976, 9 (7), 241-248.

18: A. S. Baranski, W. R. Fawcett, et al, *Anal. Chem.*, 1985, 57, 166-170.

19: Donna J. Wiedemann and R. Mark Wightman, *Anal. Chem.*, 1991, 63,

2965-2970.

20: R. Mark Wightman and David O. Wipf, *Acc. Chem. Res.*, 1990, 23, 64-70.

21: Koichi Nozaki and Satoshi Okazaki, *J. Electroanal. Chem.*, 1989, 270, 191-204.

22: David O. Wipf, Adrian C. Michael and R. Mark Wightman, *J. Electroanal. Chem.*, 1989, 269, 15-25.

23: Jean-Michel Saveant, et al., *Chem. Rev.*, 1990, 90, 723-738.

24: Jurgen Heinze, *Angew. Chem. Int. Ed. Engl.*, 1991, 30 (2), 170-171.

25: R. Mark Wightman, *Anal. Chem.*, 1981, 53 (9), 1125A-1134A.

26: Claude P. Andrieux and Jean-Michel Saveant, *J. Phys. Chem.*, 1988, 92, 5987-5992.

27: Johathon O. Howell and R. Mark Wightman, *J. Electroanal. Chem.*, 1986, 209, 77-90.

28: Hsuan-Jung Huang, Peixin He and Larry R. Faulkner, *Anal. Chem.*, 1986, 58, 2889-2891.

29: Alanah Fitch and Dennis H. Evans, *J. Electroanal. Chem.*, 1986, 202, 83-92.

30: David O. Wipf and R. Mark Wightman, *Anal. Chem.*, 1988, 60, 306-310.

31: *BAS-100A manual.*

32: W. M. Schwarz and Irving Shain, *J. Phys. Chem.*, 1965, 69, 30-40.

33: R. A. Marcus, *J. Phys. Chem.*, 1963, 67, 853-857.

34: Richard S. Nicholson and Irving Shain, *Anal. Chem.*, 1964, 36 (4), 706-723.

35: Claude P. Andrieux, Jean-Michel Saveant, *J. Phys. Chem.*, 1988, 92, 5992-5995.

36: Claude P. Andrieux and Jean-Michel Saveant, *J. Am. Chem. Soc.*, 1993, 115, 6592-6599.

References cited in chapter 5

1: Charles W. Jefford, Feng Zhang, David K. Gosser and Steven R. Meshnick, et al, *Perspectives in Medicinal Chemistry*, Chapter 29, Ed. by Bernard Testa et al., VCH, 1993.

2: Feng Zhang, David K. Gosser, Steven R. Meshnick and Charles W. Jefford, *"Interaction of cyclopenteno-1,2,4-trioxanes with heme"*, in preparation.

3: Steven R. Meshnick, Abraham Thomas, Allen Ranz, Cai-Min Xu and Hua-Zhen Pan, *Molecular and Biochemical Parasitology*, 1990, 49, 181-190.

4: C. W. Jefford, et al, *Helv. Chim. Acta.*, 1986, 69, 1778.

5: Charles W. Jefford, Yun Li, Amer Jaber and John Boukouvalas, *Synthetic Communications*, 1990, 20 (17), 2589-2596.

6: Gary H. Ponsner, Chang Ho Oh and Wilbur K. Milhous, *Tetrahedron Letters*, 1991, 32 (34), 4235-4238.

7: Charles W. Jefford, Javier Velarde and Gerald Bernardinelli, *Tetrahedron Letters*, 1989, 30 (34), 4485-4488.

8: Feng Zhang, David K. Gosser Jr. and Steven R. Meshnick, *Biochemical Pharmacology*, 1992, 43(8), 1805-1809.

9: S. R. Meshnick, M. D. Scott, et al, *J. Lab. Clin. Med.*, 1989, 114, 401.

10: B. Halliwell and J. M. C. Gutteridge, *Free Radicals in Biology and Medicine*, 2nd Ed, p. 219, Clarendon Press, Oxford, 1989.

11: M. Brezina and A. Hofmanova, *Collect Czech. Chem. Commun.*, 1973, 38, 985-993 and 3024-3031.

12: China Cooperative Research Group on Qinghaosu, *J. Tradit. Chin. Med.*, 1982, 2, 3-8.

13: A. Brossi, B. Venugopalan and L. D. Gerpe, *J. Med. Chem.*, 1988, 31, 645-650.

14: R. Eckman and J. W. Eaton, *Nature*, 1979, 278, 754-756.

15: T. G. Traylor, et al, *J. Am. Chem. Soc.*, 1989, 111, 8413-8420 and 1990, 112,

178-186.

16: S. R. Meshnick, A. Thomas, A. Ranz, C. M. Xu and H. Z. Pan, *Mol. Biochem. Parasitol.*, 1991, 49, 181-190.